

**INNOVATIVE PHARMACEUTICAL FORMULATIONS
AND EXCIPIENTS FOR NASAL DELIVERY OF DRUGS
TO TARGET THE SYSTEMIC CIRCULATION**

Ph.D. thesis

Levente Kürti

**Szeged
2012**

DEPARTMENT OF PHARMACEUTICAL TECHNOLOGY
UNIVERSITY OF SZEGED

AND

BIOLOGICAL RESEARCH CENTRE
OF THE HUNGARIAN ACADEMY OF SCIENCES, SZEGED

**INNOVATIVE PHARMACEUTICAL FORMULATIONS
AND EXCIPIENTS FOR NASAL DELIVERY OF DRUGS
TO TARGET THE SYSTEMIC CIRCULATION**

Ph.D. thesis

Levente Kürti
Pharmacist

Supervisors:

Prof. Dr. habil. Piroska Szabó-Révész, Pharm.D., D.Sc.

Dr. habil. Mária A. Deli, M.D., Ph.D.

SZEGED
2012

CONTENTS

PUBLICATONS RELATED TO THE SUBJECT OF THE THESIS

OTHER PUBLICATIONS

ABBREVIATIONS

1. INTRODUCTION	1
1.1. Nasal delivery of drugs to the systemic circulation – General considerations	2
1.2. Drug nanoparticles – Innovations in pharmaceutics with nanotechnology	3
1.3. Permeability enhancers – Innovative pharmaceutical excipients	5
1.4. Models for studying nasal drug delivery – <i>In vitro</i> and cell culture techniques	7
1.5. Cell culture model of the nasal epithelium – RPMI 2650 nasal epithelial cell line	8
2. AIMS	10
3. MATERIALS AND METHODS	11
3.1. Materials	11
3.2. Methods	13
3.2.1. Preparation and characterization of meloxicam nanoparticles	13
3.2.1.1. Preparation of co-ground formulations and their physical mixtures	13
3.2.1.2. Design of experiments	13
3.2.1.3. Determination of particle size by electron microscopic image analysis	14
3.2.1.4. Investigations of the optimized products	14
3.2.2. Franz cell diffusion – <i>In vitro</i> permeability studies	15
3.2.3. Cell culture	15
3.2.3.1. Electron microscopy	16
3.2.3.2. Immunohistochemistry	16
3.2.3.3. Cytotoxicity assays – Real-time cell microelectronic sensing, LDH release test, MTT conversion assay and fluorescent staining of cell nuclei	17
3.2.3.4. Nasal epithelial permeability studies	19
3.2.4. Statistical analysis	20
4. RESULTS	21
4.1. Preparation and characterization of meloxicam nanoparticles	21
4.1.1. Co-grinding process of meloxicam and polymer excipients	21
4.1.2. Scanning electron microscopy of meloxicam particles	21
4.1.3. Influence of different parameters on meloxicam particle size diameters	22

4.1.4. X-ray powder diffraction analysis	25
4.1.5. Dissolution of meloxicam nanoparticles	26
4.1.6. <i>In vitro</i> release of meloxicam from different pharmaceutical compositions	26
4.2. Characterisation and optimization of the RPMI 2650 cell culture model	27
4.3. Permeability of meloxicam nanoparticles across the <i>in vitro</i> nasal barrier	31
4.4. Effects of sucrose esters on RPMI 2650 cell viability	31
4.5. Effects of sucrose esters on epithelial barrier integrity	34
5. DISCUSSION	37
5.1. Meloxicam nanoparticles – Novel alternatives in pain management	37
5.2. Cell culture model of nasal epithelial toxicity and permeability	39
5.3. Permeability enhancers – Risks and benefits	41
5.4. Significance, pharmaceutical relevance	43
6. SUMMARY	44
7. REFERENCES	45
ACKNOWLEDGEMENTS	
APPENDIX	

PUBLICATIONS RELATED TO THE SUBJECT OF THE THESIS

- I. Kürti L., Deli M., Szabóné Révész P.
Intranazális gyógyszerbevitel újabb lehetőségei szisztémás hatás elérése céljából
Gyógyszerészet 53, 67–73 (2009)
IF: -
- II. Kürti L., Kukovecz Á., Kozma G., Ambrus R., Deli M.A., Szabó–Révész P.
Study of the parameters influencing the co-grinding process for the production of meloxicam nanoparticles
Powder Technology 212, 210–217 (2011)
IF: 1.887 (2010)
- III. Kürti L., Veszelka S., Bocsik A., Dung N.T.K., Ózsvári B., Puskás L.G., Kittel Á., Szabó–Révész P., Deli M.A.
The effect of sucrose esters on a culture model of the nasal barrier
Toxicology in Vitro 26, 445–454 (2012)
IF: 2.546 (2010)
- IV. Kürti L., Veszelka S., Bocsik A., Dung N.T.K., Ózsvári B., Puskás L.G., Kittel Á., Szabó–Révész P., Deli M.A.
Retinoic acid and hydrocortisone strengthen the barrier function of human RPMI 2650 cells, a model for nasal epithelial permeability
Cytotechnology (submitted on 18th January 2012, manuscript number: CYTO700)
- V. Kürti L., Bocsik A., Veszelka S., Ózsvári B., Puskás L.G., Csizmazia E., Csányi E., Deli M.A., Szabó–Révész P.
In vitro permeability screening of meloxicam nanoparticles for nasal delivery
(manuscript in preparation)

OTHER PUBLICATIONS

- I. Horvát S., Fehér A., Balogh G., Wolburg H., Veszelka S., Kurunczi A., Kürti L., Erős I., Szabó–Révész P., Deli M.A.
Sodium hyaluronate as a mucoadhesive component in nasal formulation enhances delivery of molecules to brain tissue.
European Journal of Pharmeceutics and Biopharmaceutics 72, 252–259 (2009)
IF: 4.304 (2010)
- II. Sipos E., Kurunczi A., Fehér A., Penke Z., Fülöp L., Kasza Á., Horváth J., Horvát S., Veszelka S., Balogh G., Kürti L., Erős I., Szabó–Révész P., Párducz Á., Penke B., Deli M.A.
Intranasal delivery of human β -amyloid peptide in rats: effective brain targeting
Cellular and Molecular Neurobiology 30/ 405–413 (2010)
IF: 2.423 (2010)

ABBREVIATIONS

ATCC	American Type Culture Collection
BBB	blood–brain barrier
β -cat	β -catenin
BCS	Biopharmaceutical Classification System
COST	change one separate factor at time
COX-2	cyclo-oxygenase-2
cAMP	3'-5'-cyclic adenosine monophosphate
C_{\max}	maximal plasma concentration
CPT	8-(4-chlorophenylthio)
CR	Cremophor RH40
d_{SEM}	mean particle diameter [nm]
FBS	featal bovine serum
FDA	Food and Drug Administration
FITC	fluorescein isothiocyanate labeled
HA	sodium hyaluronate
HC	hydrocortisone
HLB	hydrophile–lipophile balance
i.m.	intramuscular
i.v.	intravenous
LDH	lactate dehydrogenase
MEL	meloxicam
MEM	Eagle's minimal essential medium
MTT	3-(4,5-dimethylthiazol-2-yl)-2,5-diphenyltetrazolium bromide
NSAID	non-steroidal anti-inflammatory drug
PAMPA	parallel artificial membrane permeability assay
P_{app}	apparent permeability coefficient
PBS	phosphate buffer
PEG	polyethylene glycol
Ph. Eur.	European Pharmacopoea
PVP	polyvinylpyrrolidone
RA	retinoic acid
RO20-1724	4-(3-butoxy-4-methoxybenzyl)-2-imidazolidinone
rpm	revolutions per minute
RT-CES	real-time cell electronic sensing
SD	standard deviation
SE	sucrose ester
SEM	scanning electron microscopy
TEER	transepithelial electric resistance
TJ	tight junction
TW	Tween 80
US DMF	United States drug master file
XRPD	X-ray powder diffraction
ZO	zonula occludens protein

1. INTRODUCTION

There are several areas in pharmaceutical technology which aim to solve problems with innovative approaches. These fields include: (i) the investigation of alternative sites of drug administration, such as pulmonary, nasal and transdermal delivery, (ii) innovative ways to increase the poor aqueous solubility of pharmaceuticals and drug candidates, (iii) the nanotechnology, formulation of drug nanoparticles, (iv) the delivery of biopharmaceuticals, peptides and proteins, (v) testing the toxicity and efficacy of innovative pharmaceutical excipients and (vi) the establishment of *in vitro* test systems for pharmaceutical screening purposes.

The use of the nasal pathway for the delivery of drugs is an emerging field in both pharmaceutical sciences and pharmaceutical industry. While the great majority of nasal formulations are designed and used for local delivery to treat nasal allergy, congestion or infections, other applications of nasal delivery have gained importance in recent years (Illum, 2003). The nasal route offers possibilities for systemic and vaccine delivery which are increasingly exploited. This alternative pathway can be especially useful in the case of drugs with systemic action that are difficult to deliver via routes other than injection. There is a growing number of such drugs marketed as nasal formulations abroad and in Hungary. The main advantages of the nasal administration of drugs include (i) circumvention of the first-pass elimination by the liver and gastrointestinal tract, (ii) rapid onset of action, (iii) non-invasive, easy daily administration, good compliance of the patients.

In the experimental work summarized in the thesis, two model compounds were used, meloxicam, a drug with poor aqueous solubility and dextran, a hydrophilic paracellular marker with an average molecular weight of 4.4 kDa, a size of a peptide. Innovative pharmaceutical formulations and excipients were applied to develop pharmaceutical compositions for systemic nasal drug delivery. Nanonization of the active agent meloxicam to increase its solubility and permeability, and modifying the paracellular permeability of the larger molecular weight compound dextran with pharmaceutical excipients were performed.

Cell culture investigations offer novel perspectives for pharmaceutical technology. Cytotoxicity and permeability assays are routinely used on different primary isolated cells and immortalised cell lines. To screen drug formulations, excipients and pharmaceutical compositions for their nasal epithelial toxicity and permeability we have developed and characterized an *in vitro* cell culture model.

1.1. Nasal delivery of drugs to the systemic circulation – General considerations

Intranasal administration is an effective way to deliver drugs into the systemic circulation as an alternative to the oral and parenteral routes for some therapeutic agents (Fig. 1). Undoubtedly, the nasal administration of medicines has been widely used for the treatment of topical nasal conditions such as nasopharyngitis or allergic rhinitis for many years. The nasal pathway may circumvent the blood–brain barrier and allow centrally acting pharmacons a direct transport route to the central nervous system as reviewed by Illum (2003). Previous studies from our laboratory also indicated the presence of this pathway (Wolburg et al., 2008; Horvát et al., 2009). Concerning systemic delivery, drugs can be rapidly absorbed through the nasal mucosa, resulting in a quick onset of action, and avoiding degradation in the gastrointestinal tract and first-pass metabolism in the liver (Ugwoke et al., 2001; Arora et al., 2002).

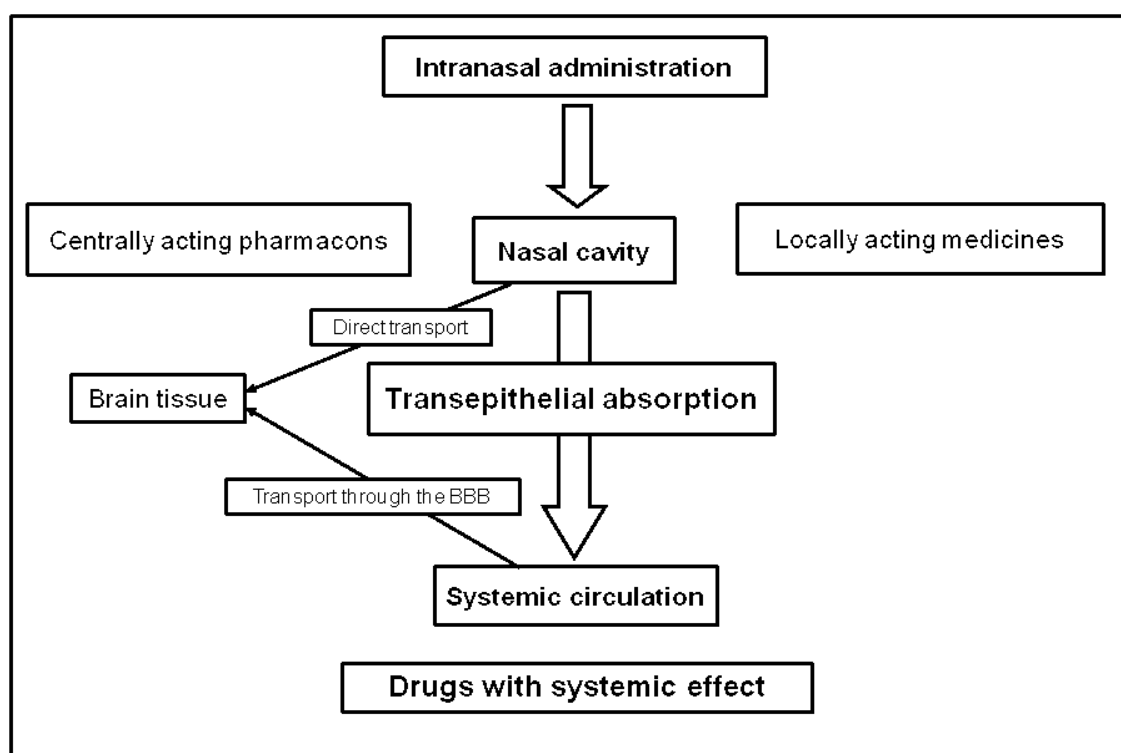


Fig. 1: Intranasal administration of drugs. The target for drug delivery can be the nasal mucosa, the central nervous system or the systemic blood circulation.

Nasal absorption is affected by physicochemical, anatomical and physiological, as well as formulation factors. The bioavailability of different active agents varies between 1% and 90%. Many drugs display high bioavailability by the nasal route, particularly if they have lipophilic characteristics (Davis and Illum, 2003). The number of nasal formulations which are available on the pharmaceutical market is rapidly growing. The use

of nasal administration of drugs is especially important in the treatment of migraine, severe pain and hormone replacement (Illum, 2003).

Lipophilic drugs can be expected to demonstrate rapid and efficient absorption when given nasally, but more polar compounds are poorly absorbed. Bioavailabilities of about 1% are to be expected for biopharmaceuticals such as insulin, calcitonin or leuprolin, and even less for higher molecular weight peptides and proteins such as growth hormone, interferons and growth factors (Kissel and Werner, 1998). The low uptake of drugs from the nasal cavity can be associated with three major factors, (i) poor transport, permeation across the nasal epithelium; (ii) possible enzymatic degradation in the nasal cavity; (iii) rapid mucociliary clearance from the site of absorption (Schmidt et al., 1998).

During the formulation of a pharmaceutical dosage form intended for intranasal application, several factors should be taken into consideration (Ugwoke et al., 2005). The poor solubility of a drug and its low rate of dissolution can lead to insufficient absorption or delayed therapeutical effect. Indeed the nasally administered pharmaceutical preparations will be cleared rapidly from the nasal cavity into the gastrointestinal tract by the mucociliary clearance system (Chien et al., 1992). Sodium hyaluronate is the sodium salt of hyaluronic acid, a naturally occurring linear polysaccharide with excellent mucoadhesive capacity (Prestwich and Vercruysse, 1998) can be selected as an excipient of nasal compositions (Liao et al., 2005). Although hyaluronan is used in diverse drug delivery systems e.g. ophthalmic, pulmonary and vaginal (Liao et al., 2005; Ludwig, 2005; Bonferoni et al., 2006), it has not been widely exploited for nasal drug delivery to the systemic blood circulation. Our research group has already used sodium hyaluronate as a viscosity-increasing and mucoadhesive component in a nasal formulation (Horvát et al., 2009). Due to the mucoadhesive properties of this biopolymer, sodium hyaluronate can enhance the permeability of drugs via mucosal tissues by increasing residence time on the site of absorption (Lim et al., 2000; Cho et al., 2003; Ludwig, 2005; Schiller et al., 2011). The low epithelial toxicity of this polymer is also favourable in nasal compositions (Miyazaki et al., 1996; Horvát et al., 2009).

1.2. Drug nanoparticles – Innovations in pharmaceutics with nanotechnology

Nanotechnology, a quickly developing area in the last decade, has a significant influence on pharmaceutical sciences by offering new solutions for existing problems. Transfer of drugs into the nano-dimension changes their physicochemical properties;

nanoparticles are used in pharmaceuticals to develop a novel formulation principle for poorly soluble active agents (Junghaus and Müller, 2008).

Over the last ten years, the number of poorly soluble drugs has continuously increased. Nanonization of pharmaceuticals offers a great possibility to increase their solubility (Ambrus et al., 2009) and to enhance permeability through mucosal barriers (Morgen et al., 2012). Nano-sized drug particles with carriers can overcome the resistance offered by biological barriers (Rawat et al., 2006).

Two basic approaches are involved in the production of nanoparticles, the bottom-up technologies (controlled precipitation, crystallization) and the top-down (high pressure homogenisation, wet milling, co-grinding) technologies. Precipitation methods are in research phases due to the complexity of the process and there are no pharmaceutical products on the market based on these technologies. Although crystalline nanoparticles have already introduced to the market, amorphous nanoparticles might belong to the second improved generation, because of their dissolution velocity and higher solubility (Shegokar and Müller, 2010). Importantly, there are no such data on meloxicam, a poorly soluble non-steroid antiinflammatory drug, widely used in clinical therapy.

Size reduction of drugs is often performed by dry milling (Delagrammatikas et al., 2007; Vegt et al., 2009), although the size limit is around 3 μm due to the aggregation of the particles. Recently studies focusing on particle size reduction to the submicron region by co-grinding process have been attempted (Sugimoto et al., 1998; Wanawongthai et al., 2009; Tozuka et al., 2011).

Co-grinding is a disintegration procedure for the preparation of nanoparticles by grinding the drug with polymers (Moribe, 2006). A main advantage of co-grinding as compared to other methods is its simplicity and organic solvents are not needed for the preparation of nanoparticles; therefore it is an economically and environmentally desirable technology (Barzegar-Jalali et al., 2010).

Breakage of drug crystals into nanoparticles creates an increased particle surface area, which is thermodynamically unfavourable. Thus, nano-sized particles tend to agglomerate to reduce their surface area. Particle agglomeration can be prevented by steric stabilization using polymeric excipients (Rabinow et al., 2004).

Water-soluble polymers have been typically used as excipients of the co-grinding process (Shakhtshneider et al., 1996; Jafar et al., 2010). In a study of Vogt et al. (2007) the rate of dissolution of poorly soluble drug was improved by co-grinding them with various excipients (lactose monohydrate, corn starch, polyvinylpyrrolidone, hydroxypropylmethyl

cellulose and sodium lauryl sulphate) using a jet-milling technique (Vogt et al., 2007). The unique properties of polyvinylpyrrolidone (PVP), such as its good solubility, its solubilising and film-forming abilities, its stabilizing effects in suspensions and emulsions, and its binding properties, make it a versatile excipient of pharmaceutical technology. PVP can form stable association compounds or complexes with a number of active agents (eg. PVP–iodine). The ability of PVP to form a water-soluble complex with insoluble active agents can be used in pharmaceuticals to improve the solubility and the dissolution rate of drugs (Foltmann and Quadir, 2008). Polyethylene glycol (PEG) is a semi-crystalline grinding excipient and it can be also used in grinding processes (Dehghan and Jafar, 2006).

The co-grinding of MEL with polymers was performed by Dehghan and Jafar (2006); in their experiments MEL solid dispersions were prepared, although the solvent evaporation method was favourable concerning the elevation of the rate of MEL dissolution.

Previously MEL drug nanoparticles have been prepared by using an emulsion-diffusion method, high-pressure homogenization or sonication (Ambrus et al., 2009). In an other study MEL nanoparticles were produced by combining anti-solvent precipitation and high pressure homogenisation approaches in presence of selected stabilizers and converting into dry powders by spray-drying (Raval and Patel, 2011).

Nasal delivery of MEL was studied by Wang et al. (2011), and pharmacokinetics after nasal administration was comparable to intravenous administration. The combination of nanotechnology with drug administration using alternative sites has perspectives in the development of efficient and safe medications.

1.3. Permeability enhancers – Innovative pharmaceutical excipients

A critical factor for nasal absorption is the permeation across the nasal epithelial cell layers. The pathways for absorption across the nasal respiratory epithelium are similar to those across other epithelia in the body (Fig. 2). Lipophilic drugs, like meloxicam, are transported transcellularly by passive lipid-mediated free diffusion, whereas hydrophilic small compounds, peptides or proteins and biomolecules, cross the barrier passively via the paracellular pathway, or use active carrier- or receptor-mediated processes (Deli, 2009).

The paracellular permeability, one of the most important determinants of drug transport, of various epithelial tissues and barriers differs greatly (Deli, 2009). Transepithelial resistance, measuring paracellular ion flux and reflecting the tightness of the intercellular junctional complex, is low in the nasal mucosa, which is considered as a

leaky epithelial tissue. The tight junctions in the small intestine, the stomach and the colon are of intermediate tightness, while brain capillaries and the skin epithelial cells form very tight paracellular barriers (Deli, 2009).

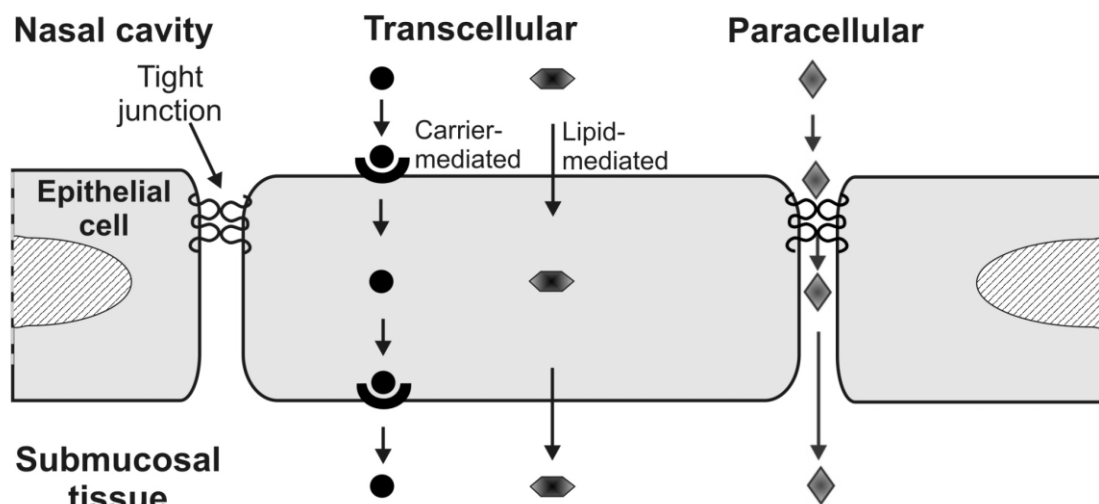


Fig. 2: Pathways through the nasal epithelium. Lipophilic drugs cross the epithelial layers transcellularly, hydrophilic compounds pass the barrier para- or transcellularly.

Since the junctions between epithelial cells constitute the strongest barrier in the nasal system (Wolburg et al., 2008), considerable effort has been directed towards the development of technologies that can improve the permeation across these cells (Illum, 2003). Methods to enhance or promote absorption by using formulation additives have therefore been extensively studied. Absorption enhancers can increase permeation of drug molecules through the barriers of the body, including the nasal epithelium (Deli, 2009). Surfactants, cationic polymers, cyclodextrins and many other types of compounds have been applied so far (Alpar et al., 2005).

Surfactants are solubilising excipients widely used in oral, injectable and nasal formulations (Behl et al., 1998; Davis and Illum, 2003). Non-ionic surfactants have been shown to be less toxic than ionic surfactants to biological membranes (Arechabala et al., 1999). Macrogol-glycerolhydroxystearate 40 (Cremophor RH40) and polysorbate 80 (Tween 80) are non-ionic solubilising and emulsifying agents. These surfactants can be used to increase bioavailability of drugs by solubilising of poorly soluble compounds, increasing cell membrane fluidity, or augmenting paracellular absorption (MacDonald et al., 2010).

Polyoxyethylene castor oil derivatives (Cremophors) are a series of compounds obtained by reacting varying amounts of ethylene oxide with either castor oil or

hydrogenated castor oil. Cremophors are used in oral, topical and parenteral pharmaceutical formulations (Wade and Weller, 1994). We have a favorable experience with Cremophor RH 40 in nasal formulations. Cremophor could enhance the nasal absorption and targeting of a peptide-size test molecule in combination with the mucoadhesive hyaluronic acid in rats (Horvát et al., 2009).

Polyoxyethylene sorbitan fatty acid esters (polysorbates) are a series of fatty acid esters of sorbitol and its anhydrides copolymerized with approximately 20 moles of ethylene oxide for each mole of sorbitol and its anhydrides. Polysorbates are hydrophilic non-ionic surfactants used widely as emulsifying, solubilising and wetting agents. Polysorbates 20, 40, 60 and 80 are included in the FDA Inactive Ingredients Guide for i.m., i.v., oral, rectal, topical and vaginal preparations (Wade and Weller, 1994).

Innovative pharmaceutical excipients, sucrose fatty acid esters are non-ionic surface-active agents consisting of sucrose as hydrophilic group and fatty acids as lipophilic groups. Sucrose contains 8 hydroxyl groups, and it is therefore possible to produce sucrose esters containing from 1 to 8 fatty acid moieties. In sucrose esters, the fatty acids are attached to sucrose, a disaccharide consisting of two monosaccharides, glucose and fructose. The commercial sucrose esters are mixtures of sucrose esters with various esterification degrees. Due to their complexity, they exhibit very diverse behaviour, like the glycerides. Sucrose esters are commonly used in food and cosmetic industries as emulsifiers, antibacterial agents or crystallization inhibitors (Garti et al., 2000; Csáki, 2011). Recently there has been great interest to use them also in the field of pharmaceuticals. There are data about the applicability of sucrose esters as permeation enhancers through the skin (Csóka et al., 2007), and our group demonstrated that sucrose esters can be successfully used in hot melt technology (Szűts et al., 2007, 2008). We have recently described an improved dissolution of gemfibrozil from a ternary solid dispersion system containing laurate sucrose ester (Szűts et al., 2011). Due to their good solubilising properties there is an interest to use sucrose esters as pharmaceutical excipients for nasal drug delivery. However there are no data on their toxicity and effect on human nasal epithelial cells.

1.4. Models for studying nasal drug delivery – *In vitro* and cell culture techniques

For successful formulation of a nasal delivery system, testing with reliably established *in vitro*, cell culture, *ex vivo* tissue and *in vivo* animal models are crucial (Fig. 3).

Vertical Franz diffusion cell model is a valid *in vitro* model for evaluating drug penetration from pharmaceutical preparations (Siewert et al., 2003). Basically, donor and acceptor compartments are separated by a membrane of artificial, animal or human origin. The *in vitro* permeability experiments are performed through cellulose acetate synthetic membranes. Lipophilic characteristics of the artificial membrane can be created by proper impregnation (eg. with isopropyl myristate). Generally, these membranes are reported to be more permeable than biological membranes.

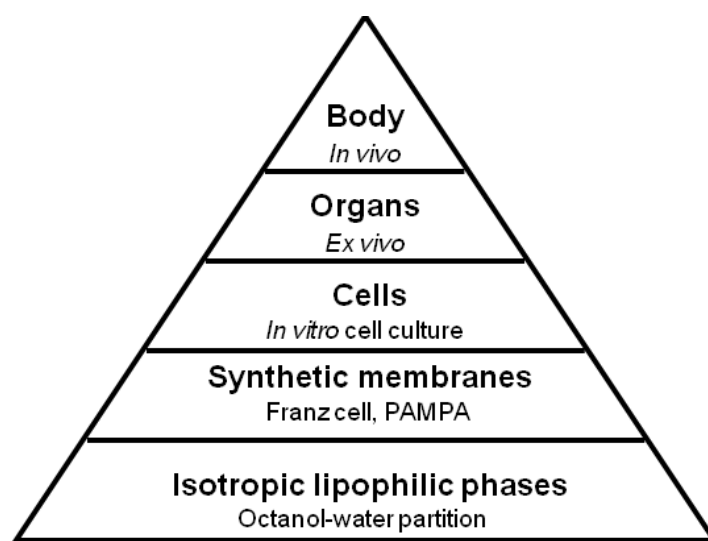


Fig. 3: Complexity pyramid of test systems used in pharmaceutical studies for prediction of drug permeability. Cell cultures can be classified as systems with medium complexity.

There are several limitations of the *ex vivo* tissue and animal models, including differences between the species in enzyme activities or in cell type distribution, and specialities in many anatomical and physiological features in various animal nasal cavities, compared with those of the human (Chien, 1992).

Several *in vivo* models of rat, rabbit, dog, sheep, and monkey were reported to deliver pharmacons via the nasal route (Chien, 1992; Costantino et al., 2007; Horvát et al., 2009). However, there are several disadvantages of the *ex vivo* tissue and *in vivo* animal models, including differences between the species in enzyme activities or in cell type distribution, and specialities in many anatomical and physiological features in various animal nasal cavities, compared with those of the human (Chien, 1992).

1.5. Cell culture models of the nasal epithelium – RPMI 2650 nasal epithelial cell line

The criteria for transport experiments with any nasal epithelial cell culture model are (i) the formation of confluent cell layers; (ii) the expression and correct localization of

intercellular junctional proteins; (iii) the functional barrier properties measured by transepithelial electric resistance and permeability coefficients for drug or marker molecules.

In vitro cell culture models of the human nasal epithelium based on primary culture technologies have proven to be useful for studies of nasal epithelial permeability and drug absorption (Lin et al., 2005). However limiting factors hinder the widespread usage and usefulness of primary nasal cell culture models. The shortage of human nasal tissue and the low reproducibility have prompted to seek an alternative to primary cultures of nasal epithelial cells, that is, the use of nasal epithelial cell lines. The use of an immortalized cell line has the advantages of ease of culture, lower costs, genetic homogeneity and reproducibility of the results.

The most relevant anatomical region in the nasal cavity concerning systemic nasal drug delivery is the respiratory epithelium lining the middle and inferior turbinate (Schmidt et al., 1998). RPMI 2650 is a human nasal epithelial cell line derived from a spontaneously formed tumour. Although this cell line originates from an anaplastic nasal septum tumour, its properties are closely related to normal human nasal epithelium concerning its karyotype (Moorhead, 1965), its cytokeratin polypeptide pattern (Moll et al., 1983), and the presence of mucoid material on the cell surface (Moore and Sandberg, 1964). This particular cell line has been mostly used for nasal metabolism studies and toxicity assays and less for permeability studies, since there are conflicting reports with regard to the ability of these cells to form monolayer. Some experts claim that RPMI 2650 nasal epithelial cells are able to form monolayers (Bai et al., 2008) while others described that they grow in clumps rather than in monolayers (De Fraissinette et al., 1995). Poor differentiation and lack of polarization have also been reported for this cell line (Werner et al., 1996). Furthermore, there is inconclusive data on the ability of RPMI 2650 cells to form tight junctions, though there is evidence that they can form perijunctional F-actin rings (Werner et al., 1996). Due to these reasons RPMI 2650 human nasal epithelial cell line is rarely used for nasal transport studies (Bai et al., 2008; Wengst and Reichl, 2009).

2. AIMS

For the development of relevant strategies to overcome biological barriers (eg. nasal mucosa) and in order to screen the feasibility of drug nanoparticles, innovative excipients and novel pharmaceutical compositions for nasal delivery targeting the systemic blood circulation, *in vitro* permeability models are useful and relevant tools.

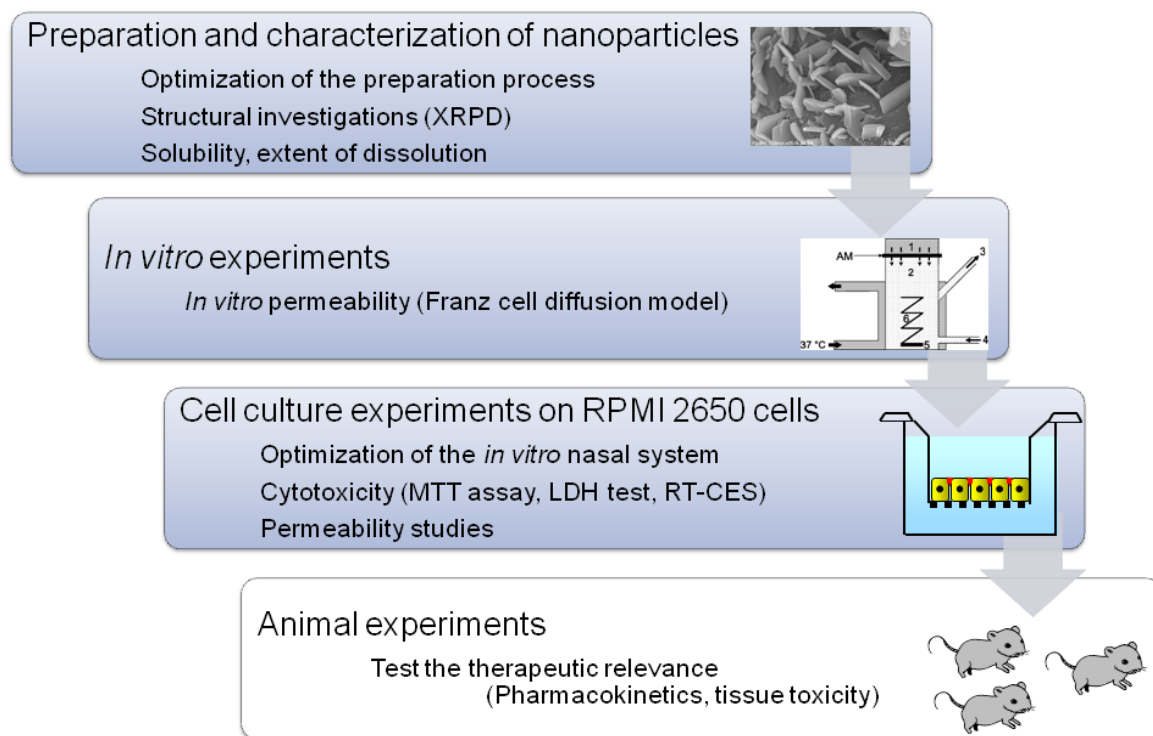


Fig. 4: The steps of a nasal investigational protocol to screen innovative formulations (nanoparticles) and novel pharmaceutical excipients (permeation enhancers).

The aim of my scientific work was to establish an *in vitro* investigational protocol for drugs intended to use in nasal delivery (Fig. 4). The application of cell-based assays as well as conventional investigational methods of pharmaceutical technology is crucial for understanding the toxicity and efficacy of an innovative pharmaceutical composition.

The main steps of our experiments were the following:

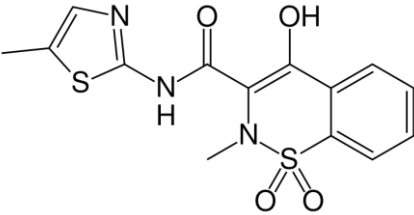
- (i) preparation and characterisation of meloxicam nanoparticles by co-grinding
- (ii) optimization of the preparation process by factorial experiment design
- (iii) establishment of *in vitro* methods for studying permeability of drugs in nasal formulations
- (iv) optimization of a culture model of the nasal system using RPMI 2650 cells
- (v) screen of the toxicity and efficacy of drug nanoparticles and pharmaceutical excipients by *in vitro* methods

3. MATERIALS AND METHODS

3.1. Materials

All reagents were purchased from Sigma–Aldrich, Hungary, unless otherwise indicated. Meloxicam (MEL), a BCS II drug was obtained from EGIS Ltd. (Hungary; Table 1).

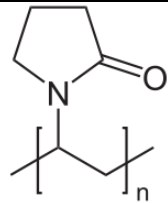
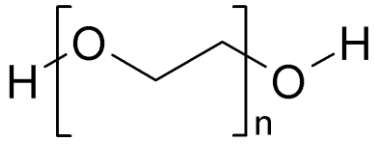
Table 1 *Properties of the active agent*

	Meloxicam
Chemical structure	
Chemical name	4-hydroxy-2-methyl-N-(5-methyl-2-thiazolyl)-2H-benzothiazine-3-carboxamide-1,1-dioxide
Molecular weight	351.4
Trade name	Movalis [®] , Meloxep [®]
Physical properties	yellow powder, poorly water-soluble, crystalline, high melting point
Applications	NSAID, selective COX-2 inhibitor

COX-2, cyclo-oxygenase-2; NSAID, non-steroidal anti-inflammatory drug.

The grinding additives, polyvinylpyrrolidone (PVP) K25 and C30 were purchased from BASF (Germany). Polyethylene glycol (PEG) 6000 and 20 000 were from Sigma–Aldrich Chemie GmbH, Germany (Table 2). Sodium hyaluronate (HA; Mw=1400 kDa) was obtained as a gift from Gedeon Richter Ltd. (Hungary).

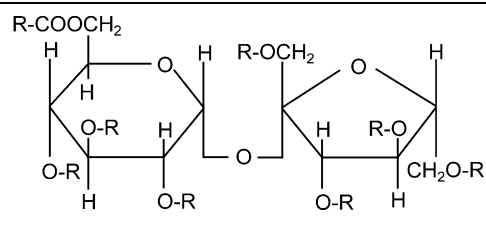
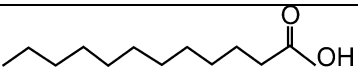
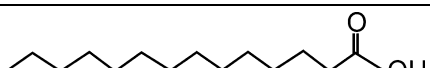
Table 2 *Polymer additives of the co-grinding process*

	Polyvinylpyrrolidone (Ph. Eur.)	Polyethylene glycol (Ph. Eur.)
Chemical structure		
Synonyms	Povidone, Kollidon	Macrogol, Polyoxyethylene
Physical properties	white-to-yellow-white powder soluble in water absorb large quantities of water amorphous temperature-resistant	white waxy powder soluble in water hygroscopic semi-crystalline low glass forming temperature
Applications	binder, solubilising agent, crystallization inhibitor, suspension stabilizer	binder, film coating, lubricant

Ph. Eur., European Pharmacopoea.

Laurate sucrose ester was of pharmaceutical grade, and myristate sucrose ester of analytical grade (Mitsubishi Kagaku Foods Co., Japan; Table 3).

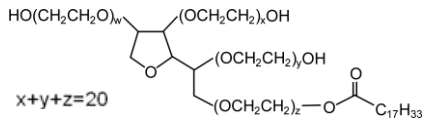
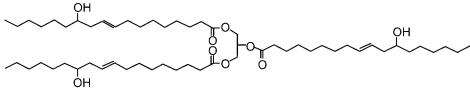
Table 3 Structure and properties of sucrose esters

	Sucrose fatty acid esters	
Chemical structure		
Chemical name	laurate sucrose ester	myristate sucrose ester
Trade name	Surfhope SE Pharma D-1216 (US DMF)	Ryoto sugar ester M-1695
Fatty acid	lauric acid (C ₁₂ H ₂₄ O ₂)	myristic acid (C ₁₄ H ₂₈ O ₂)
R-		
Solubility	soluble in water	soluble in water
HLB	16	16
Applications	non-ionic surface-active agent, emulsifier, antibacterial agent, crystallization inhibitor, permeation enhancer	

HLB, hydrophile–lipophile balance; US DMF, US drug master file.

Tween 80 and Cremophor RH40 (BASF, Germany) were of pharmaceutical grade (Table 4).

Table 4 Structure and properties of reference surfactants

	Polysorbate 80 (Ph. Eur.)	Macrogol-glycerolhydroxystearate 40 (Ph. Eur.)
Chemical structure		
Chemical name	polyethoxylated sorbitan and oleic acid	polyethoxylated 40 hydrogenated castor oil
Trade name	Tween 80	Cremophor RH40
Composition	70%: oleic acid (C ₁₈ H ₃₄ O ₂) 30%: linoleic, palmitic and stearic acid	90%: ricinoleic acid (C ₁₈ H ₃₄ O ₃) 10%: linoleic, oleic, palmitic and stearic acid
Physical properties	viscous water-soluble yellow liquid	white to yellowish thin paste at 20 °C
HLB	15	15
Applications	non-ionic surfactant and emulsifier	

HLB, hydrophile–lipophile balance; Ph. Eur., European Pharmacopoea.

3.2. Methods

3.2.1. Preparation and characterization of meloxicam nanoparticles

3.2.1.1. Preparation of co-ground formulations and their physical mixtures

Binary mixtures of MEL powder and the carriers PVP–C30, PVP–K25, PEG 6000 and PEG 20 000 were mixed and charged into the chamber of the planetary monomill (Fritsch Pulverisette 6, Fritsch GmbH, Germany) in various drug–carrier ratios. The grinding was performed in an 80 cm³ silicon nitride (Si₃N₄) milling drum containing 25 silicon nitride balls. In each experiment, 1.0 g of MEL was ground together with the calculated amount of polymer additive.

The milling parameters are given in Table 5 and the investigated parameters are listed in Table 6. After grinding, the samples were stored in plastic vials until use.

Table 5 General parameters of co-grinding, independent variables

Material of the grinding pot	Si ₃ N ₄
Material of the grinding balls	Si ₃ N ₄
Number of the grinding balls	25
Volume of the grinding pot	80 mL
Diameter of the grinding balls	10 mm
Duration of the grinding	2 h

The physical mixtures of drug–carrier were prepared by accurately weighing the calculated amounts of MEL and carrier, mixing them well in a porcelain mortar and storing in plastic vials until use.

3.2.1.2. Design of experiments

In a series of pre-screening experiments the following parameters were fixed: (i) the milling drum size and material, (ii) the ball size and number, and (iii) the milling duration. The remaining variables were the parameters featuring in the optimization (Table 6). A full factorial design plan was created and carried out with the MEL particle size distribution defined as response factor. All calculations were performed by using Minitab 14 (Minitab Statistical Software, PA, USA).

Table 6 Compositions of different samples, parameters of optimization

Meloxicam/excipient ratio	1:0.5, 1:1, 1:2
Excipients	PVP–C30, PVP–K25, PEG 6000, PEG 20 000
Revolutions per minute (rpm)	200, 300, 400

3.2.1.3. Determination of particle size by electron microscopic image analysis

Co-ground products were washed and centrifuged three times in distilled water to separate the water-soluble excipient from the water-insoluble MEL (the aqueous solubility of MEL is $4.4 \pm 0.7 \mu\text{g/mL}$ (Ambrus et al., 2009)), so that individual MEL particles could be studied. The particle size and the surface morphology of the MEL particles were visualised by scanning electron microscopy (SEM). Samples were fixed onto a metallic stub with double-sided conductive tape (diameter 12 mm, Oxford Instruments, UK). Images were taken in secondary electron image mode on a Hitachi S-4700 Type II instrument (Japan) at an acceleration voltage of 10 kV.

MEL particle diameter distributions were obtained by analysing SEM images with the ImageJ software environment (Abramoff et al., 2004). Over 150 individual particle measurements were made in at least five different images in order to determine the particle size accurately. Although less frequently used than TEM or dynamic light scattering, SEM image analysis is an established method for nanoparticle size analysis: for instance, it was applied successfully for the characterization of carbon nanotube networks (Smajda et al., 2007), Zn-glycerolate microstacks (Remias et al., 2009) and co-grinding products of PVP and CaCO_3 (Zapata-Massot et al., 2004).

3.2.1.4. Investigations of the optimized products

The physical state of MEL in the different samples was evaluated by X-ray powder diffraction (XRPD) analysis. Diffraction patterns were analysed with a Miniflex II X-ray diffractometer (Rigaku Co., Japan), where the tube anode was Cu with $K_\alpha = 1.5405 \text{ \AA}$. The pattern was collected with a tube voltage of 30 kV and a tube current of 15 mA in in-step scan mode ($4^\circ/\text{min}$). The instrument was calibrated by using Si.

The solubility of MEL was determined at physiological conditions (pH 7.4, 37°C) by addition of an excess of the drug to the solvent, after which the mixture was stirred on a magnetic stirrer for 8 h, then filtered (Minisart SRP 25, Sartorius, Germany), and the content of dissolved drug was analysed spectrophotometrically at 362 nm (Unicam UV/vis spectrophotometer, Germany). The extent of dissolution of MEL was studied in 50 mL phosphate buffer (PBS) at physiological conditions with Pharmatest equipment (Germany) at a paddle speed of 100 rpm. The dissolution experiments were conducted in triplicate.

3.2.2. Franz cell diffusion – *In vitro* permeability studies

In vitro permeability studies were performed with a vertical Franz–diffusion cell system (Microette Topical and Transdermal Diffusion Cell System, Hanson Research, USA) containing six cells (Makai et al., 2003; Csóka et al., 2005) at physiological conditions (Fig. 5). The donor phase contained MEL at 1 mg/mL and sodium hyaluronate at 5 mg/mL concentration, which were placed on the synthetic membrane impregnated with isopropyl myristate. The effective diffusion surface was 1.8 cm². PBS was used as an acceptor phase. The rotation of the stir-bar was set to 100 rpm. Experiments were performed at 37 °C (± 0.5 °C) water bath. At predefined time points, samples of 0.8 mL were taken from the acceptor phase by the autosampler (Microette Autosampling System, Hanson Research, USA) and were replaced with fresh receiving medium. Six Franz cells for each group were set.

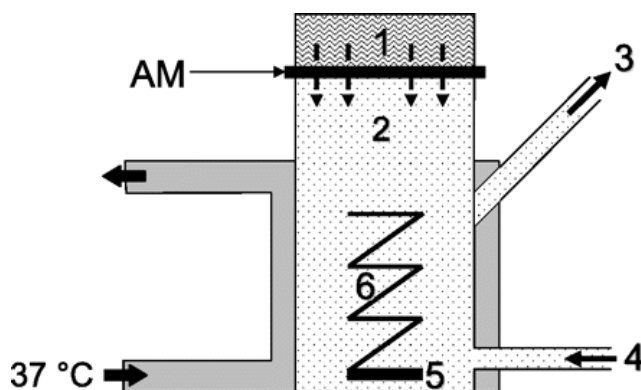


Fig. 5: Schematic drawing of the Franz cell. The donor compartment (1) above the artificial membrane (AM) contains meloxicam. The compartment below is the acceptor phase (2), from which samples are taken through the sampling port (3), and fresh medium is added to the acceptor phase by the replacing port (4). The acceptor compartment is surrounded by a water jacket kept at 37 °C. At the bottom of the acceptor phase, a stir-bar (5) and a helix mixer (6) are rotated magnetically (Resch et al., 2010).

3.2.3. Cell culture

RPMI 2650 (ATCC cat.no. CCL 30) cells were grown in Eagle's minimal essential medium (MEM) supplemented with 10% foetal bovine serum (FBS) and 50 µg/mL gentamicin in a humidified 37 °C incubator with 5% CO₂. The cells were seeded on rat tail collagen (0.05 v/v%) coated culture dishes at a density of 5×10^5 cells/cm² and the medium was changed every 2 days. When RPMI 2650 cells reached approximately 80–90% confluency in the dish they were trypsinized with 0.05% trypsin–EDTA solution. For the cell viability assays cells were passaged to 96-well plates, for immunohistochemistry and nucleus staining cells were cultured on glass coverslips. For permeability studies cells were cultured on Transwell filter inserts (polycarbonate membrane, 0.4 µm pore size, 1.1 cm² surface area, Corning Costar Co., MA, USA; Fig. 6). All surfaces were coated with

0.05 v/v% rat tail collagen before cell seeding. Cell growth and morphology were monitored using a Nikon Eclipse TE2000 microscope (Nikon, Japan).

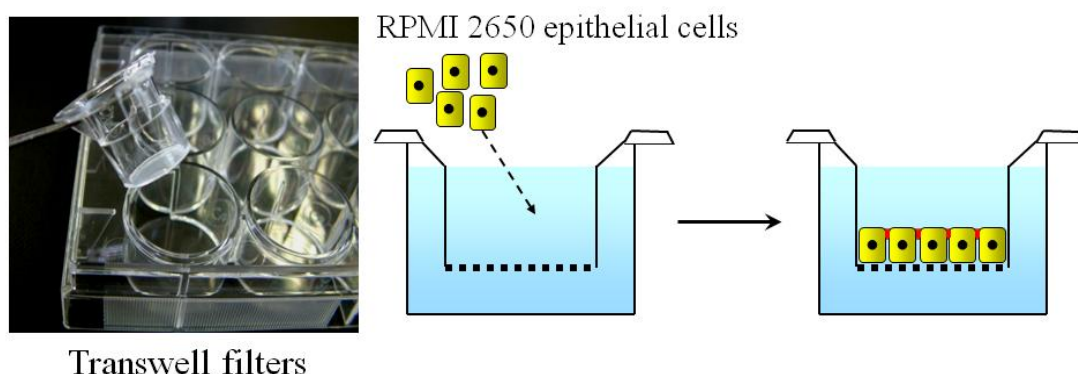


Fig. 6: Human RPMI 2650 cells were cultured on Transwell filter inserts for permeability experiments.

The culture model was optimised by testing the 24-h effect of retinoic acid (RA) in three different concentrations: 0.01, 100, 300 $\mu\text{g/mL}$. Hydrocortisone (HC) was examined at 500 nM; 8-(4-chlorophenylthio) adenosine 3',5'-cyclic monophosphate sodium salt (CPT-cAMP) at 250 μM in the presence of 17.5 μM 4-(3-butoxy-4-methoxybenzyl)-2-imidazolidinone (RO20-1724, Calbiochem, Germany), a phosphodiesterase inhibitor.

3.2.3.1. Electron microscopy

RPMI 2650 cells grown on Transwell filter membrane were fixed with 3% paraformaldehyde in 0.05 M cacodylate buffer (pH 7.5) for 30 min at 4 °C. After washing with cacodylate buffer several times, the membranes of the culture inserts with the cells were removed from their support and placed into 24-well chamber slide and were postfixed in 1% OsO_4 for 30 min. Finally the membranes of the culture inserts with the cells were removed from their support and embedded in Taab 812 (Taab, UK). Following polymerisation at 60 °C for 12 h, ultrathin sections were cut perpendicularly for the membrane using a Leica UCT ultramicrotome (Leica Microsystems, UK) and examined using a Hitachi 7100 transmission electron microscope (Hitachi Ltd., Japan). Electron micrographs were made by Megaview II (lower resolution, Soft Imaging System, Germany). Brightness and contrast were adjusted if necessary using Adobe Photoshop CS3 (CA, USA).

3.2.3.2. Immunohistochemistry

To stain for junctional proteins RPMI 2650 cells cultured on rat tail collagen coated glass coverslips were washed in PBS and fixed with 4% paraformaldehyde–PBS for 30 min.

After washing with PBS cells were blocked with 3% bovine serum albumin in PBS and incubated with primary antibodies anti- β -catenin and anti-ZO-1 (both from Invitrogen, CA, USA) for 1 h and 30 min. Incubation with secondary antibody Cy3-labeled anti-rabbit IgG and Hoechst dye 33342 to stain cell nuclei lasted for 1 h. Between and after incubations cells were washed three times with PBS. Coverslips were mounted in Gel Mount (Biomed, USA) and staining was examined by Olympus Fluoview FV1000 confocal laser scanning microscope.

3.2.3.3. Cytotoxicity assays – Real-time cell microelectronic sensing, LDH release test, MTT dye conversion assay and fluorescent staining of cell nuclei

Real-time cell electronic sensing (RT-CES) is a label-free technique for dynamic monitoring of living cells (Xing et al., 2005; Xia et al., 2008; Fig. 7A). The xCELLigence system (Roche, Switzerland) utilises an electronic readout called impedance to non-invasively quantify adherens cell proliferation and viability. A special 96-well E-plate (Roche, Hungary) contains microelectronic sensor arrays. The interaction between cells and electrode generates impedance response that correlates linearly with cell index reflecting cell number, adherence and cell growth (Ózsvári et al., 2010). The E-plate was coated with 0.2% gelatine-PBS solution for 20 min at 37 °C. Culture medium (80 μ L) was added to each well for background readings than 80 μ L cell suspension was dispensed at the density of 6×10^3 cells/well. The cells were kept in an incubator at 37 °C for 24 h and monitored every 5 min. The cell index at each time point was defined as $(R_n - R_b)/15$, where R_n is the cell-electrode impedance of the well when it contains cells and R_b is the background impedance of the well with the culture medium alone.

Lactate dehydrogenase (LDH) release, the indicator of cell membrane damage, was determined from culture supernatants by a commercially available kit (Cytotoxicity detection kit LDH, Roche, Switzerland; Fig. 7B). For LDH release assay RPMI 2650 cells were cultured in 96-well plates. After treatments 50 μ L samples from culture supernatants were incubated with equal amounts of reaction mixture for 15 min. The enzyme reaction was stopped by 0.1 M HCl. Absorbance was measured at a wavelength of 450 nm with a microplate reader (Fluostar Optima, BMG Labtechnologies, Germany). Toxicity was calculated as percentage of the total LDH release from cells treated by 10 mg/mL Triton X-100 detergent.

Living cells convert the yellow dye 3-(4,5-dimethylthiazol-2-yl)-2,5-diphenyltetrazolium bromide (MTT) to purple, insoluble formazan crystals (Fig. 7C).

RPMI 2650 cells were cultured in 96-well plates. After treatments the cells were incubated with 0.5 mg/mL MTT solution for 3 h in CO₂ incubator. The amount of formazan crystals was dissolved in dimethyl sulfoxide and determined by measuring absorbance at 570 nm with a microplate reader (Fluostar Optima, BMG Labtechnologies, Germany).

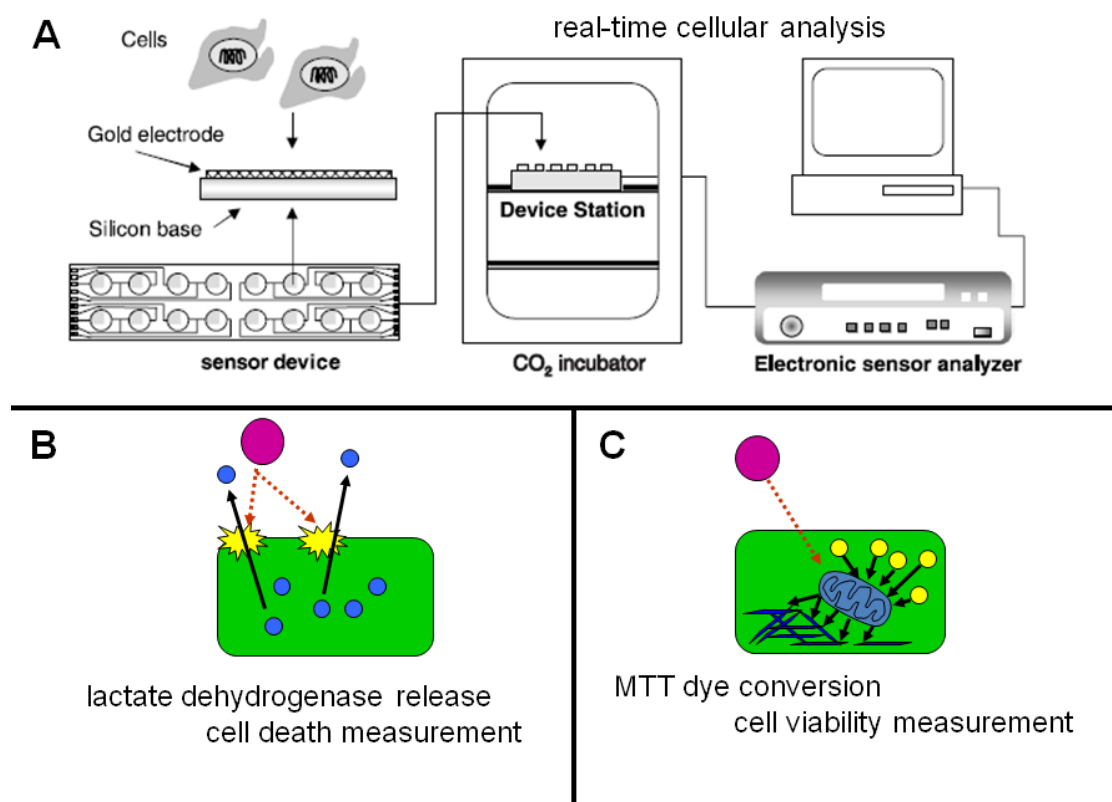


Fig. 7: Cytotoxicity assays. *A: real-time cell microelectronic sensing (Xing et al., 2005); B: LDH release test indicating cell membrane damage; C: MTT dye conversion assay showing the metabolic activity of living cells.*

Viability and nuclear morphology of RPMI 2650 cells were confirmed by double fluorescent staining. *Bis*-benzimidazole (Hoechst dye 33342) labels the nuclei of both viable and dead cells. Ethidium-homodimer-1 (Molecular Probes, USA) cannot pass through the plasma membrane of viable cells, therefore only stains dead cells. Cell layers grown on collagen-coated coverslips were treated with surfactants for 30 min, then 10 μ M *bis*-benzimidazole and ethidium-homodimer-1 was added for another 30 min. At the end of incubation cells were fixed in 4% paraformaldehyde in PBS for 30 min, washed three times in PBS, mounted, and analysed using a fluorescent microscope (Nikon Eclipse TE2000, Japan) and photographed by a Spot RT digital camera (Diagnostic Instruments, USA).

3.2.3.4. Nasal epithelial permeability studies

The flux of MEL and fluorescein isothiocyanate labeled dextran (FITC-dextran, mw: 4.4 kDa) across epithelial cell layers was determined in permeability assays (Fig. 8). RPMI 2650 cells were seeded onto Transwell filter inserts and grown for 2 days. The inserts were transferred to 12-well plates containing 1.5 mL Ringer–Hepes solution (118 mM NaCl, 4.8 mM KCl, 2.5 mM CaCl₂, 1.2 mM MgSO₄, 5.5 mM *D*-glucose, 20 mM Hepes, pH 7.4) in the basolateral compartments. In the apical chambers the culture medium was replaced by 500 µL of formulations containing 1 mg/mL MEL prepared in Ringer–Hepes. In experiments studying permeability enhancers culture medium was replaced by 500 µL Ringer–Hepes containing 100 µg/mL FITC-dextran and the selected concentrations of permeability enhancers in the apical chambers. The plates were kept in a 37 °C incubator with 5% CO₂ for 1 h on a rocking platform. After incubation the concentrations of the drug and the marker molecule were determined from the basolateral compartments spectrophotometrically in the case of MEL (Unicam UV/vis spectrophotometer, Germany) and by a fluorescent microplate reader in the case of FITC-dextran (Fluostar Optima, BMG Labtechnologies, Germany; emission: 485 nm, excitation: 520 nm).

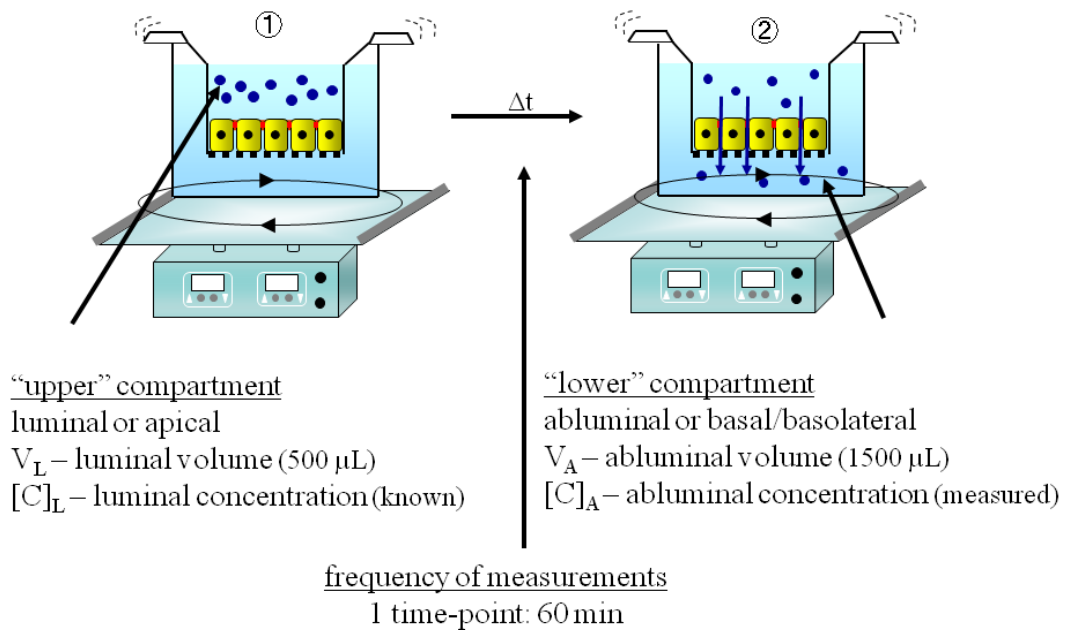


Fig. 8: Measurement of permeability across RPMI 2650 nasal epithelial cell layers.

The apparent permeability coefficients (P_{app}) were calculated. by the following equation (Youdim et al., 2003) and expressed as 10⁻⁶ cm/s:

$$P_{app} \text{ (cm/s)} = \frac{\Delta[C]_A \times V_A}{A \times [C]_L \times \Delta t}$$

Cleared volume was calculated from the concentration difference of the tracer in the basolateral compartment ($\Delta[C]_A$) after 1 h incubation and in the apical compartments at 0 h the start of the experiment ($[C]_L$), the volume of the basolateral compartment (V_A ; 1.5 mL) and the surface area available for permeability (A ; 1.1 cm²).

3.2.4. Statistical analysis

Co-grinding

Multivariate problems similar to the co-grinding process are often optimized by using the change one separate factor at a time (COST) approach: all parameters but one are fixed, and the response of the system is studied as a function of the changing variable. Each variable is scanned in this way, and the combination of their optimum values is accepted as the overall optimum.

Cell culture experiments

All data presented are means \pm SD. The values were compared using the analysis of variance followed by Dunnett tests using GraphPad Prism 5.0 software (GraphPad Software Inc., USA). Changes were considered statistically significant at $p < 0.05$. All independent experiments were repeated at least three times, the number of parallel samples within assays varied between 4 and 12. Inter-assay precision was calculated for all types of assays, and the coefficients of variation (CV%) were below 15%.

4. RESULTS

4.1. Preparation and characterization of meloxicam nanoparticles

4.1.1. Co-grinding process of meloxicam and polymer excipients

The particle size of MEL was reduced by roughly one order of magnitude, regardless of the additive used. This primary effect originated from the high-energy collisions taking place in the planetary ball mill (Alkebro et al., 2002). Ball milling is a process with complex mechanics, analysed in detail by Chattopadhyay et al. 2001. On the basis of their model, it was possible to calculate the energetics of the co-grinding experiments performed. The results in Table 7 indicate that the total energy transferred to the MEL–excipient mixture via collisions in our system lies in the range 2.85–68.50 kJ g⁻¹.

Table 7 Milling energetics map of the experiments performed

		Cumulative collision energy transferred (kJ g ⁻¹)			
		Meloxicam to additive weight ratio			
Rotation speed (rpm)	Collision frequency (s ⁻¹)	No additive	1:0.5	1:1	1:2
200	240	8.56	5.71	4.28	2.85
300	360	28.89	19.27	14.45	9.63
400	480	68.50	45.67	34.25	22.83

4.1.2. Scanning electron microscopy of meloxicam particles

A closer analysis of the SEM micrographs revealed that there were considerable differences in particle size distribution as a function of the excipient type used (Fig. 9).

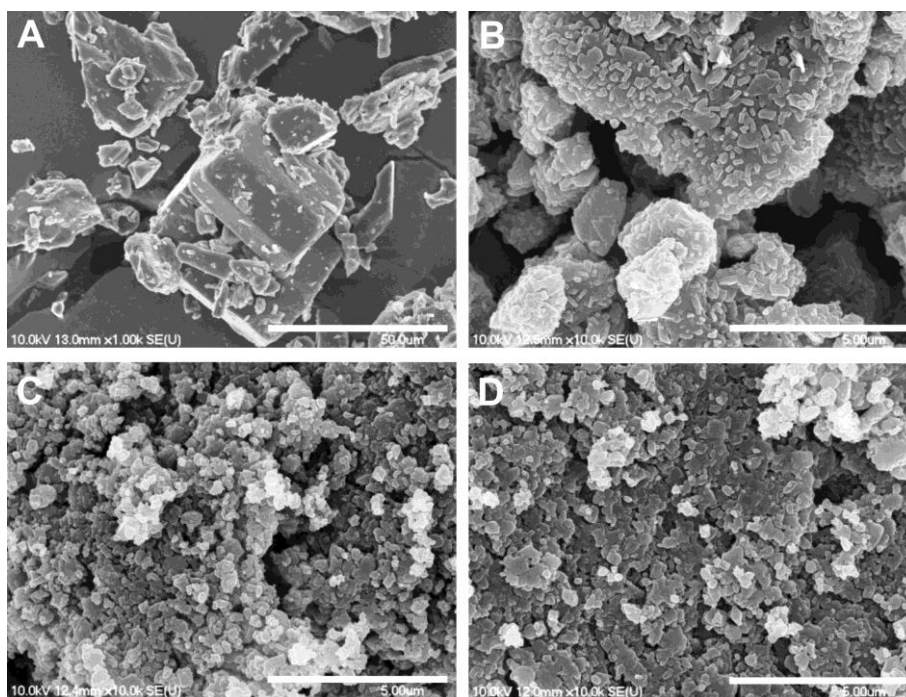


Fig. 9: Scanning electron microscopic images from meloxicam before grinding, bar: 50 µm (A), after co-grinding with PVP–K25 in a ratio of 1:0.5 at 300 rpm, bar: 5 µm (B), with PEG 20 000 in a ratio of 1:0.5 at 400 rpm, bar: 5 µm (C), with PEG 6000 in a ratio of 1:0.5 at 400 rpm, bar: 5 µm (D).

4.1.3. Influence of different parameters on meloxicam particle size diameters

The size distribution function is characterized by the mean particle diameter and the standard deviation of the diameter. The relationship of particle size with the grinding variables is analysed quantitatively in the main effects plots (Fig. 10 and Fig. 11) and interaction plots (Fig. 12 and Fig. 13).

The main effects plot shows the average response for each value of each variable, combining the effects of the other variables as if all variables were independent. The main effects plots for the MEL particle diameter indicate that the tested excipients can all promote size reduction (Fig. 10).

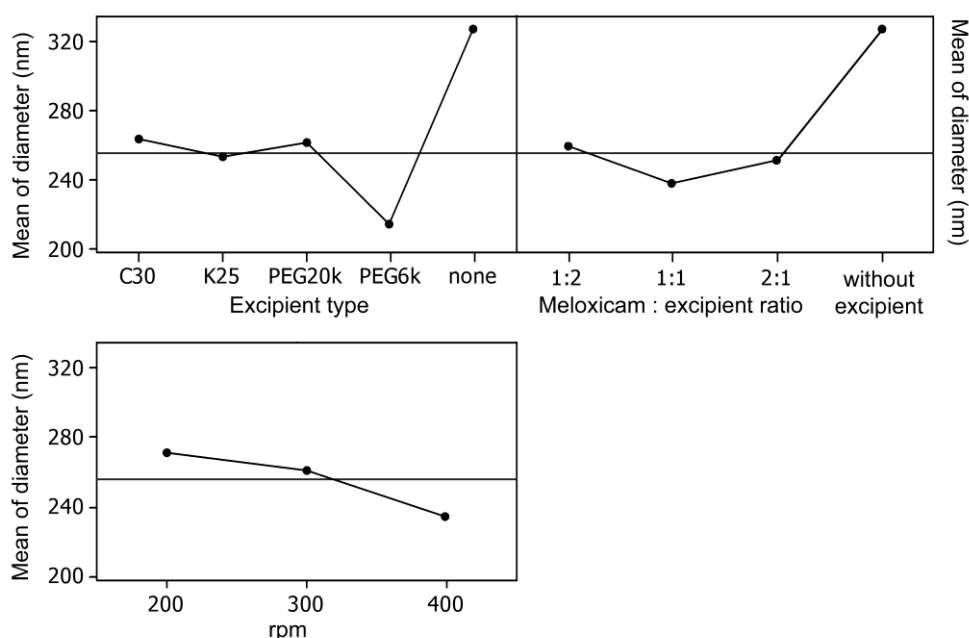


Fig. 10: Influence of different parameters (main effects plot, data means) on meloxicam particle diameter. C30, PVP–C30; K25, PVP–K25; PEG20k, PEG 20 000; PEG6k, PEG 6000.

Increasing the relative amount of MEL in the system resulted in larger product particles, whereas increasing the milling energy (grinding rate) reduced the particle size. Since our goal was to grind MEL into uniformly small particles so that its administration can be controlled, it was important to study the main effects plots characterizing the broadness of the particle size distribution curve (Fig. 11).

It is evident from Fig. 11 that the excipients PVP–K25 and PEG 6000 provide significantly broader and narrower MEL diameter distributions, respectively, than the other two tested additives. Increase of the MEL to additive ratio resulted in a less uniform

product. On the other hand, the distribution uniformity as a function of the milling energy exhibited a minimum at 300 rpm.

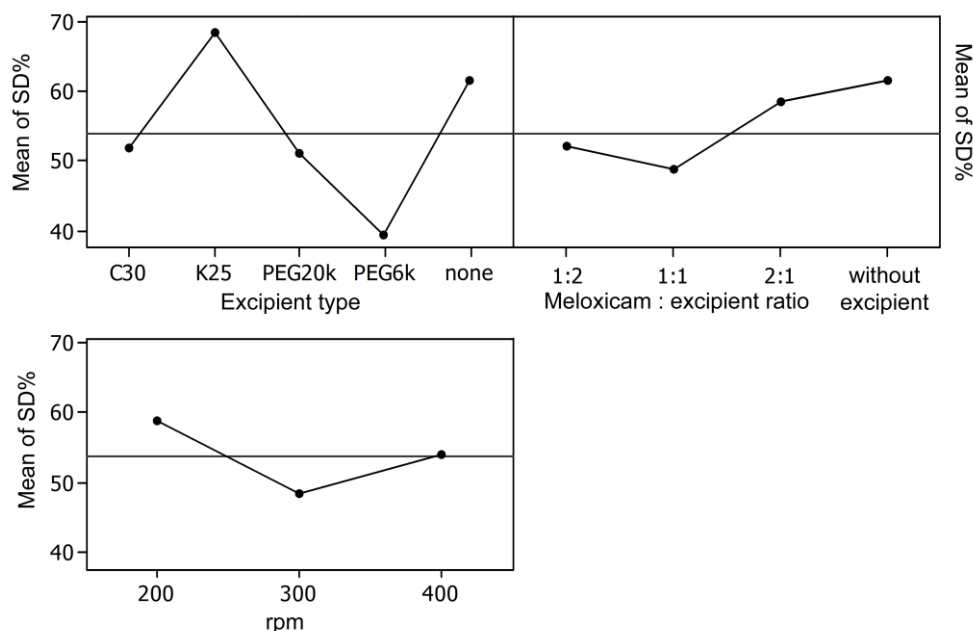


Fig. 11: Main effects plot (data means) for standard deviation% (SD%). C30, PVP-C30; K25, PVP-K25; PEG20k, PEG 20 000; PEG6k, PEG 6000.

Interaction plots illustrate the effects between variables, which are not independent by showing the means of the responses for each level of a factor for each level of a second factor pairwise for all factors involved in the study. Therefore, the interaction plots presented in Fig. 12 and Fig. 13 for the mean diameter and the SD%, respectively, can be used to gain insight into the complex interactions between the grinding parameters.

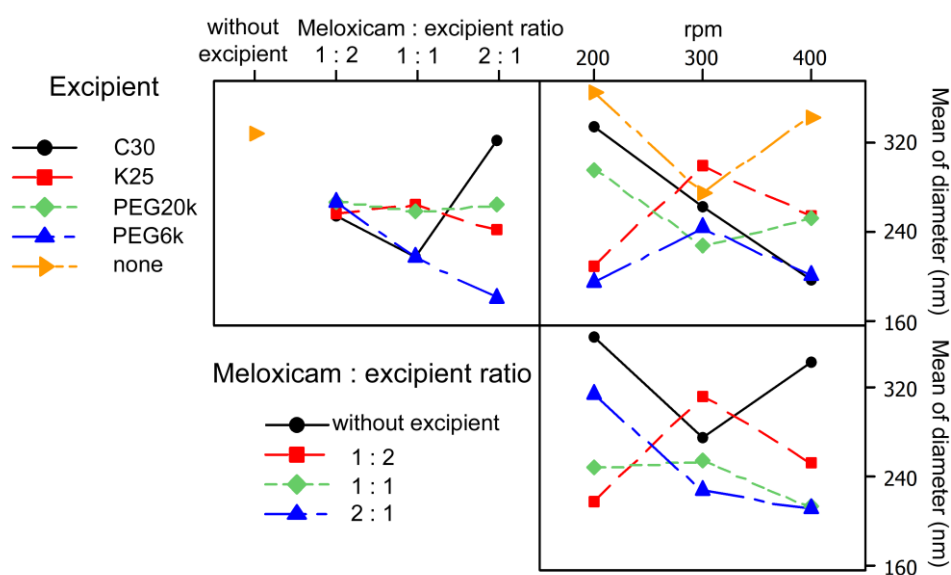


Fig. 12: Interaction plot (data means) for diameter. C30, PVP-C30; K25, PVP-K25; PEG20k, PEG 20 000; PEG6k, PEG 6000.

For example: (i) all additives but PVP–C30 result in a particle diameter increase at higher milling rates; (ii) increasing the milling frequency can compensate the diameter differences introduced by changing the MEL to additive ratio; (iii) the use of PEG 6000 as additive results in particularly narrow size distributions, regardless of the choice of the other two parameters.

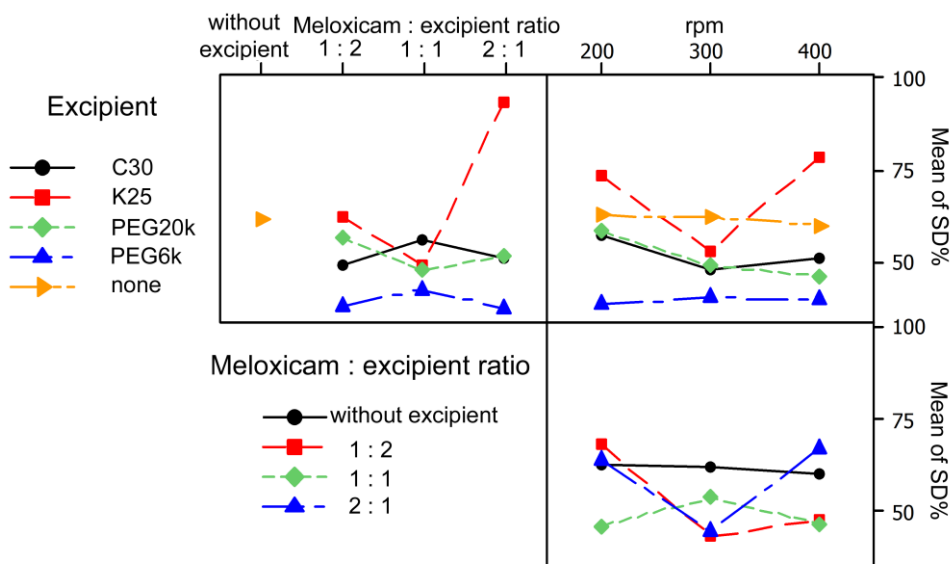


Fig. 13: Interaction plot (data means) for SD%. C30, PVP–C30; K25, PVP–K25; PEG20k, PEG 20 000; PEG6k, PEG 6000.

To summarize the grinding behaviour of MEL in a high-energy ball mill with Si_3N_4 as grinding material: in the absence of any grinding additives, the final product particles are too large at low milling energy ($d_{\text{SEM}}=364$ nm at 200 rpm) and aggregate rapidly at high energy ($d_{\text{SEM}}=343$ nm at 400 rpm). There is an optimum at 300 rpm. However, even at this setting, the average product particle size is above $d_{\text{SEM}}=270$ nm. It is interesting to note that, without additives, the relative broadness of the particle size distribution function was independent of the milling energy (SD~61%).

With PVP–C30, it was possible to decrease the average MEL particle size below 250 nm and the average SD below 50%. This was a significant improvement relative to the additive-free grinding result. The optimum co-grinding parameter set for PVP–C30 was a MEL to excipient ratio 1:1, and a rotation frequency of 400 rpm.

The optimized products selected for further studies are shown in Table 8 and Fig. 14.

Table 8 Optimized products of the co-grinding process

Grinding excipient	Drug to excipient ratio	Rotation speed (rpm)	$d_{\text{SEM}} \pm \text{SD}$ (nm)
PVP–C30	1:1	400	140.4 ± 69.2
PEG 6000	1:2	400	173.8 ± 60.3

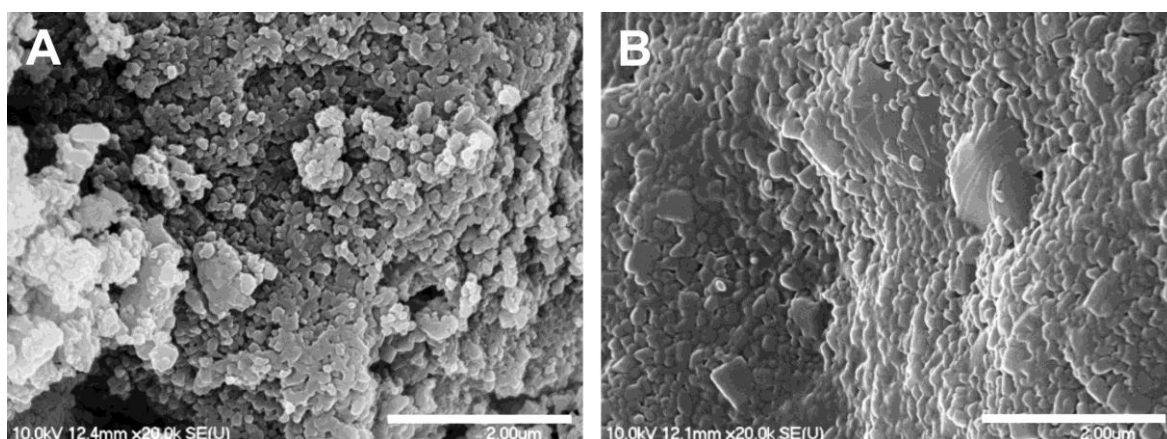


Fig. 14: Scanning electron microscopic images from the optimized products: meloxicam after co-grinding with PVP-C30 in a ratio of 1:1 at 400 rpm, bar: 2 μm (A), meloxicam after co-grinding with PEG 6000 in a ratio of 1:2 at 400 rpm, bar: 2 μm (B).

4.1.4. X-ray powder diffraction analysis

The most promising products of the co-grinding process were further investigated by XRPD analysis. The XRPD patterns of MEL, physical mixtures and products containing MEL and excipients in the optimized ratio are presented on Fig. 15. The optimized products (Table 8, Fig. 14) differ in their crystallinity, which can be observed in the diffraction spectra. The presence of numerous distinct peaks in the XRPD spectrum indicates that MEL is a crystalline material; its characteristic peaks appear at diffraction angles 2θ of 13.22, 15.06, 26.46 and 26.67°.

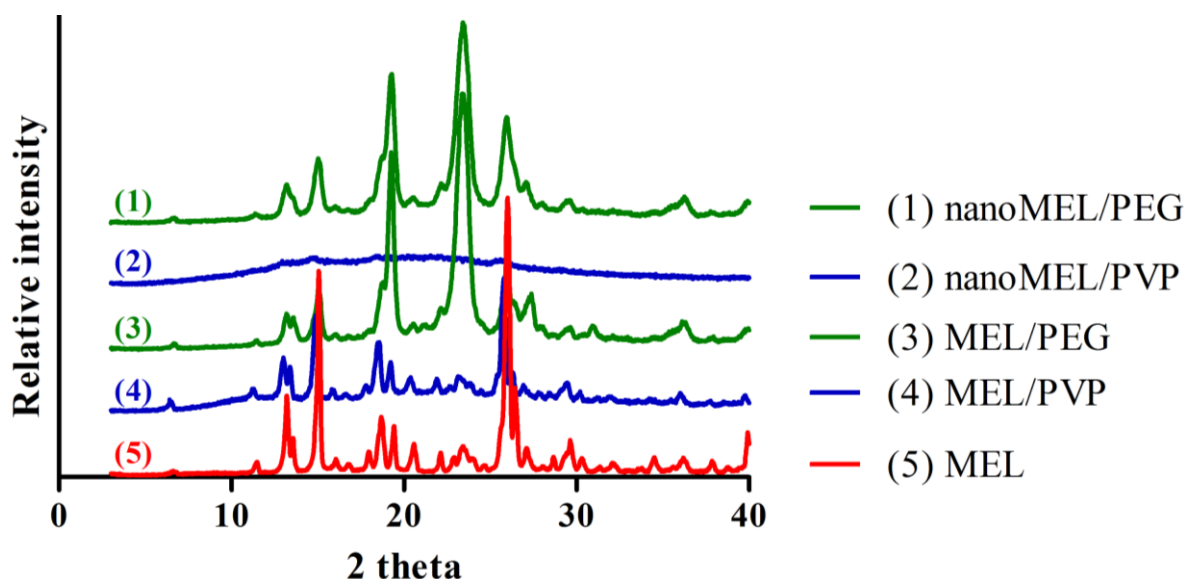


Fig. 15: X-ray powder diffraction spectra of the optimized products (1, 2), the physical mixtures of the components (4, 3) and meloxicam (5). MEL/PVP, meloxicam and polyvinylpyrrolidone C30 mass ratio 1:1; MEL/PEG, meloxicam and polyethylene glycol 6000 mass ratio 1:2.

The crystallinity of MEL was decreased in the co-grinding process with PVP–C30; in the other optimized product, which contains PEG 6000 the crystallinity of MEL did not change significantly comparing to the physical mixture. The crystalline MEL was altered in the co-grinding process with the amorphous excipient, PVP–C30, leading to amorphous nanoparticles. With PEG 6000 as excipient, the crystallinity of MEL was proved (Fig. 15), i.e. MEL nanocrystals were prepared. Based on these data nanoMEL/PVP product was selected for *in vitro* dissolution, permeability and cell culture studies.

4.1.5. Dissolution of meloxicam nanoparticles

Amorphous nanoMEL/PVP nanoparticles showed favourable dissolution properties at physiological conditions. In one hand the solubility of MEL elevated up to about 1 mg/mL (Fig. 16A), on the other hand the extent of dissolution also increased, complete dissolution of MEL was observed in 15 min (Fig. 16B).

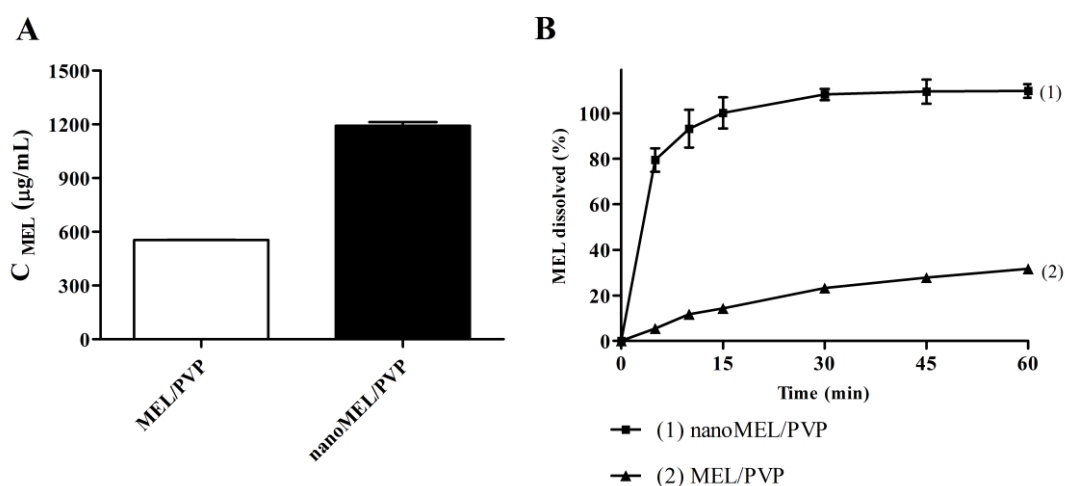


Fig. 16: A: Solubility of meloxicam (MEL) in case of the physical mixture (MEL/PVP) and the co-ground product (nanoMEL/PVP) in phosphate buffer (pH 7.4, 37 °C). B: The extent of dissolution of MEL in case of the physical mixture (MEL/PVP) and the co-ground product (nanoMEL/PVP) in phosphate buffer (pH 7.4, 37 °C). MEL/PVP, meloxicam and polyvinylpyrrolidone C30 mass ratio 1:1.

4.1.6. *In vitro* release of meloxicam from different pharmaceutical compositions

The cumulative amount of MEL that diffused through a synthetic membrane from the different pharmaceutical compositions was measured against time (Fig. 17). The diffusion from the composition containing MEL nanoparticles and sodium hyaluronate was quicker, 25% of MEL was released from the formulation containing MEL in nanonized form vs. 10% in case of the physical mixture in the first 2 h.

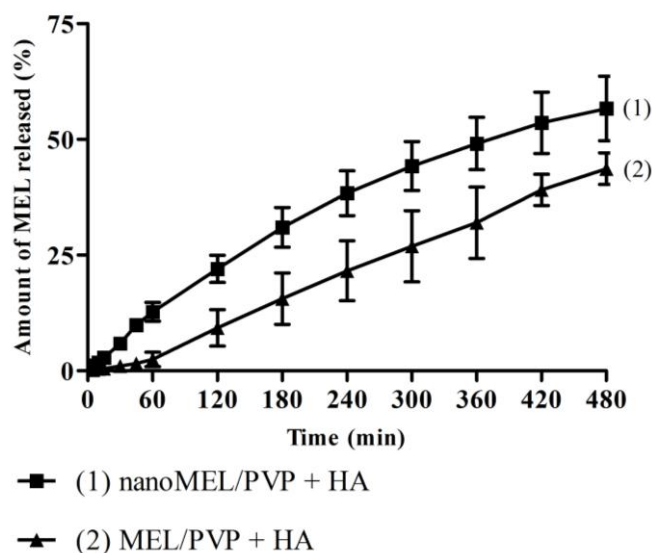


Fig. 17: *In vitro* permeability of meloxicam through an artificial membrane in case of the physical mixture (MEL/PVP) and the coground product (nanoMEL/PVP) in phosphate buffer (pH 7.4, 37 °C). MEL/PVP, meloxicam and polyvinylpyrrolidone C30 mass ratio 1:1; HA, sodium hyaluronate (5 mg/mL).

4.2. Characterisation and optimization of the RPMI 2650 cell culture model

Confluent layers of RPMI 2650 human nasal epithelial cells were obtained on collagen-coated surfaces (Fig. 18). RPMI 2650 cells achieved confluency within 2 days on collagen coated polycarbonate membranes. The presence of intercellular junctions was confirmed by electron and immunofluorescent microscopy. Besides morphological characterisation, the functional properties of RPMI 2650 nasal epithelial layers, like transepithelial electric resistance and paracellular permeability, were also investigated. Intercellular adherens junctional protein β -catenin was detected on the border of RPMI 2650 cells by immunofluorescent microscopy. Faint cytoplasmic staining was also visible in agreement with the known signalling mechanism of this protein.

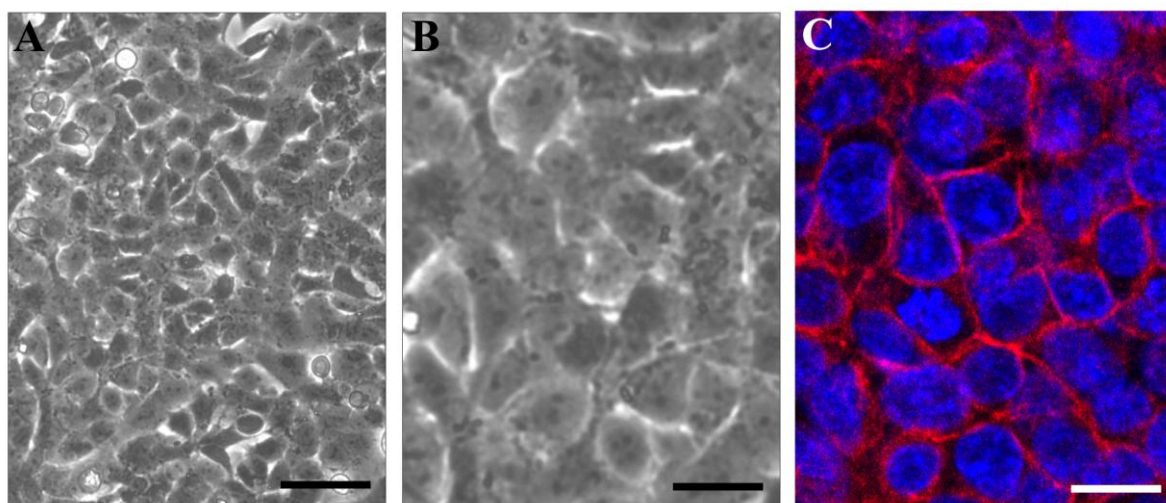


Fig. 18: Confluent RPMI 2650 human nasal epithelial cell layers visualised by phase contrast microscopy (A, bar 40 μ m; B, bar: 10 μ m) and by confocal fluorescent microscopy after immunostaining for β -catenin (C, bar: 10 μ m).

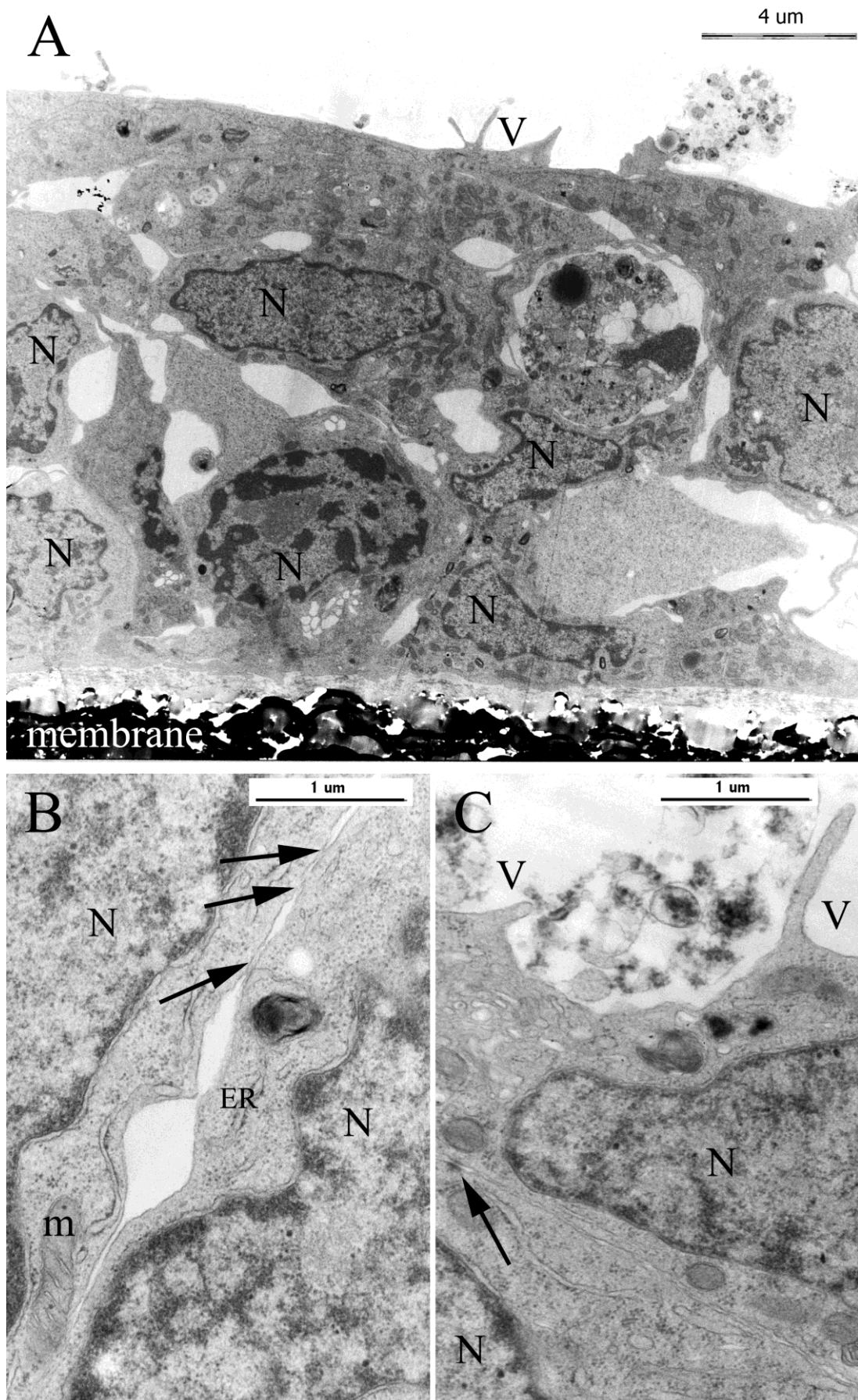


Fig. 19: Electron microscopic image of the ultrastructure of RPMI 2650 cell layers. Arrows show intercellular junctions. N, nucleus; m, mitochondrion; ER, endoplasmatic reticulum; V, microvilli.

RPMI 2650 cells grew in mono- or multilayers as *in vivo* as demonstrated by the electron microscopic images (Fig. 19A). A cubic and polarized cell morphology, microvilli and mucoid material on the apical surface could be observed. Healthy, intact cell constituents, like mitochondria, endoplasmic reticulum and large cell nuclei with few cytoplasm were visualised. Intercellular junctions are important in the paracellular barrier function of the cell layers (Fig. 19B–C). These characteristics are typical for epithelial cells *in vivo* as well. Tight intercellular junctions were visualised by electron microscopy.

Growth and differentiating factors: retinoic acid, hydrocortisone and cAMP were tested to improve the RPMI 2650 *in vitro* model for pharmaceutical screening purposes. The barrier function of the nasal epithelial cell layers was confirmed by morphological and functional methods.

The immunostaining and localization of adherens and tight junctional proteins were changed in human RPMI 2650 cells by treatments. Immunostaining for adherens junction protein β -catenin and tight junction related protein ZO-1 were more intense and better localized to the cell periphery in RPMI 2650 cells treated with retinoic acid, hydrocortisone or cAMP then in the control group (Fig. 20).

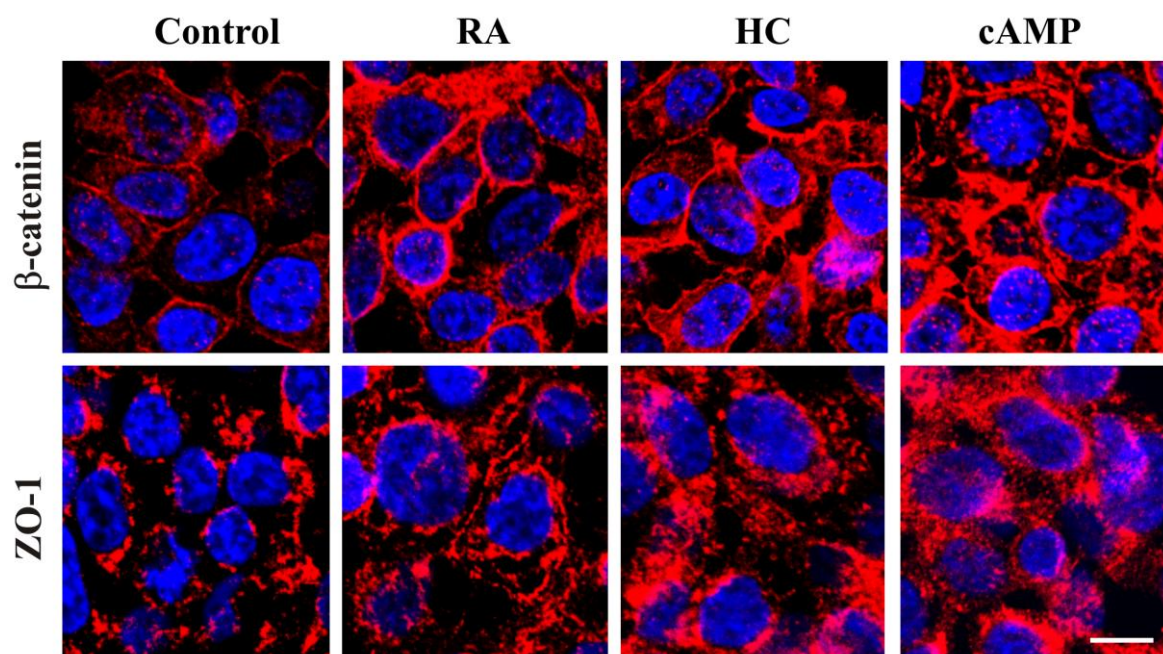


Fig. 20: Immunohistochemical staining of RPMI 2650 cells for junctional proteins β -catenin and zonula occludens-1 (ZO-1) visualised by confocal fluorescent microscopy. Cells were treated with retinoic acid (RA, 300 μ g/mL), hydrocortisone (HC, 500 nM) or 3'-5'-cyclic adenosine monophosphate (cAMP, 250 μ M) for 24 h; bar: 10 μ m.

Retinoic acid and hydrocortisone significantly decreased the paracellular permeability for FITC-dextran 4.4 kDa and increased the transepithelial resistance of nasal epithelial cell layers (Fig. 21). These parallel effects indicate strengthened barrier formation in agreement with the morphological observations. While cAMP did not change the epithelial paracellular permeability, interestingly, it significantly decreased the electric resistance of RPMI 2650 cells (Fig. 21).

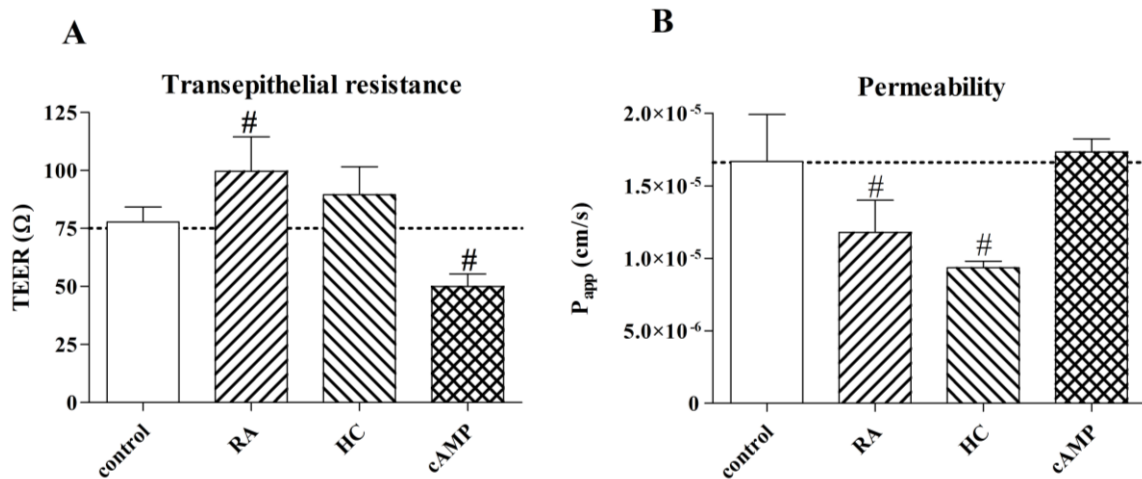


Fig. 21: Barrier functions measured by transepithelial resistance (A) and permeability for FITC-labeled dextran 4.4 kDa (B) of RPMI 2650 layers treated with retinoic acid (RA, 300 $\mu\text{g/mL}$), hydrocortisone (HC, 500 nM) or 3'-5'-cyclic adenosine monophosphate (cAMP, 250 μM). P_{app} , apparent permeability coefficient.

The flux of FITC-dextran 4.4 kDa from the apical to the basolateral compartments is around 4.5% in the control group. Treatments with retinoic acid, hydrocortisone and cAMP resulted in 3.2, 2.5 and 4.7% flux of the marker molecule from the donor to the acceptor compartment.

The transepithelial electric resistance values of the confluent cell layers in the optimized model system were around 150–200 Ω calculated from the RT-CES results. The apparent permeability coefficient of RPMI 2650 cell layers for paracellular marker 4.4 kDa FITC-dextran was 9.7×10^{-6} cm/s (Table 9).

Table 9 The optimised in vitro nasal system

RPMI 2650 human nasal epithelial cell line	
surface treatment	rat tail collagen coating
initial seeding density	5×10^5 cells/cm ²
concentration of serum in the culture medium	10%
24-h treatments before permeability experiments	300 $\mu\text{g/mL}$ retinoic acid 500 nM hydrocortisone
TEER values calculated from RT-CES analysis	150-200 Ω
P_{app} for FITC-dextran 4.4 kDa	9.7×10^{-6} cm/s

P_{app} , apparent permeability coefficient; TEER, transepithelial electric resistance.

4.3. Permeability of meloxicam nanoparticles across the *in vitro* nasal barrier

To test the biological effects of the MEL nanoparticles human RPMI 2650 cells were used. Impedance measured by RT-CES non-invasively quantifies adherens cell proliferation, viability and cell layer integrity. The RT-CES results indicated no sign of disruption of the integrity of the RPMI 2650 cell layers (Fig. 22A), which could be observed in the toxicity control group (10 mg/mL TritonX-100 detergent).

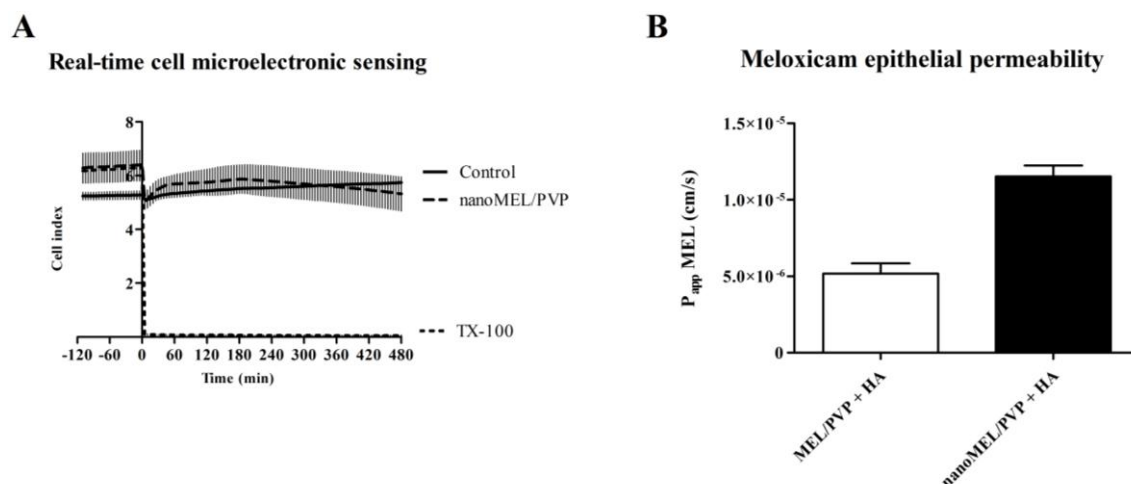


Fig. 22: A: Real-time cell microelectronic sensing measurement of cell viability and integrity of human RPMI 2650 nasal epithelial cells treated by vehicle and the co-ground product (nanoMEL/PVP). B: Apparent permeability coefficients (P_{app}) of MEL in case of the physical mixture (MEL/PVP) and the co-ground product (nanoMEL/PVP) measured across human RPMI 2650 nasal epithelial cell layers. MEL/PVP, meloxicam and polyvinylpyrrolidone C30 mass ratio 1:1; HA, sodium hyaluronate (5 mg/mL); TX-100, TritonX-100 (10 mg/mL).

The flux of MEL through the human RPMI 2650 cell layers was significantly slower than in the case of the Franz cell diffusion model, reflecting the higher complexity of the cell culture system. The permeability coefficient of MEL for the composition containing MEL nanoparticles and sodium hyaluronate was significantly higher than in case of the physical mixture (1.2×10^{-5} cm/s vs. 0.5×10^{-5} cm/s; Fig. 22B).

4.4. Effects of sucrose esters on RPMI 2650 cell viability

The toxicity of surfactants on RPMI 2650 cells was tested by RT-CES method. Cell index, reflecting cell viability, was not reduced significantly by laurate and myristate sucrose esters at 0.1 mg/mL concentrations, but profound effect was found in concentrations higher than 0.1 mg/mL after 1-h treatment (Fig. 23A). Tween 80 had no influence on the cell index after 1-h treatment at 1 mg/mL, but decreased the cell index below 50% at 10 mg/mL concentration (Fig. 23B). After 1-h treatment none of the studied

concentrations of Cremophor RH40 (1, 10, 50 mg/mL) caused alterations in cell index, indicating no cell damage. Our toxicity control, TritonX-100 caused 90% reduction in cell index values. This drastic reduction indicates cellular death, in agreement with MTT and LDH release data (Fig. 24).

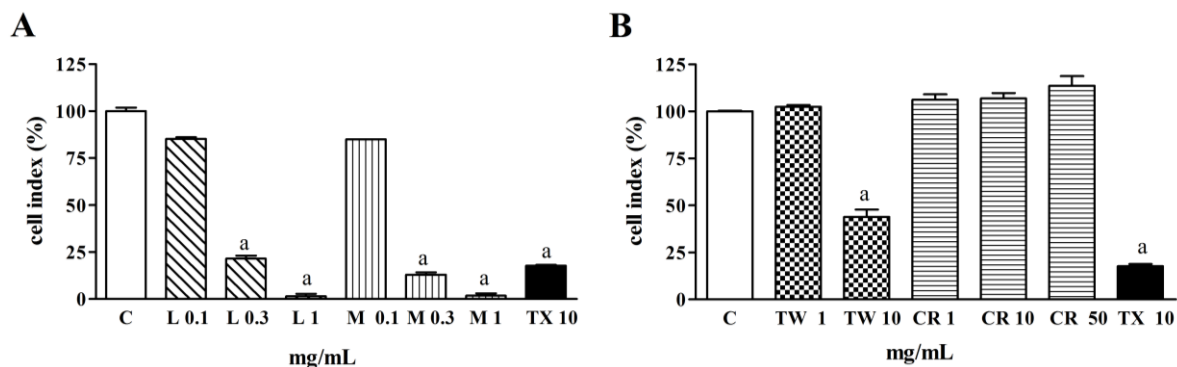


Fig. 23: Changes in cell index indicating viability of RPMI 2650 cells after 1-h treatment with sucrose esters (A) and with reference surfactants (B). a: significantly different as compared to control group, $p < 0.05$. Data are presented as mean \pm SD, $n = 4$. C, control; CR, Cremophor RH40; TW, Tween 80; L, laurate sucrose ester; M, myristate sucrose ester; TX, TritonX-100.

The effect of surfactants on the plasma membrane integrity of RPMI 2650 cells were determined by LDH release and on epithelial cell viability by MTT dye conversion assay (Fig. 24). Laurate and myristate sucrose esters increased significantly the LDH release from RPMI 2650 cells into the extracellular space in a dose-dependent way above 0.3 mg/mL concentration (Fig. 24A–B). A maximal LDH release indicating 100% toxicity was observed for both sucrose esters at 1 mg/mL dose comparable to the effect of Triton X-100. The reference surfactants Tween 80, Cremophor RH40 were non-toxic for RPMI 2650 cells under 10 mg/mL concentration for 1 h treatment period. The 4-h MTT dye conversion cell viability test, reflecting intracellular enzyme activities, and endo- and exocytosis, proved to be more sensitive than the LDH release assay. Sucrose esters over 0.03 mg/mL concentration significantly reduced the viability of RPMI 2650 cells in a dose-dependent way (Fig. 24C–D). In agreement with the findings measured by LDH release, a complete loss of cell viability could be detected at sucrose ester doses higher than 1 mg/mL, comparable to the effect of the toxicity control. In these experiments reference surfactants were toxic over 3 mg/mL concentration.

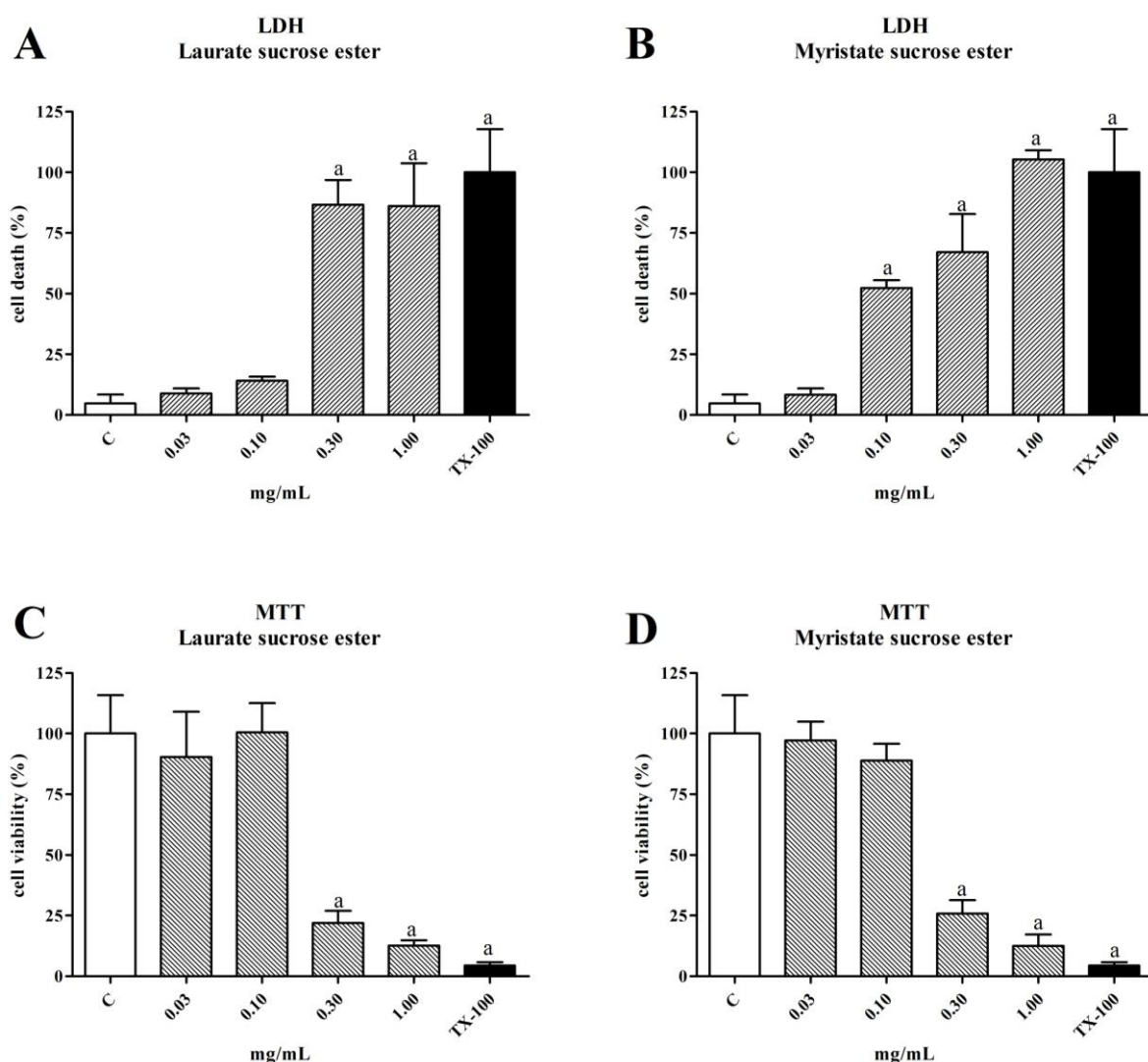


Fig. 24: Toxicity of sucrose esters on RPMI 2650 cells after 1-h treatment measured by LDH release assay (A, B) and after 4-h treatment measured by MTT reduction assay (C, D). *a*: significantly different as compared to control group. All values presented are means \pm SD, $n=8$, $p<0.05$. LDH, lactate dehydrogenase; MTT, 3-(4,5-dimethylthiazol-2-yl)-2,5-diphenyltetrazolium bromide; TX, TritonX-100.

Besides functional tests the toxicity of excipients was proved by morphological methods as well. The double fluorescent staining of nasal epithelial cell nuclei was performed after 1-h treatment of the cells with surfactants (Fig. 25). In agreement with the results of other viability assays, the toxicity of 1 mg/mL sucrose esters and 5 mg/mL Tween 80 was confirmed, while at lower concentrations no sign of cytotoxicity was detected on RPMI 2650 cells (Fig. 25). Cremophor RH40 at both 1 and 5 mg/mL concentrations had negligible effect on cell viability.

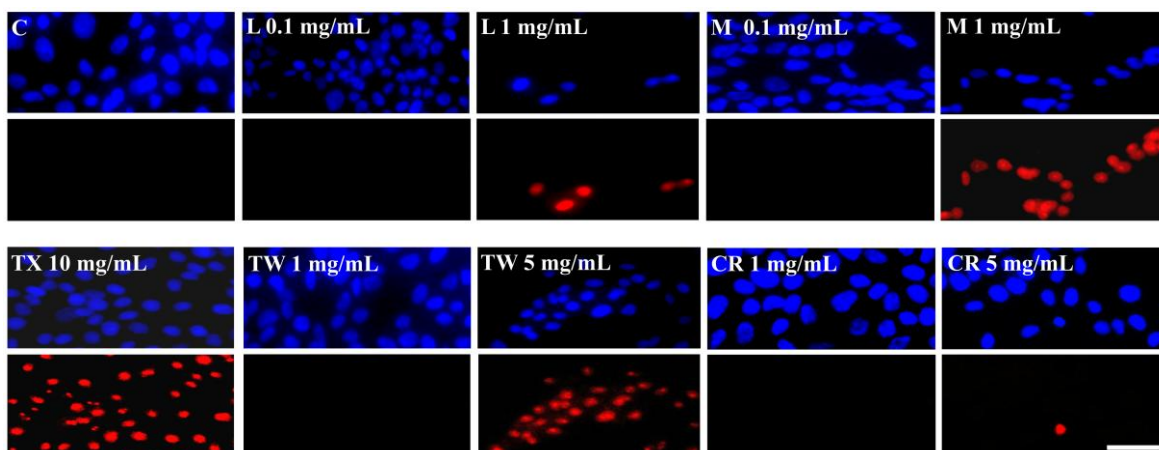


Fig. 25: Double fluorescent staining of nuclei of RPMI 2650 cells shows the cytotoxicity of excipients after 1-h treatment. Blue colour indicates cell nuclei of living and dead cells, red colour indicates cell nuclei of dead cells. C, control; CR, Cremophor RH40; L, laurate sucrose ester; M, myristate sucrose ester; TW, Tween 80; TX, TritonX-100. Bar: 30 μ m.

Results from the toxicity assays on RPMI 2650 cells for all four excipients are summarised in Table 10. The non-toxic concentrations of sucrose esters as compared to Tween 80 and Cremophor RH40 were at least one order of magnitude higher.

Table 10 Comparison of cellular toxicity of surfactants measured by different methods

Surfactant	RT-CES			LDH release assay			MTT reduction assay			Nucleus staining* 1h
	1h	4h	24h	1h			4h			
	TD 0 mg/mL	TD 0 mg/mL	TD 0 mg/mL	TD 0 mg/mL	TD 50 mg/mL	TD 100 mg/mL	TD 0 mg/mL	TD 50 mg/mL	TD 100 mg/mL	TD 0 mg/mL
Laurate SE	0.1	0.1	0.1	0.1	0.2	0.3	0.1	0.2	1.0	< 1.0
Myristate SE	0.1	0.1	<0.1	0.03	0.1	1.0	0.1	0.2	1.0	< 1.0
TW	1.0	1.0	<1.0	10.0	>100.0	>100.0	3.0	>100.0	>100.0	< 5.0
CR	>50.0	>50.0	1.0	10.0	>100.0	>100.0	3.0	60.0	>100.0	>5.0

CR, Cremophor RH40; LDH, lactate dehydrogenase; MTT, 3-[4,5-dimethylthiazol-2-yl]-2,5-diphenyl tetrazolium bromide; RT-CES, real-time cell electric sensing; SE, sucrose ester; TD 0, non-toxic dose; TD 50, dose causing 50% cellular toxicity; TD 100, dose causing 100% cellular toxicity; TW, Tween 80.

* Nucleus staining was done by fluorescent dyes bis-benzimide and ethidium-homodimer-1.

We could confirm with the cell electric sensing method, that the non-toxic dose of laurate sucrose ester was still safe after 24-h treatment period, while the non-toxic dose of Cremophor RH40 has drastically dropped to 1 mg/mL at 24 h as compared to previous time-points.

4.5. Effects of sucrose esters on epithelial barrier integrity

Sucrose esters elicited dose-dependent TEER changes (Fig. 26A–B). At 0.1 mg/mL concentrations both laurate and myristate sucrose esters led to a significant and transient TEER decrease, while 0.3 mg/mL and higher concentrations caused an irreversible drop of

TEER. Tween 80 at 10 mg/mL dose also resulted in a significant TEER decrease, while the smaller concentration, similarly to 1 and 10 mg/mL concentration of Cremophor RH40 did not cause changes as compared to control group.

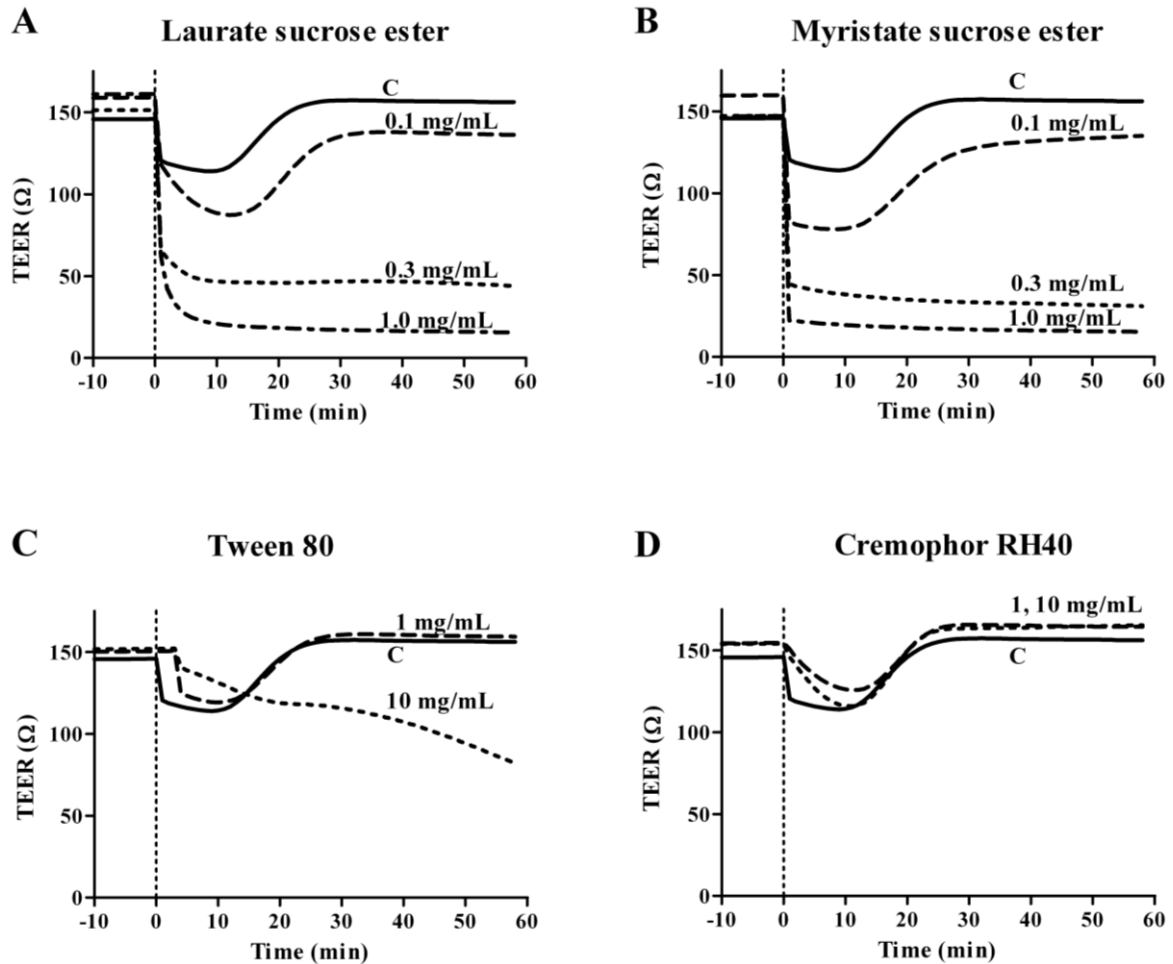


Fig. 26: Kinetics of the changes in transepithelial resistance of RPMI 2650 cells after treatment with surfactants. Broken line at 0 minutes indicates the onset of treatment. Data are presented as mean, $n=4$. C, control; TEER, transepithelial electric resistance.

By treating the confluent layers of RPMI 2650 epithelial cells with previously determined safe, non-toxic concentrations of various surfactants, permeability experiments with FITC-dextran, a hydrophilic paracellular marker with an average molecular weight of 4.4 kDa, the size of a peptide were performed. Laurate sucrose ester increased significantly the permeability of RPMI 2650 cell layers in a concentration-dependent manner (Fig. 27A). After 1-h treatment with 0.1 mg/mL laurate sucrose ester the permeability coefficient of FITC-dextran was increased by 50%.

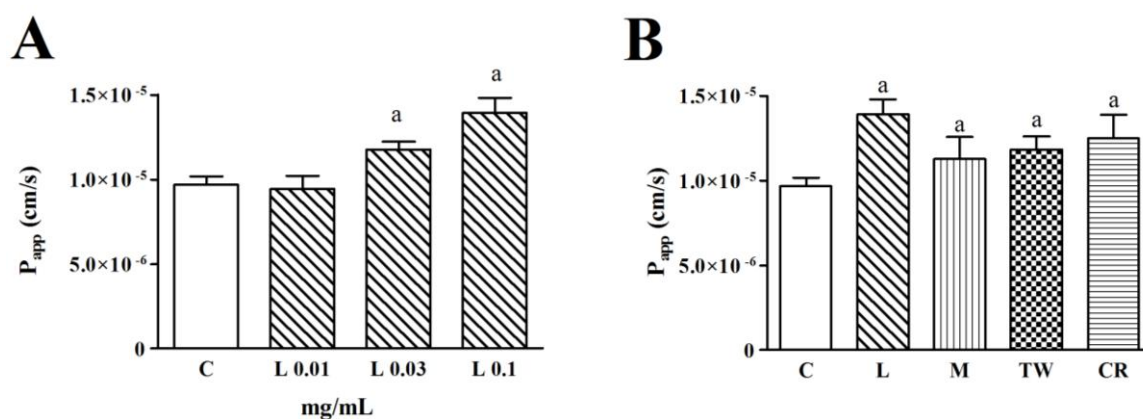


Fig. 27: The effect of non-toxic doses (0.01, 0.03, 0.1 mg/mL) of laurate sucrose ester (A) and of excipients applied in the same concentration of 0.1 mg/mL (B) on the apparent permeability coefficients of 4.4 kDa FITC-dextran on confluent RPMI 2650 cell layers. a: significantly different as compared to control group, $p < 0.05$. Data are presented as mean \pm SD, $n = 3$. C, control; CR, Cremophor RH40; L, laurate sucrose ester; M, myristate sucrose ester; TW, Tween 80; P_{app} , apparent permeability coefficient.

Comparing the effects of sucrose esters and the reference surfactants on the permeability for the marker molecule across epithelial cell layers, the same, non-toxic concentration of 0.1 mg/mL was chosen for all compounds. All excipients increased significantly the epithelial paracellular permeability; the largest increase was seen in case of laurate sucrose ester, the P_{app} values were elevated from 9.7×10^{-6} cm/s to 1.4×10^{-5} cm/s after 1-h treatment (Fig. 27B).

DISCUSSION

5.1. Meloxicam nanoparticles – Novel alternatives in pain management

MEL, a non-steroidal anti-inflammatory drug (NSAID) with analgesic properties, is an enolic acid oxicam derivative (Hanft et al., 2001; Fahmy, 2006). The aqueous solubility of MEL is poor and the rate of dissolution is low (15% in 5 min). MEL has low molecular mass and relatively well-permeable, its permeability coefficient on the Caco-2 cell model is 17.6×10^{-6} cm/s. The poor dissolution property of the drug is a limiting factor for its absorption rate and its onset of action. Its bioavailability is 89% after dissolution (Del Tacca et al., 2002). The usual recommended oral dose is 7.5–15 mg/day; a dose as high as 30 mg/day may also be applied (Euller-Ziegler et al., 2001). A parenteral formulation of MEL (15 mg/1.5 mL) has been developed for situations requiring rapid analgesia, such as acute mechanical lower back pain, sciatica and acute flares of osteoarthritis (Davies and Skjodt, 1999). The mean C_{\max} value was achieved within four to five hours after oral administration of MEL, indicating elongated drug absorption. Due to the low quantity of a single dose of MEL and the need for its rapid onset of action in the case of crisis treatment nanotechnology can offer solutions to increase its solubility and enhance the dissolution rate.

NSAIDs, including MEL, can cause serious gastrointestinal adverse events including inflammation, bleeding, ulceration, and perforation of the stomach, small intestine, or large intestine, which can be fatal (Hanft et al., 2001). Therefore nasal pathway of drug administration is preferable to reduce gastrointestinal side-effects and to circumvent the first-pass metabolism in the liver.

Multivariate problems such as MEL grinding are often optimized by using the COST approach. Each variable of the grinding process is scanned in this way, and the combination of their optimum values is accepted as the overall optimum. Unfortunately, this method is slow, since the number of necessary experiments increases considerably with the number of variables. Moreover, the COST approach can seldom find the true overall optimum of a system since it assumes that the effects of all variables are completely independent, whereas the response of a real system to change in any single parameter often appears as the overall effect of several parameter alterations, i.e. real-life multidimensional parameter spaces are seldom orthogonal. A good strategy for finding the overall optimum of a multivariate problem is to fit the response surface on the basis of the responses obtained from well-chosen parameter sets. Since the effect of any single variable can usually be accounted for by a second-order polynomial, it is customary to test

parameters at three different levels: a high, a medium and a low setting. Such designs, called three-level full factorial designs, have been applied successfully in the past to optimise the synthesis of carbon nanotubes (Kukovecz et al., 2005; Smajda et al., 2007), the deposition of titanate nanowires on glass (Daranyi et al., 2008) and the wet peroxidation of aqueous phenol solution (Melero et al., 2007). The simplest three-level full factorial design is to pick three values for one independent variable (x_1 : rotation speed), chart the three corresponding response (d : particle diameter) values in a standard two dimensional Cartesian coordinate system and fit the $d=f(x_1)$ function by a parabola. In case of two independent variables (x_1 : rotation speed and x_2 : MEL to excipient ratio) we need to sample $3 \times 3 = 9$ points in the x_1x_2 plane and chart the corresponding d values as elevation above the x_1x_2 plane in a three dimensional coordinate system.

PVP, an amorphous excipient which does not melt during the co-grinding process helped to reduce particle size and to prevent the agglomeration, as a stabiliser agent in our experiments. Our data are in accordance with the findings of other groups on PVP used in other systems (Taylor and Zografi, 1997; Watanabe et al., 2003). On the contrary, PEG is a semi-crystalline grinding additive with low melting point which could melt due to friction work. As a consequence PEG was not as efficient as PVP in the size reduction of our model drug MEL.

Ambrus et al. (2009) improved the dissolution rate of MEL with other methods, the drug was formulated in a nanosuspension by applying an emulsion-diffusion method, high pressure homogenisation or sonication. The formation of MEL nanosuspensions with a particle size of 200–900 nm was observed, the extent of MEL dissolution reached 90% in 5 min. As a comparison in our experiments in the case of the optimised co-ground product (nanoMEL/PVP) an uniform size distribution and smaller particle size of MEL was obtained.

The increased solubility and the elevated extent of dissolution of nanoMEL/PVP can be explained by (i) the reduction of the particle size, according to Ambrus et al. (2009), (ii) the increased specific surface area of the particles, according to the Noyes–Whitney equation (Noyes and Whitney, 1897), (iii) the presence of hydrophilic polymers, according to Leuner and Dressman (2000) and (iv) the loss of crystallinity of the active agent, according to the paper of Jójárt-Laczkovich and Szabó-Révész (2010). Amorphous drug nanoparticles possess a higher saturation solubility compared to equally sized drug nanocrystals in the crystalline state. Therefore, to reach the highest saturation solubility increase, a combination of nanometer size and amorphous state is ideal.

Information on toxicity is very important for pharmaceutical use of nanoparticles. *In vitro* cell culture assays are useful tools to investigate the toxicity of nanonized drugs. In comparison to animal models, cell viability assays allow for a simpler, faster and more cost-efficient assessment of toxicity. Limitation of *in vitro* test systems is the lack of the complexity of animal models or the human body. Nanoparticles can interfere with conventional end-point colorimetric *in vitro* toxicity assays due to the following reasons, (i) high adsorption capacity; (ii) optical properties; (iii) catalytic activity; (iv) acidity/alkalinity; (v) dissolution (Kroll et al., 2009). Therefore novel technologies such as marker-free, real-time assays greatly help to reveal the interaction of nanoparticles with cells. Furthermore the continuous monitoring of the biological status of the cells can be integrated in conventional medium or high-throughput plate formats (Ressler et al., 2004; Ózsvári et al., 2010). Using a real-time assay we demonstrated for the first time that the pharmaceutical composition containing nanoMEL/PVP and sodium hyaluronate is not toxic for human nasal epithelial cells. By comparing the results of RT-CES on nasal epithelial cells with other data from the epithelial toxicity of sucrose esters, the lack of change in cell index indicates that MEL nanoparticles are not toxic and do not influence the paracellular pathway through RPMI 2650 cell layers.

The *in vitro* permeability results on a synthetic membrane and the cell-based assays suggest the potential usefulness of the pharmaceutical composition containing nanoMEL/PVP for systemic nasal delivery. The higher permeability of MEL in the formulation containing nanoparticles and sodium hyaluronate may be explained by the increased solubility and the elevated extent of dissolution. Further experiments are planned to study the bioavailability and pharmacokinetics of this innovative pharmaceutical composition.

5.2. Cell culture model of nasal epithelial toxicity and permeability

Due to the importance of systemic nasal drug delivery there is a need for cell culture models of the nasal barrier for testing various compounds and pharmaceutical compositions (Dimova et al., 2005). The properties of such *in vitro* systems need to be compared with *in vivo* circumstances.

The culture conditions and applicability of RPMI 2650 cells as an epithelial model are contradictory in the literature. De Fraissinette et al. (1995) discussed the limits of the use of this cell line as an *in vitro* nasal model for drug absorption. In their experiments RPMI 2650 cells formed cell clusters on filters, although they also had tendency to spread

in a cell layer. The cells never showed cell polarization, nor microvilli or tight junctions, and were not able to form tight cell layers. In another study RPMI 2650 cells grew in multilayers, typical for the nasal epithelium, but cell polarisation and differentiation could not be detected (Schmidt et al., 1998). In contrast to the above mentioned studies, using different culture conditions including air–liquid interface RPMI 2650 cells formed layers suitable for permeability assays (Bai et al., 2008; Wengst and Reichl, 2010).

In our experiments RPMI 2650 cells grew as mono- or multilayers and reached confluence in liquid–liquid interface culture condition. The presence of intercellular junctions was confirmed by electron and immunofluorescent microscopy. Besides morphological investigations, the functional properties of the nasal epithelial barrier such as resistance and paracellular permeability were also proved. Our data are in agreement with results from other *in vitro* and *in vivo* models (Schmidt et al., 1998).

Retinoids regulate the growth and differentiation of different cell types, especially epithelial cells, mainly through interaction with nuclear retinoic acid and retinoid X receptors (Bogos et al., 2008). Although retinoic acid is crucial in the development of human airway epithelial cultures, its use as a medium supplementation is debated (Gray et al., 1996; Yoon et al., 2000). According to our observations retinoic acid had a significant effect on the barrier properties on RPMI 2650 cells, in agreement with literature data (Yoon et al., 2000). Hydrocortisone also increased the cell index of human nasal epithelial cells, in accordance with observations on the favourable effect of hydrocortisone on epithelial cells described previously (Wu et al., 1986; Van Scott et al., 1988). Hydrocortisone is a potent inducer of the formation of barrier properties in cultured endothelial cells (Perriere et al., 2007; Nakagawa et al., 2009), and the increase in the cell index of RPMI 2650 layers may be also related to the formation of a tighter barrier.

Advantages of the presented *in vitro* nasal system include simplicity of culture, reproducibility, suitability for permeability studies and RT-CES. RPMI 2650 cells model the respiratory zone of the human nasal epithelium which is the most important absorption surface for nasally administered drugs to the systemic circulation. The absence of cilia and air–liquid interface can be considered as limitations of this nasal model. The presented data support that RPMI 2650 cells can be successfully used to establish an *in vitro* model of the nasal barrier and to test toxicity and epithelial permeability.

The nasal pathway can be exploited for systemic peptide delivery due to the advantages of intranasal application (Kissel et al., 1998; Costantino et al., 2007). There are marketed pharmaceutical products for nasal systemic peptide delivery such as calcitonin

which is applied in the treatment of osteoporosis, and there is a growing interest for the nasal delivery of biologically active peptides (Sipos et al., 2010). The results of the permeability assays on RPMI 2650 cells could model the absorption of peptide-size molecules and nanoparticles, and proves the usefulness of the model as a test system.

5.3. Permeability enhancers – Risks and benefits

Sucrose esters are widely used in the cosmetic and food industry. Due to their advantageous properties as emulsifiers, solubilisers and permeation enhancers, the potential of sucrose esters to be used as pharmaceutical excipients has been investigated recently (Csóka et al., 2007; Szűts et al., 2007, 2008, 2011). The applicability of surface active agents as permeability enhancers is limited by their toxicity (Deli, 2009), therefore it is essential to determine their safe, non-toxic concentrations.

The toxicity of sucrose esters was tested for the first time in an *in vitro* model of the nasal barrier. Four different independent methods were used to measure cell viability, a label-free, real-time cell electric sensing technique, two colorimetric methods, LDH release and MTT conversion tests, and finally a morphological method, cell nucleus staining. Colorimetric methods are advisable only for the preliminary phase of a cell death study (Weyermann et al., 2005; Galluzzi et al., 2009; Fernández Freire et al., 2009). These assays suffer from several drawbacks, they are endpoint determinations, and higher concentrations of surfactants may interfere with the detection method (Weyermann et al., 2005). In our experiments the highest non-toxic concentrations of reference surfactants were determined by LDH release assay. This result might be due either to the interference of the excipients with the enzyme reaction or to their inability to affect cellular plasma membrane. The MTT test was more sensitive, and lower concentrations of excipients were found non-toxic. The increased sensitivity might be related not only to the longer assay time but also to the higher complexity of the MTT reduction where several cellular processes are involved (Liu et al., 1997). The nucleus staining method was suitable for the morphological confirmation of the toxic concentrations of the excipients, but could not provide kinetic data and exact determination of the non-toxic or toxic doses.

Due to the limitations mentioned above we have used a technological approach that provides kinetic measurement in cell-based assays (Ózsvári et al., 2010). The real-time cell electric sensing technology monitors cell viability status in a simple homogeneous assay format over a broad time frame, from minutes to several days. It is a non-invasive, highly sensitive measurement and has a reduced interference with normal cell function (Solly et

al., 2004; Boyd et al., 2008). This method was the most sensitive to determine the safe concentrations of the excipients at different incubation times. It is noteworthy that the difference between the non-toxic concentrations of sucrose esters and reference molecules dropped drastically after 24-h treatment. The epithelial cell viability at non-toxic doses of sucrose esters remained constant. In contrast the toxicity of Cremophor RH40 and Tween 80 increased over time, which might indicate *in vivo* toxicity after longer treatment.

By applying various toxicity assays our results indicate that sucrose esters are more toxic than reference surfactants, especially for shorter incubation times in cultured cells. However, this difference significantly decreased when cells were examined with real-time monitoring for 24 h. In oral preparations the cellular toxicity of excipients can be diminished by dilution in the gastrointestinal fluids, in addition sucrose esters are hydrolysed and absorbed as sucrose and individual fatty acids in the gastrointestinal tract (Noker et al., 1997). In the nasal mucous membrane, considerable dilution cannot be expected and the mucosa is more sensitive. The enzymatic degradation of sucrose esters is unknown. Therefore, the safe concentrations of excipients determined by cellular assays need to be taken into consideration at the formulation process of nasal vehicles.

Sucrose esters can be used as potential permeability enhancers. Real-time electric sensing provided quantitative information about the biological status of RPMI 2650 human nasal epithelial cells, including cell number, viability, and adherence indicating paracellular permeability. Sucrose esters had a dose-dependent effect on epithelial permeability in non-toxic concentration range. A transient effect on the resistance of RPMI 2650 cell layers has been observed, which was unique for sucrose esters. Although these novel excipients were not found to be more effective permeability enhancers than the reference compounds, their effect on paracellular permeability of cultured human epithelial cells have been demonstrated for the first time. The increase in paracellular permeability elicited by the non-toxic concentrations of sucrose esters might be related to their effect on intercellular junctions. No LDH release was detected at these concentrations indicating an intact plasma membrane integrity. While *in vitro* cytotoxicity correlated with the paracellular permeability on Caco-2 cells (Konsoula and Barile, 2005), in the present experiments the tested excipients modified paracellular permeability at non-toxic concentrations. To reveal the mechanism of action of sucrose esters further experiments are necessary.

5.4. Significance, pharmaceutical relevance

The results presented in the thesis provide information on the evaluation of an investigational protocol to screen novel formulations like drug nanoparticles, innovative excipient such as sucrose esters and new pharmaceutical compositions (Fig. 4). The following practical conclusions can be drawn from the experimental data summarized in the thesis:

- (i) The critical parameters of the co-grinding process have been optimised as a result of the factorial experiment design.
- (ii) NanoMEL/PVP drug nanoparticles have increased solubility and faster dissolution rate in physiological conditions.
- (iii) Human RPMI 2650 nasal epithelial cells were successfully used to screen cytotoxicity and permeability of pharmaceutical compounds.
- (iv) NanoMEL/PVP drug nanoparticles showed no toxicity but enhanced permeability in nasal epithelial cells indicating safe and efficient application in nasal formulations.
- (v) Sucrose esters can alter paracellular permeability of nasal epithelial cells without toxic effects.

Biopharmaceutical studies including bioavailability experiments are needed to test nasal formulations. Before preclinical testing on animals, it is reasonable to screen drug candidates with respect to their permeability through the nasal mucosa and epithelial toxicity by using *in vitro* models. The presented *in vitro* nasal epithelial model could be applicable to test the toxicity and permeability of pharmaceutical formulations and excipients.

New formulations for systemic nasal drug delivery, like nanoparticles, need to be tested for nasal cytotoxicity, toxicokinetics and epithelial permeability. Novel excipients of nasal compositions also need to be investigated for epithelial toxicity and permeability on *in vitro* nasal models, similarly to the application of the widely used Caco-2 model for testing oral formulations.

The relevance of the presented nasal investigational protocol needs to be confirmed in preclinical tests in the future. Our findings may contribute to the development of new pharmaceutical compositions and better screening systems for nasal drug delivery of pharmacons.

6. SUMMARY

Novel sites of drug administration for systemic delivery and novel formulations offer numerous opportunities to develop innovative pharmaceutical compositions. The nasal pathway represents an alternative route for non-invasive systemic administration of drugs, although the nasal epithelium forms a restricting barrier. Nanonization of drugs is a great possibility to increase solubility and to augment permeability through mucosal barriers. Pharmaceutical excipients may help to increase the solubility of active agents and enhance the permeability of molecules with larger molecular mass like peptides via the modulation of the paracellular pathway.

An *in vitro* investigational protocol have been established to produce, characterize and screen innovative pharmaceutical solutions, namely meloxicam drug nanoparticles and sucrose esters, novel biodegradable non-ionic surface active excipients to enhance nasal drug delivery. Both conventional investigational methods of pharmaceutical technology and cell-based assays have been used.

Using meloxicam as a model drug and polyvinylpyrrolidone as an excipient nanoparticles have been successfully produced by a co-grinding process optimized in a factorial experimental design. The physicochemical properties of these amorphous drug nanoparticles were favourable as compared to physical mixture. Increased solubility, enhanced extent of dissolution and *in vitro* permeability were found which are crucial parameters for nasal delivery. A human nasal epithelial cell culture model was established, characterized and optimized by morphological and functional methods. This model based on RPMI 2650 cells was applied for toxicity and permeability measurements. Nanonization resulted in enhanced permeability for meloxicam across epithelial cell layers without cellular toxicity and damage to barrier integrity. Sucrose esters at low doses altered paracellular permeability for a peptide-sized marker molecule of nasal epithelial cells without toxic effects.

The presented nasal investigational protocol may contribute to the development of new pharmaceutical compositions and better screening systems for nasal delivery of pharmacons.

7. REFERENCES

- Abramoff, M.D., Magelhaes, P.J., Ram, S.J., 2004. Image Processing with ImageJ. *Biophotonics International* 11, 36–42.
- Alkebro, J., BeHgin-Colin, S., Mocellin, A., Warren, R., 2002. Modeling high-energy ball milling in the alumina-yttria system. *Journal of Solid State Chemistry* 164, 88–97.
- Alpar, H.O., Somavarapu, S., Atuah, K.N., Bramwell, V.W., 2005. Biodegradable mucoadhesive particulates for nasal and pulmonary antigen and DNA delivery. *Advanced Drug Delivery Reviews* 57, 411–430.
- Ambrus, R., Kocbek, P., Kristl, J., Sibanc, R., Rajkó, R., Szabó-Révész, P., 2009. Investigation of preparation parameters to improve the dissolution of poorly water-soluble meloxicam. *International Journal of Pharmaceutics* 381, 153–159.
- Arechabala, B., Coiffard, C., Rivalland, P., Coiffard, L.J., de Roeck-Holtzhauer, Y., 1999. Comparison of cytotoxicity of various surfactants tested on normal human fibroblast cultures using the neutral red test, MTT assay and LDH release. *Journal of Applied Toxicology* 19, 163–165.
- Arora, P., Sharma, S., Garg S., 2002. Permeability issues in nasal drug delivery. *Drug Discovery Today* 7, 967–975.
- Bai, S., Yang, T., Abbruscato, T.J., Ahsan, F., 2008. Evaluation of human nasal RPMI 2650 cells grown at an air–liquid interface as a model for nasal drug transport studies. *Journal of Pharmaceutical Sciences* 97, 1165–1178.
- Barzegar-Jalali, M., Valizadeh, H., Siahi Shadbad, M.R., Adibkia, K., Mohammadi, G., Farahani, A., Arash, Z., Nokhodchi, A., 2010. Cogrounding as an approach to enhance dissolution rate of a poorly water-soluble drug (gliclazide). *Powder Technology* 197, 150–158.
- Behl, C.R., Pimplaskar, H.K., Sileno, A.P., Xia, W.J., Gries, W.J., deMeireles, J.C., 1998. Optimization of systemic nasal drug delivery with pharmaceutical excipients. *Advanced Drug Delivery Reviews* 29, 117–133.
- Bogos, K., Renyi-Vamos, F., Kovacs, G., Tovari, J., Dome, B., 2008. Role of retinoic receptors in lung carcinogenesis. *Journal of Experimental Clinical Cancer Research* 27, 18–24.
- Bonferoni, M.C., Giunchedi, P., Scalia, S., Rossi, S., Sandri, G., Caramella, C., 2006. Chitosan gels for the vaginal delivery of lactic acid: relevance of formulation parameters to mucoadhesion and release mechanisms. *AAPS PharmSciTech* 7, 141–147.
- Boyd, J.M., Huang, L., Xie, L., Moe, B., Gabos, S., Li, X.F., 2008. A cell–microelectronic sensing technique for profiling cytotoxicity of chemicals. *Analalytica Chimica Acta* 615, 80–87.
- Chattopadhyay, P.P., Manna, I., Talapatra, S., Pabi, S.K., 2001. A mathematical analysis of milling mechanics in a planetary ball mill. *Materials Chemistry and Physics* 68, 85–94.
- Chien, Y.W., Su, K.S.E., Chang, S., 1992. *Nasal systemic drug delivery*. Informa Healthcare Inc., New York.
- Cho, K.Y., Chung, T.W., Kim, B.C., Kim, M.K., Lee, J.H., Wee, W.R., Cho, C.S., 2003. Release of ciprofloxacin from poloxamer-graft-hyaluronic acid hydrogels *in vitro*. *International Journal of Pharmaceutics* 260, 83–91.
- Costantino, H.R., Illum, L., Brandt, G., Johnson, P.H., Quay, S.C., 2007. Intranasal delivery: Physicochemical and therapeutic aspects. *International Journal of Pharmaceutics* 337, 1–24.
- Csáki, K.F., 2011. Synthetic surfactant food additives can cause intestinal barrier dysfunction. *Medical Hypotheses* 76, 676–681.
- Csóka, G., Marton, S., Zelkó, R., Otomo, N., Antal, I., 2007. Application of sucrose fatty acid esters in transdermal therapeutic systems. *European Journal of Pharmaceutics Biopharmaceutics* 65, 233–237.

- Csóka, I., Csányi, E., Zapantis, G., Nagy, E.; Féher-Kiss, A., Horváth, G. Blazsó, G., Erős, I., 2005. *In vitro* and *in vivo* percutaneous absorption of topical dosage forms: case studies. *International Journal of Pharmaceutics* 291, 11–19.
- Daranyi, M., Kukovecz, Á., Horváth, E., Kónya, Z., Kiricsi, I., 2008. Fine tuning the coverage of a titanate nanowire layer on a glass substrate. *Chemical Physics Letters* 460, 191–195.
- Davies, N.M., Skjodt, N.M., 1999. Clinical pharmacokinetics of meloxicam. A cyclo-oxygenase-2 preferential nonsteroidal anti-inflammatory drug. *Clinical Pharmacokinetics* 36, 115–26.
- Davis, S.S., Illum, L., 2003. Absorption enhancers for nasal drug delivery. *Clinical Pharmacokinetics* 42, 1107–1128.
- De Fraissinette, A., Brun, R., Felix, H., Vonderscher, J., Rummelt, A., 1995. Evaluation of the human cell line RPMI 2650 as an *in vitro* nasal model. *Rhinology* 33, 194–198.
- Dehghan, M.H.G., Jafar, M., 2006. Improving dissolution of meloxicam using solid dispersions. *Iranian Journal of Pharmaceutical Research* 4, 231–238.
- Delagrammatikas, G., Delagrammatikas, M., Tsimas, S., 2007. Particle size distributions a new approach. *Powder Technology* 176, 57–65.
- Deli, M.A., 2009. Potential use of tight junction modulators to reversibly open membranous barriers and improve drug delivery. *Biochimica et Biophysica Acta* 1788, 892–910.
- Del Tacca, M., Colucci, R., Fornai, M., Blandizzi, C., 2002. Efficacy and tolerability of meloxicam, a COX-2 preferential nonsteroidal antiinflammatory drug: a review. *Clinical Drug Investigation* 22, 799–818.
- Dimova, S., Brewster, M.E., Noppe, M., Jorissen, M., Augustijns, P., 2005. The use of human nasal *in vitro* cell systems during drug discovery and development. *Toxicology in Vitro* 19, 107–122.
- Euller-Ziegler, L., Velicitat, P., Bluhmki, E., Türck, D., Scheuerer, S., Combe, B., 2001. Meloxicam: a review of its pharmacokinetics, efficacy and tolerability following intramuscular administration. *Inflammation research*. 50, Suppl. 1, 5–9.
- Fahmy, M., 2006. Ca-alginate beads loaded with meloxicam: effect of alginate chemical composition on the properties of the beads and ulcerogenicity of the drug. *Journal of Drug Delivery Science and Technology* 16, 183–189.
- Fernández Freire, P., Peropadre, A., Pérez Martín, J.M., Herrero, O., Hazen, M.J., 2009. An integrated cellular model to evaluate cytotoxic effects in mammalian cell lines. *Toxicology in Vitro* 23, 1553–1558.
- Foltmann, H., Quadir, A., 2008. Polyvinylpyrrolidone (PVP) – one of the most widely used excipients in pharmaceuticals: an overview. *Drug Delivery Today* 8, 22–27.
- Galluzzi, L. et al., 2009. Guidelines for the use and interpretation of assays for monitoring cell death in higher eukaryotes. *Cell Death and Differentiation* 16, 1093–1107.
- Garti, N., Aserin, A., Fanun, M., 2000. Non-ionic sucrose esters microemulsions for food applications. Part 1. Water solubilization. *Colloids and Surfaces A* 164, 27–38.
- Gray, T.E., Guzman, K., Davis, C.W., Abdullah, L.H., Nettesheim, P., 1996. Mucociliary differentiation of serially passaged normal human tracheobronchial epithelial cells. *American Journal of Respiratory Cellular and Molecular Biology* 14, 104–112.
- Hanft, G., Turck, D., Scheuerer, S., Sigmund, R., 2001. Meloxicam oral suspension: a treatment alternative to solid meloxicam formulations. *Inflammation Research* 50, 35–37.
- Horvát, S., Fehér, A., Wolburg, H., Sipos, P., Veszélka, S., Tóth, A., Kis, L., Kurunczi, A., Balogh, G., Kürti, L., Erős, I., Szabó-Révész, P., Deli M.A., 2009. Sodium hyaluronate as a mucoadhesive component in nasal formulation enhances delivery of molecules to brain tissue. *European Journal of Pharmaceutics and Biopharmaceutics* 72, 252–259.
- Illum, L., 2003. Nasal drug delivery: possibilities, problems and solutions. *Journal of Controlled Release* 87, 187–198.

- Jafar, M., Dehgan, M.H.G., Shareef, A., 2010. Enhancement of dissolution and antiinflammatory effect of meloxicam using solid dispersions. *International Journal of Applied Pharmaceutics* 2, 22–27.
- Jórárt-Laczkovich, O., Szabó-Révész, P., 2010. Amorphization of a crystalline active pharmaceutical ingredient and thermoanalytical measurements on this glassy form. *Journal of Thermal Analysis and Calorimetry* 102, 243–247.
- Junghaus, J.-U.A.H., Müller, R.H., 2008. Nanocrystal technology, drug delivery and clinical applications. *International Journal of Nanomedicine* 3, 295–309.
- Kissel, T., Werner, U., 1998. Nasal delivery of peptides: an *in vitro* cell culture model for the investigation of transport and metabolism in human nasal epithelium. *Journal of Controlled Release* 53, 195–203.
- Konsoula, R., Barile, F.A., 2005. Correlation of *in vitro* cytotoxicity with paracellular permeability in Caco-2 cells. *Toxicology in Vitro* 19, 675–684.
- Kroll, A., Pillukat, M.H., Hahn, D., Schneckeburger, J., 2009. Current *in vitro* methods in nanoparticle risk assessment: Limitations and challenges. *European Journal of Pharmaceutics and Biopharmaceutics* 72, 370–377.
- Kukovecz, Á., Méhn, D., Nemes-Nagy, E., Szabó, R., Kiricsi, I., 2005. Optimization of CCVD synthesis conditions for single-wall carbon nanotubes by statistical design of experiments (DoE). *Carbon* 43, 2842–2849.
- Leuner, C., Dressman, J., 2000. Improving drug solubility for oral delivery using solid dispersions. *European Journal of Pharmaceutics and Biopharmaceutics* 50, 47–60.
- Liao, Y.H., Jones, S.A., Forbes, B., Martin, G.P., Brown, M.B., 2005. Hyaluronan: pharmaceutical characterization and drug delivery. *Drug Delivery* 12, 327–342.
- Lim, S.T., Martin, G.P., Berry, D.J., Brown, M.B., 2000. Preparation and evaluation of the *in vitro* drug release properties and mucoadhesion of novel microspheres of hyaluronic acid and chitosan. *Journal of Controlled Release* 66, 281–292.
- Lin, H., Yoo, J.W., Roh, H.J., Lee, M.K., Chung, S.J., Shim, C.K., Kim, D.D., 2005. Transport of anti-allergic drugs across the passage cultured human nasal epithelial cell monolayer. *European Journal of Pharmaceutical Sciences* 26, 203–210.
- Liu, Y., Peterson, D.A., Kimura, H., Schubert, D., 1997. Mechanism of cellular 3-(4,5-dimethylthiazol-2-yl)-2,5-diphenyltetrazolium bromide (MTT) reduction. *Journal of Neurochemistry* 69, 581–593.
- Ludwig, A., 2005. The use of mucoadhesive polymers in ocular drug delivery. *Advanced Drug Delivery Reviews* 57, 1595–1639.
- MacDonald, C., Lyzenga, W., Shao, D., Agu, U. R., 2010. Water-soluble organic solubilizers for *in vitro* drug delivery studies with respiratory epithelial cells: Selection based on various toxicity indicators. *Drug Delivery* 17, 434–442.
- Makai, A., Csányi, E., Németh, Z., Pálkás, J., Erős, I., 2003. Structure and drug release of lamellar liquid crystals containing glycerol. *International Journal of Pharmaceutics* 256, 95–107.
- Melero, J.A., Calleja, G., Martinez, F., Molina, R., Pariente, M.I., 2007. Nanocomposite Fe₂O₃/SBA-15: an efficient and stable catalyst for the catalytic wet peroxidation of phenolic aqueous solutions. *Chemical Engineering Journal* 131, 245–256.
- Moll, R., Krepiere, R., Franke, W.W., 1983. Complex cytokeratin polypeptide patterns observed in certain human carcinomas. *Differentiation* 23, 256–269.
- Moore, G.E., Sandberg, A.A., 1964. Studies of a human tumor cell line with a diploid karyotype. *Cancer* 17, 170–175.
- Moorhead, P.S., 1965. Human tumor cell line with a quasi-diploid karyotype (RPMI 2650). *Experimental Cell Research* 39, 190–196.

- Morgen, M., Bloom, C., Beyerinck, R., Bello, A., Song, W., Wilkinson, K., Steenwyk, R., Shamblin, S., 2012. Polymeric nanoparticles for increased oral bioavailability and rapid absorption using celecoxib as a model of a low-solubility, high-permeability drug. *Pharmaceutical Research* 29, 427–440.
- Moribe, K., Pongpeerapat, A., Tozuka, Y., Yamamoto, K., 2006. Drug nanoparticle formation from drug/HPMC/SDS ternary ground mixtures. *Pharmazie* 61, 97–101.
- Miyazaki, T., Miyauchi, S., Nakamura, T., Takeshita, S., Horie, K., 1996. The effect of sodium hyaluronate on the growth of rabbit corneal epithelial cells *in vitro*. *Journal of ocular pharmacology and therapeutics* 12, 409–415.
- Nakagawa, S., Deli, M.A., Kawaguchi, H., Shimizudani, T., Shimono, T., Kittel, Á., Tanaka, K., Niwa, M., 2009. A new blood–brain barrier model using primary rat brain endothelial cells, pericytes and astrocytes. *Neurochemistry International* 54, 253–263.
- Noker, P.E., Lin, T.H., Hill, D.L., Shigeoka, T., 1997. Metabolism of ¹⁴C-labelled sucrose esters of stearic acid in rats. *Food and Chemical Toxicology* 35, 589–595.
- Noyes, A., Whitney, W., 1897. The rate of solution of solid substances in their own solutions. *Journal of the American Chemical Society* 19, 930–934.
- Ózsvári, B., Puskás, G.L., Nagy, L.I., Kanizsai, I., Gyuris, M., Madácsi, R., Fehér, L.Z., Gerő, D., Szabó, Cs., 2010. A cell-microelectronic sensing technique for the screening of cytoprotective compounds. *International Journal of Molecular Medicine* 25, 525–530.
- Perrière, N., Yousif, S., Cazaubon, S., Chaverot, N., Bourasset, F., Cisternino, S., Declèves, X., Hori, S., Terasaki, T., Deli, M.A., Scherrmann, J.M., Temsamani, J., Roux, F., Couraud, P.O., 2007. A functional *in vitro* model of rat blood-brain barrier for molecular analysis of efflux transporters. *Brain Research* 1150, 1–13.
- Prestwich, G.D., Vercruysse, K.P., 1998. Therapeutic application of hyaluronic acid and hyaluronan derivatives. *Pharmaceutical Science & Technology Today* 1, 42–43.
- Rabinow, B.E., 2004. Nanosuspensions in drug delivery. *Nature Reviews Drug Discovery* 3, 785–796.
- Raval, A.J., Patel, M.M., 2011. Preparation and characterization of nanoparticles for solubility and dissolution rate enhancement of meloxicam. *International Research Journal of Pharmaceuticals* 1/2.
- Rawat, M., Singh, D., Saraf, S., 2006. Nanocarriers: promising vehicle for bioactive drugs. *Biological and Pharmaceutical Bulletin* 29, 1790–1798.
- Remias, R., Kukovecz, Á., Daranyi, M., Kozma, G., Varga, S., Kónya, Z., Kiricsi, I., 2009. Zn-glycerolate microstacks. *European Journal of Inorganic Chemistry* 24, 3622–3627.
- Resch, M.D., Resch, B.E., Csizmazia, E., Imre, L., Németh, J., Révész, P., Csányi, E., 2010. Permeability of human amniotic membrane to ofloxacin *in vitro*. *Investigative Ophthalmology and Visual Science* 51, 1024–1027.
- Ressler, J., Grothe, H., Motrescu, E., Wolf, B., 2004. New concepts for chip-supported multi-well-plates: realization of a 24-well-plate with integrated impedancesensors for functional cellular screening applications and automated microscope aided cell-based assays. *Conf. Proc. IEEE Eng. Med. Biol. Soc.* 3, 2074–2077.
- Schiller, J., Volpi, N., Hrabárová, E., Soltés, L., 2011. Hyaluronic acid: a natural biopolymer, in: Kalia, S., Avérous, L. (Eds.), *Biopolymers: Biomedical and Environmental Applications*. Scrivener Publishing LLC, Massachusetts, pp. 3–34.
- Schmidt, M.C., Peter, H., Lang, S.R., Ditzinger, G., Merkle, H.P., 1998. *In vitro* cell models to study nasal mucosal permeability and metabolism. *Advanced Drug Delivery Reviews* 29, 51–79.
- Shakhtshneider, T.P., Vasilchenko, M.A., Politov, A.A., Boldyrev, V.V., 1996. The mechanochemical preparation of solid disperse systems of ibuprofen-polyethylene glycol, *International Journal of Pharmaceutics* 130, 25–32.

- Shegokar, R., Müller, R.H., 2010. Nanocrystals: Industrially feasible multifunctional formulation technology for poorly soluble actives. *International Journal of Pharmaceutics* 399, 129–139.
- Siewert, M., Dressman, J., Brown, C.K., Shah, V.P., 2003. FIP/AAPS Guidelines to dissolution/*in vitro* release testing of novel/special dosage forms. *AAPS PharmSciTech* 4, 1–10.
- Sipos, E., Kurunczi, A., Fehér, A., Penke, Z., Fülöp, L., Kasza, Á., Horváth, J., Horvát, S., Veszelka, S., Balogh, G., Kürti, L., Erős, I., Szabó-Révész, P., Párducz, Á., Penke, B., Deli, M.A., 2010. Intranasal delivery of human beta-amyloid peptide in rats: effective brain targeting. *Cellular and Molecular Neurobiology* 30, 405–413.
- Smajda, R., Kukovecz, Á., Kónya, Z., Kiricsi, I., 2007. Structure and gas permeability of multi-wall carbon nanotube buckypapers. *Carbon* 45, 1176–1184.
- Solly, K., Wang, X., Xu, X., Strulovici, B., Zheng, W., 2004. Application of real-time cell electronic sensing (RT-CES) technology to cell-based assays. *Assay and Drug Development Technology* 2, 363–372.
- Sugimoto, M., Okagaki, T.S., Narisawa, S., Koida, Y., Nakajima, K., 1998. Improvement of dissolution characteristics and bioavailability of poorly water-soluble drugs by novel cogrinding method using water-soluble polymer. *International Journal of Pharmaceutics* 160, 11–19.
- Szűts, A., Pallagi, E., Regdon jr., G., Aigner, Z., Szabó-Révész, P., 2007. Study of thermal behaviour of sugar esters. *International Journal of Pharmaceutics* 336, 199–207.
- Szűts, A., Makai, Zs., Rajkó, R., Szabó-Révész, P., 2008. Study of the effects of drugs on the structures of sucrose esters, the effects of solid-state interactions on drug release. *Journal of Pharmaceutical and Biomedical Analysis* 48, 1136–1142.
- Szűts, A., Láng, P., Ambrus, R., Kiss, L., Deli, M.A., Szabó-Révész, P., 2011. Applicability of sucrose laurate as surfactant in solid dispersions prepared by melt technology. *International Journal of Pharmaceutics* 410, 107–110.
- Taylor, L.S., Zografi, G., 1997. Spectroscopic characterization of interactions between PVP and indomethacin in amorphous molecular dispersion. *Pharmaceutical Research* 14, 1691–1698.
- Tozuka, Y., Imono, M., Uchiyama, H., Takeuchi, H., 2011. A novel application of α -glucosyl hesperidin for nanoparticle formation of active pharmaceutical ingredients by dry grinding. *European Journal of Pharmaceutics and Biopharmaceutics* 79, 559–65.
- Ugwoke, M.I., Verbeke, N., Kinget, R., 2001. The biopharmaceutical aspects of nasal mucoadhesive drug delivery. *Journal of Pharmacy and Pharmacology* 53, 3–22.
- Ugwoke, M.I., Agu, R.U., Verbeke, N., Kinget, R., 2005. Nasal mucoadhesive drug delivery: background, applications, trends and future perspectives. *Advanced Drug Delivery Reviews* 57, 1640–1665.
- Van Scott, M.R., Lee, N.P., Yankaskas, J.R., Boucher, R.C., 1988. Effect of hormones on growth and function of cultured canine tracheal epithelial cells. *American Journal of Physiology* 255, 237–245.
- Vegt, O., Vromans, H., Toonder, J., Maarschalk, J.V., 2009. Influence of flaws and crystal properties on particle fracture in a jet mill. *Powder Technology* 191, 72–77.
- Vogt, M., Kunath, K., Dressman, J.B., 2008. Dissolution improvement of four poorly water soluble drugs by cogrinding with commonly used excipients. *European Journal of Pharmaceutics and Biopharmaceutics* 68, 330–337.
- Wade, A., Weller, P.J., 1994. *Handbook of Pharmaceutical Excipients*, Second Edition, American Pharmaceutical Association, The Pharmaceutical Press, 375–378.
- Wanawongthai, C., Pongpeerapat, A., Higashi, K., Tozuka, Y., Moribe, K., Yamamoto, K., 2009. Nanoparticle formation from probucol/PVP/sodium alkyl sulfate co-ground mixture. *International Journal of Pharmaceutics* 376, 169–75.
- Wang, S., Chow, M.S.S., Zuo, Z., 2011. An approach for rapid development of nasal delivery of analgesics – Identification of relevant features, *in vitro* screening and *in vivo* verification. *International Journal of Pharmaceutics* 420, 43–50.

- Watanabe, T., Hasegawa, S., Wakiyama, N., Kusai, A., Senna, M., 2003. Comparison between polyvinylpyrrolidone and silica nanoparticles as carriers for indomethacin in a solid state dispersion. *International Journal of Pharmaceutics* 250, 283–286.
- Wengst, A., Reichl, S. 2010. RPMI 2650 epithelial model and three-dimensional reconstructed human nasal mucosa as *in vitro* models for nasal permeation studies. *European Journal of Pharmaceutics and Biopharmaceutics* 74, 290–297.
- Werner, U., Kissel, T., 1996. *In vitro* cell culture models of the nasal epithelium: a comparative histochemical investigation of their suitability for drug transport studies. *Pharmaceutical Research* 13, 978–988.
- Weyermann, J., Lochmann, D., Zimmer, A., 2005. A practical note on the use of cytotoxicity assays. *International Journal of Pharmaceutics* 288, 369–376.
- Wolburg, H., Wolburg-Buchholz, K., Sam, K., Horvát, S., Deli, M.A., Mack, A.F., 2008. Epithelial and endothelial barriers in the olfactory region of the nasal cavity of the rat. *Histochemistry and Cell Biology* 130, 127–140.
- Wu, R., Sato, G.H., Whitcutt, M.J., 1986. Developing differentiated epithelial cell cultures: airway epithelial cells. *Fundamental and Applied Toxicology* 6, 580–590.
- Xia, M., Huang, R., Witt, L.K., Southall, N., Fostel, J., Cho, M.H., Jadhav, A., Smith, C.S., Inglese, J., Portier, C.J., Tice, R.R., Austin, C.P., 2008. Compound cytotoxicity profiling using quantitative high-throughput screening. *Environmental Health Perspectives* 116, 284–291.
- Xing, J.Z., Zhu L., Gabos, S., Xie, L., 2005. Microelectronic cell sensor assay for detection of cytotoxicity and prediction of acute toxicity. *Toxicology in Vitro* 20, 995–1004.
- Yoon, J.H., Kim, K.S., Kim, S.S., Lee, J.G., Park, I.Y., 2000. Secretory differentiation of serially passaged normal human nasal epithelial cells by retinoic acid: expression of mucin and lysozyme. *Annual Otology, Rhinology, Laryngology* 109, 594–601.
- Youdim, K.A., Avdeef, A., Abbott, N.J., 2003. *In vitro* trans-monolayer permeability calculations: often forgotten assumptions. *Drug Discovery Today* 8, 997–1003.
- Zapata-Massot, C., Frances, C., Le Bolay, N., 2004. On the use of scanning electron microscopy for the modelling of co-grinding kinetics in a tumbling ball mill. *Powder Technology* 143, 215–229.

ACKNOWLEDGEMENTS

I am grateful to my supervisors **Prof. Dr. Piroska Révész** and **Dr. Mária Deli** for their scientific guidance, encouragement and support throughout my Ph.D. studies.

I am thankful to Dr. Rita Ambrus, Alexandra Bocsik, Dr. András Fehér, Lóránd Kiss, Dr. Szilvia Veszélka and Fruzsina Walter for their inspiring help in my studies.

I would like to thank Ngo Thi Khue Dung, Klára Kovács and Zoltánné Lakatos for the excellent technical assistance.

We are indebted to all cooperating partners, namely Dr. Ágnes Kittel for the electron microscopy; Dr. Ákos Kukovecz and Gábor Kozma for the preparation of meloxicam nanoparticles and the optimization of the co-grinding process of meloxicam; Dr. László Puskás and Dr. Béla Ózsvári for the real-time cell microelectronic sensing; Dr. Erzsébet Csányi and Dr. Eszter Csizmazia for the Franz cell diffusion experiments.

Finally, I am especially thankful to my family for their love and untiring support during my studies.

Financial support

The research was supported by grants from the Project named „TÁMOP-4.2.1/B-09/1/KONV-2010-0005 – Creating the Center of Excellence at the University of Szeged” is supported by the European Union and co-financed by the European Regional Development Fund; the Foundation of Gedeon Richter and the Hungarian Research Fund (OTKA-NNF 78920 project).

APPENDIX

PUBLICATION I.

TOVÁBBKÉPZŐ KÖZLEMÉNYEK

Gyógyszerészet 53. 67-73. 2009.

Intranazális gyógyszerbevitel újabb lehetőségei szisztémás hatás elérése céljából

Kürti Levente¹, dr. Deli Mária², Szabóné dr. Révész Piroska¹

1. Bevezetés

Biofarmáciai szempontból elsődleges gyógyszer alkalmazási módnak tekinthető a folyamatos intravénás infúzió meghatározott program szerinti adagolása. Ebben az esetben nem kell esetleges gasztrointesztinális inkompatibilitással, a máj *first-pass* metabolizmusával számolni, és nyújtott, konstans vérszint érhető el a terápiás tartományban. Ez a biofarmáciai szempontból ideális gyógyszeralkalmazási mód azonban számos hátránnyal, potenciális rizikótényezőkkel, költséges előállításal és egyes betegek rossz compliance-ével jár, ezért szükséges alternatív beviteli kapukat keresni. A transzdermális alkalmazási úttal (pl. tapasz) lipofil farmakonok tartós, egyenletes vérszintje biztosítható, de gyors hatáskifejtésre nem számíthatunk, és a bőr permeabilitása hidrophil ill. nagyobb molekulatömegű farmakonok számára korlátozott. Intranazális alkalmazás esetén szintén számolhatunk szisztémás támadáspontú farmakonokkal, viszont az orrnyálkahártya permeabilitási tulajdonságai előnyösebbek [1].

Hatóanyagok nazális úton való bejuttatása a szisztémás keringésbe ezért kap egyre nagyobb figyelmet. Az orrnyálkahártya számos előnyös tulajdonsággal rendelkezik: nagy felszívódási felületet biztosít a gyógyszerabszorpcióhoz, gyors hatás érhető el, alternatív út le-

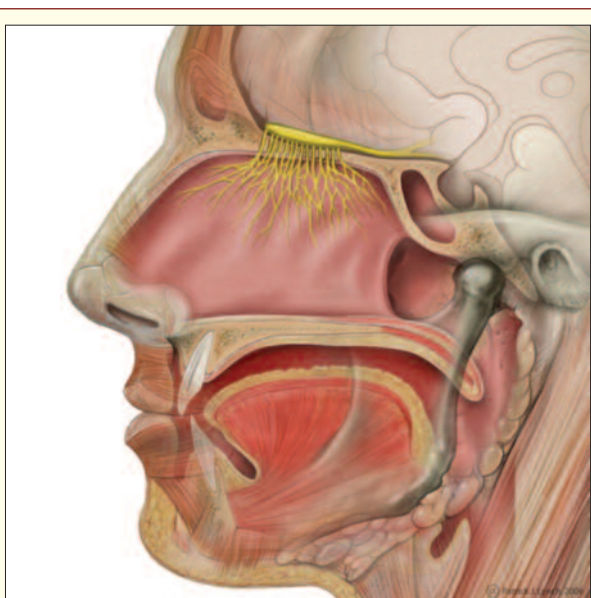
Napjainkban a figyelem az orrnyálkahártyára, mint alternatív beviteli kapura terelődik a gyorsabb és nagyobb mértékű gyógyszerabszorpció vonatkozásában. Már ősidők óta ismert az orrnyálkahártya nagy permeabilitása és gyógyszerbeviteli útként való alkalmazhatósága, viszont csak az elmúlt három évtizedben kezdtek valóban kihasználni az orrnyálkahártyát terápiás lehetőséggént. Az intravénás alkalmazás alternatívája lehet az intranazális gyógyszerbevitel a szisztémás keringésbe. A nazális szisztémás bevitelt a nagy felszívódási felület, a pórusokat tartalmazó endotél membrán, a gazdag vérellátottság, a máj first-pass metabolizmusának elkerülése és a könnyű alkalmazhatóság egyaránt kedvelt alkalmazási móddá teszik. Az utóbbi években széles körben vizsgáltak intranazálisan alkalmazott szisztémás támadásponttal rendelkező hatóanyagokat. További kutatások szükségesek azonban olyan új nazális terápiás rendszerek kialakítására, melyekkel a gyógyszerfelszívódás növelhető lenne az orrnyálkahártya normál funkciójának károsítása nélkül.

hetséges a vér-agy gát megkerülésével a központi idegrendszerbe és nem szenvednek *first-pass* metabolizmust a hatóanyagok a májban (**1. táblázat**). Rendkívül sokféle hatóanyagot lehet bejuttatni nazális úton a szisztémás keringésbe, még relatív nagy molekulákat is, mint például peptideket és proteineket, különösen penetrációt fokozó segédanyagok jelenlétében [2].

2. Terápiás megfontolások

A nazális készítményekről először majdnem mindenkinek a *lokális hatással* rendelkező orrcseppek, orrkenőcsök jutnak eszébe. A megfázás esetén alkalmazott dekongesztánsok és az allergiás tünetek enyhítésére szolgáló H₁-antihisztaminok helyileg hatnak, jelentős felszívódással nem kell számolni.

Az orrnyálkahártya felépítése azonban a *vakcináció nazális lehetőségét* is magában rejt, különösen a légúti infekciókkal szembeni védettség kialakításában lehetnek hatásosak. Megfelelő antigén prezentálása az orrhoz kapcsolódó limfoid szövethez humorális és celluláris immunválaszt is kiválthat. A vakcináció nazális formájának eredményessége abban rejlik, hogy nemcsak szisztémás immunválaszt eredményeznek, hanem



1. ábra: Anatómiai ábra az orrüregről, a sárga szín a nervus olfactorius-t jelzi (forrás: Wikipedia)

I. táblázat

A nazális gyógyszerbevitel előnyei és hátrányai**Előnyök**

nem invazív módszer
nem szükséges steril készítményt előállítani
nem jár fájdalommal
könnyű és egyszerű alkalmazás
a beteg önmagának is be tudja adni
gyors felszívódás, gyors hatás
nincs first-pass metabolizmus
nagy permeabilitás sok hatóanyag esetén
gastrointesztinális mellékhatások elkerülése, mérséklése
nem szenvednek a farmakonok bomlást a gyomorban
kisebb a gyógyszer-túladagolás veszélye
nyelési nehézségben szenvedő betegek esetén is alkalmazható
hányinger, hányás esetén is hatékony
jobb compliance
direkt út a központi idegrendszerbe

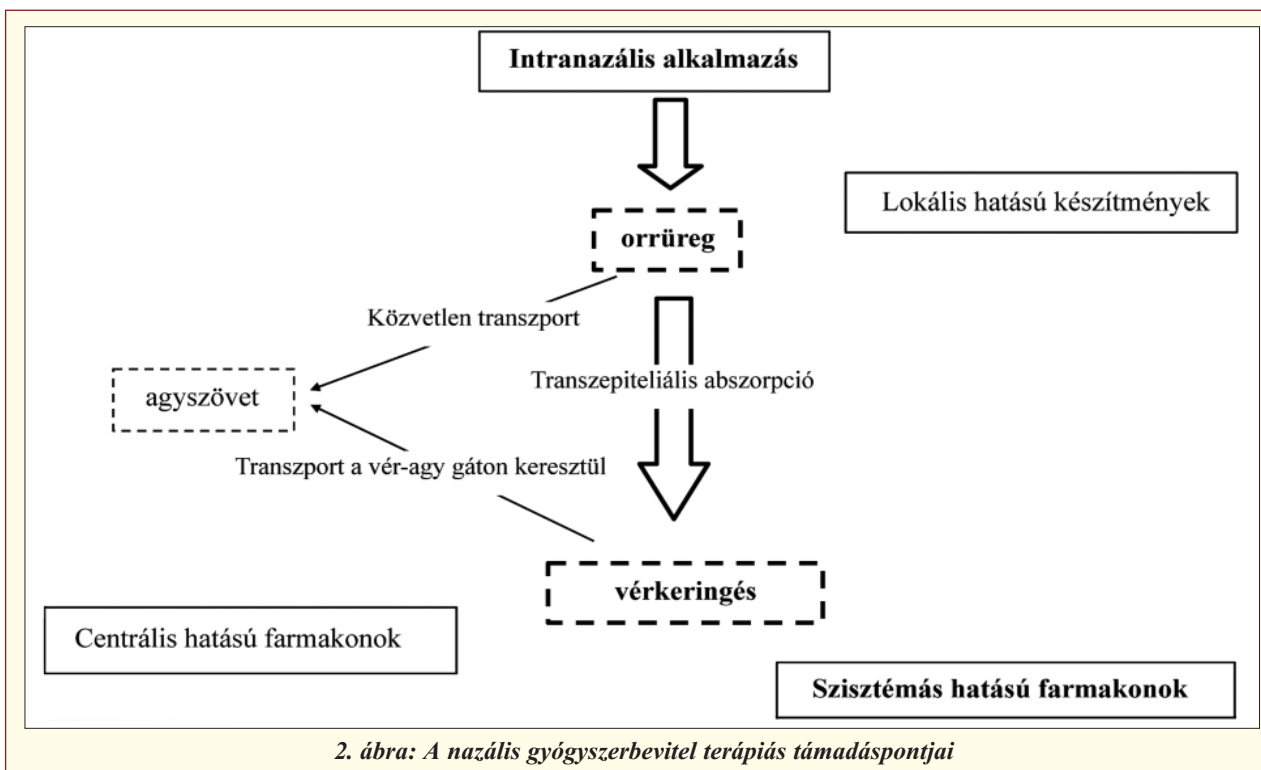
Hátrányok

orrmnyálkahártya érzékenysége
irritáció
25-200 µl közötti térfogatú lehet az egyszeri adag
rövid tartózkodási idő az orrmnyálkahártyán
mucociliaris clearance általi gyors elimináció
enzimatis barrier
patológias állapotok (pl. rhinitis) megváltoztatják a felszívódást

lokálisan az orrmnyálkahártyán is immunválaszt hoznak létre, ezáltal sokkal nagyobb mértékű védetség érhető el [3]. Az intranazális immunizáció esetén tehát helyi és szisztémás immunitás egyaránt megjelenik. Továb-

bi előnye, hogy nem szükséges steril készítményt előállítani, ami a gyártási költségeket jelentősen csökkenti, ez az anyagi tényező különösen nagy jelentőségű a fejlődő országokban.

Az orrüreg és agyszövet közötti transzport közismert, hiszen a kokacserje (*Erythroxylon coca*) leveleiből nyert kokain pszichostimuláns kábítószer egyik beviteli módja a szer orrüregbe történő felszippantása. A kokain közvetlen bejutását a központi idegrendszer specifikus területeire különféle állatkísérletekkel bizonyították. Nazális bevitel esetén a kezdeti koncentrációk az agyban magasabbak voltak, mint intravénás bevitel esetén. Sok más gyógyszernél is hasonló eredményeket figyeltek meg [7, 12]. Ezek különösen olyan poláris hatóanyagok esetén bírnak hatalmas jelentőséggel, amelyek nem jutnának át a vér-agy gáton. A legtöbb eddig vizsgált anyag agyszövetbe jutott mennyisége intranazális bevitelkor a beadott dózis 1-10%-át tette ki. Ez a korlátozott mértékű, de közvetlen transzport az orrmnyálkahártyán keresztül a központi idegrendszerbe a vér-agy gát megkerülésével lehetséges, amit a szaglóhám egyedülálló anatómiai és élettani tulajdonságai tesznek lehetővé. Az itt elhelyezkedő neuronok sejtestjei az epitéliumban helyezkednek el, dendrites idegsejt-nyúlványaik pedig közvetlenül érintkeznek a környezettel, míg axonjaik átkapcsolódás nélkül a központi idegrendszerbe futnak. A szervezetben egyedül itt található primer érzékhám. A neuronok axonjai a rostacsont szitaszerű szerkezetén áthatolva a szaglógumóban végződnek, mely már a központi idegrendszer részét képezi.



2. ábra: A nazális gyógyszerbevitel terápiás támadáspontjai

II. táblázat

**Forgalomban és kutatási fázisban lévő szisztémás hatással rendelkező
nazális készítmények hatóanyagai, indikációi és gyógyszernevei**

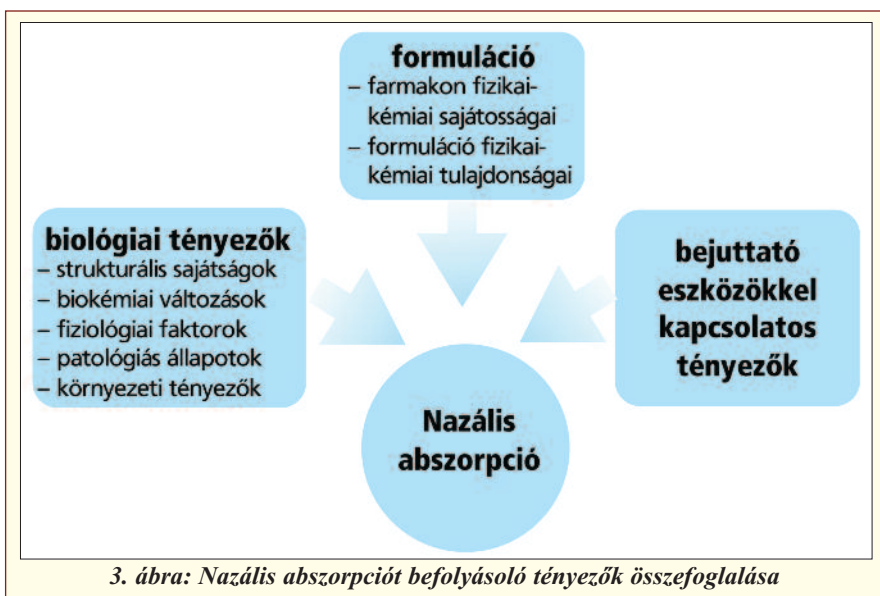
Farmakon	Indikáció	Forgalomban lévő készítmények
Morfin, butofanol-tartarát	fájdalomcsillapítás	<i>Stadol Nasal Spray</i> (Bristol)
Midazolám	gyermekkori status epilepticus	-
Szumatriptán, zolmitriptán, ergotamin	migrén és cluster típusú fejfájás	<i>Imigran orrspray</i> (GlaxoSmithKline)
Galantamin	Alzheimer-kór	-
Apomorfin	erektilis diszfunkció, Parkinson-kór	-
Interferon β_{1A}	sclerosis multiplex	-
Kalcitonin	osteoporosis	<i>Calcitonin-ratiopharm oldatos orrspray</i> (Ratiopharm); <i>Biostin orrspray</i> (TEVA); <i>Calco oldatos orrspray</i> (Medico Uno Pharma); <i>Miacalcic orrspray</i> (Novartis)
Ösztradiol	menopausa, osteoporosis prevenció	<i>Calidiol orrspray</i> (Servier)
Dezmopresszin-acetát	haemophilia A és von Willebrand betegség; centrális diabetes insipidus; enuresis nocturna	<i>Octostim orrspray</i> (Ferring); <i>Minirin orrspray</i> (Ferring); <i>Nocutil oldatos orrspray</i> (Gebro Pharma)
Oxitocin	laktáció fokozása	<i>Syntocinon Nasal Spray</i> (Sandoz)
Metoklopramid, szkopolamin, ondanszetron	hányinger, hányás	-
Propranolol	angina pectoris	-
Buszerelin, goszerelin	hormon-dependens prosztatacarcinoma	<i>Suprefact orrspray</i> (Sanofi-Aventis)
Nafarelin-acetát	centrális pubertas praecox, endometriosis	<i>Synarel Nasal Solution</i> (Roche)
Cianokobalamin (B ₁₂ -vitamin)	B ₁₂ -vitamin defficiencia	<i>Nascobal</i> (Questor Pharmaceuticals)
Influenza-vakcinák	influenza	<i>FluMist</i> (MedImmun Vaccines Inc.); <i>Influvac</i> (Solvay Pharmaceuticals)
Protirelin (TRH)	diagnosztikum	<i>Relefact TRH</i>

A 2. ábra alapján látható, hogy a nazálisan beadott hatóanyag egy része felszívódik a szisztémás keringésbe és kifejti terápiás hatásait, a vér-agy gáton keresztül elérheti a központi idegrendszert, vagy felhalmozódhat a szervekben, szövetekben, de eliminálódhat is a szervezetből. A hatóanyag egy másik hányada a vér-agy gátat megkerülve a szaglóhámon keresztül közvetlenül jut az agyszövetbe.

Kijelenthetjük, hogy a beteg-compliance növekedéséhez nagymértékben hozzájárul az egyszerű adagolás és a gyors hatás. A fentiek alapján, tehát akut és krónikus terápiában egyaránt szerepet kaphat a nazális gyógyszerbeviteli kapu. Sürgősségi fájdalomcsillapítás nazális analgetikumokkal azonnali hatást eredményez, krónikus betegségek (pl. osteoporosis, vérzékenység, centrális diabetes insipidus) esetén hosszú, akár egész életen át tartó terápia szükséges és lehetséges nazális alkalmazásra szánt készítményekkel.

Nem véletlen tehát, hogy a szisztémás hatással rendelkező nazálisan alkalmazott gyógyszerek száma egyre növekszik. A II. táblázat mutatja be a forgalomban és kutatási fázisban lévő nem lokális hatású nazális készítményeket. Olyan betegségek esetén érdemes (lehetne) ilyen készítményeket alkalmazni, amikor azonnali gyors hatásra van szükség (pl. sürgősségi fájdalomcsillapítás), a betegség a bélmotilitást is érinti (pl. diabetes mellitus, parkinsonismus), így az enterális felszívódás változik, valamint amelyek esetén hosszantartó gyógyszeres terápia szükséges és ezzel az egyszerű adagolási móddal növelhető lenne a beteg-compliance.

A szisztémás keringésbe történő abszorpció nagy jelentőséggel bír és a gyógyszertechnológusok számára sok új kihívást jelent. Új összetételek keresése és a megfelelő nazális gyógyszerformák fejlesztése számos ismert hatóanyagnak új indikációs területet nyithatna meg és sok farmakon-jelölt bejuttatási problémáit is megoldhatná.



3. Intranazális gyógyszerbevitelt befolyásoló tényezők

Számos tényező képes befolyásolni a nazálisan beadott hatóanyagok felszívódását, amelyeket az alábbiakban foglaltunk össze (lásd még a 3. ábrát).

Nazális abszorpció vonatkozásában sem javasolt az orrüreg normál fiziológiai viszonyainak megváltoztatása. Különösen igaz ez az állítás krónikus alkalmazásra szánt készítmények esetén, mert a hosszantartó adagolás során mellékhatásként patológiás elváltozások jöhetnek létre az érzékeny ornyálkahártyán.

3.1. Biológiai tényezők

3.1.1. Strukturális sajátosságok

Az orrüregben található strukturális sajátosságok közül lényeges megemlíteni, hogy öt anatómiai régiót (köztük a szagló- és légzőhámot) különítünk el, ezek tulajdonságai különböznek felszívódás szempontjából is [6].

3.1.2. Biokémiai változások

Az ornyálkahártya védelmi mechanizmusát enzimatis barrier is segíti. A nyálkahártya szöveteiben és a váladékban egyaránt találhatók metabolikus enzimek, melyek elsősorban a protein és peptid típusú hatóanyagoknál jelentenek problémát. A nazális metabolizmust a citokróm P-450-függő monooxigenáz rendszer biztosítja, proteáz- és peptidáz-aktivitás szintén megfigyelhető, enziminhibícióval növelhető az abszorpció mértéke. Kifelé irányuló, ún. efflux-transzport rendszereket – mint például a P-glikoproteint – megfigyeltek az ornyálkahártyán is, szerepük a nazális ab-

szorpcióban nem teljesen tisztázott [2]. Prodrugok alkalmazásával a komponensek stabilitása, oldékonysága és permeációja is fokozható [6].

3.1.3. Fiziológiai faktork

Az orrüregek belső felülete emberben körülbelül 150 cm², melyet 4 mm vastag csillósörös nyálkahártya borít, teljes térfogatát tekintve 15 ml (1. ábra) [4]. A szaglóhám (regio olfactoria) felülete az orrüregek csupán 10%-át teszi ki [7]. Más epitel-barriersekhez képest nagy permeabilitással rendelkező felület az ornyálkahártya, amit a

gazdag vérellátottságának és az idegi szabályozásának köszönhet. Az autonóm és a szomatikus rendszer egyaránt behálózta. Paraszimpatikus stimuláció az arteriolák dilatációját és permeabilitás-fokozódást eredményez.

A nazális abszorpció történhet *transzcelluláris* és *paracelluláris* úton egyaránt. Lipofil gyógyszerek transzcelluláris úton szívódnak fel passzív diffúzióval a koncentráció-grádienseknek megfelelően. A fentanil esetén, annak lipofil tulajdonságainak köszönhetően, majdnem 80%-os biohasznosíthatóságot figyeltek meg nazális alkalmazás esetén [8]. Az orrüreg nagy felülete és jó vérellátottsága ellenére az ornyálkahártya alacsony permeabilitással rendelkezik poláris molekulák számára. Ennek az oka, hogy a poláris vagy hidrofil molekulák számára az epitel sejtek közötti út áll rendelkezésre, azonban a sejtek közötti zárókapcsolatok ezt erősen korlátozzák. A zárókapcsolatok dinamikus struktúrák, bizonyos mértékig megnyílhatnak, azonban a méretük miatt a paracelluláris út kevésbé hatékony nagyobb molekulák számára. Az 1000 Da-nál nagyobb molekulatömegű anyagok nem jutnak át ezen a módon. Kis molekulatömegű poláris molekulák megközelítőleg 10%-os biohasznosíthatósággal rendelkeznek nazális bevitel esetén, viszont peptidok (például kalcitonin, inzulin) biohasznosíthatósága 1% alatti tartományba esik. A nagyobb peptidok és a proteinek endocitotikus transzportfolyamatokon keresztül juthatnak át a nazális nyálkahártyán [9]. Harmadik lehetséges útja a nazális abszorpciónak az intracelluláris axonális transzport a szaglóhám neuronjain keresztül, elsősorban a szaglógumóba (*bulbus olfactorius*). Ez a transzport viszont nagyon lassú, akár órákba is telhet, hogy a hatóanyag bejusson a központi idegrendszerbe, míg a transzcelluláris és paracelluláris transzport percek alatt a szövetekbe juttathatja a hatóanyagot [7].

3.1.3.1. Nazális szekrérum

A nyálkahártyában lévő kehelysejtek és mirigyek nyákos szekrérumot termelnek. Az orrváladék 2-3% mucint és 1-2% szervesen sós tartalmaz, valamint 95%-ban vízből áll [7]. Az orrüregben folyamatosan termelődő nyálka mennyisége megközelítőleg napi 1,5-2 liter, ami vékony, 5 μ m vastagságú, alul szol, felül gél állapotú rétegben borítja az epitél sejteket [10]. Ez a nazális nyálkahártyaréteg 15-20 percenként teljesen megújul [11]. Ez a folyamat a mukociliáris clearance. Az orrnyálkahártyán keresztüli permeabilitást befolyásolja az orrszekrérum viszkozitása, az hogy a hatóanyag oldódik-e a szekréumban, valamint az orrüregben uralkodó pH viszonyok is. A nazális szekréció és clearance éjszaka alacsonyabb aktivitást mutat, tehát circadián ritmus figyelhető meg [6].

3.1.3.2. Mucociliaris clearance

A csillós hámnak nagy jelentősége van a nyálkahártya normális működése szempontjából. A ciliák állandó ostorozó mozgást végeznek (300-500 csapás/perc). A garat felé mereven csapnak, az orrnyílások felé visszahajlanak. Ezzel a mozgással az orrváladékot, a benne levő szennyeződések és a bevitt gyógyszereket is a garat felé sodorják [12]. A mucociliaris clearance az egyik legfontosabb élettani védelmi mechanizmusa a légzőrendszernek. A védelmi rendszer érzékenységének következtében nemcsak az ártalmas anyagok, hanem a hatóanyagok is gyorsan eliminálódnak az orrnyálkahártya felületéről a gasztrointesztinális traktus irányába. Mukoadhezív tulajdonságokkal nem rendelkező készítményeknél 10-15 perces felezési idővel kell számolni. Csökkent mucociliaris clearance esetén megnövekszik az érintkezési idő a hatóanyag és a nyálkahártya között, ami nagyobb mértékű felszívódást eredményez [6]. Sok hatóanyagnál nem a permeabilitás a korlátozó tényező az abszorpció szempontjából, hanem a mucociliaris clearance általi gyors elimináció, amit segédanyagokkal szabályozni lehet [13].

3.1.3.4. Patológiás állapotok

A gyógyszer-permeációt különféle betegségek is befolyásolják, mint például az egyszerű megfázás, a rhinitis, az atopiás rhinitis vagy az orrpolip. A betegségek a mucociliaris clearance funkciójának károsodásához, hipo-, illetve hiperszekrécióhoz és az orrnyálkahártya irritációjához vezetnek [6].

3.1.3.5. Környezeti tényezők

Általánosságban megállapítható, hogy a csillók csapási frekvenciája és a mucociliaris clearance lineáris növeke-

dést mutat a hőmérséklet emelkedésének függvényében [14]. A cigarettafüst csökkenti a mucociliaris clearance hatékonyságát a mucus reológiai tulajdonságainak befolyásolásával és/vagy a csillók számának redukciójával, de a csillók csapási frekvenciája változatlan marad [10].

3.2. A nazális alkalmazás eszközei

A hatóanyag mennyiségének pontos adagolása nagyon lényeges szempont a gyógyszerkészítmények adagoló eszközeinek kialakítása során. Folyékony gyógyszerformák esetén cseppentők és spray-k jöhetnek szóba. A legkevésbé pontos adagolást orrcseppenként lehet megfigyelni, mert a folyadék túlcsorog a garat felé a gasztrointesztinális rendszer irányába. Napjainkban a legelterjedtebbek az oldatos orrspray-k, melyek használatával a gyógyszerkészítmény adagolása pontos és egyszerű. Szuszpenziós orrspray-k esetén szintén pontos adagolás érhető el, viszont ezek formulációjánál különös figyelmet kell szánni a részecskék méretére és morfológiájára.

Nazális porok adagolása hasonló eszközzel történik, mint az asztma kezelésében használt por-inhalátor.

Gélek, kenőcsök és más felszilárd készítmények nazális alkalmazása megfelelően kialakított tubusból történhet.

4. Intranazális gyógyszerbevitelt befolyásoló formulációs tényezők

A farmakon fizikai kémiai sajátosságai: a molekulatömeg, a molekulaméret, az oldékonyság, a lipofilitás és a pK_a érték alapvetően fontos tényezők az abszorpció szempontjából [6]. Így megfelelő körültekintéssel kell kiválasztani a segédanyagokat (**III. táblázat**) és a gyógyszerhordozó rendszereket (**IV. táblázat**).

4.1. Farmakonok tulajdonságai

A farmakonok oldékonyságának növelése azért lényeges, hogy a farmakon feloldódjon az orrnyálkahártya felületén és így jusson be a szisztémás keringésbe, valamint, hogy kis térfogatú (200-300 μ l pro dosi), de te-

III. táblázat
Nazális alkalmazásra szánt gyógyszerformák segédanyagai

Nazális készítmények segédanyagai
szolubilizáló szerek: poliszorbát
illat- és ízjavítók: mentol
pufferek: primer és szekunder foszfát
tartósítószer: benzalkónium-klorid
ozmotikus sajátosságú segédanyagok: mannit
gélképző és viszkozitás-növelő anyagok: kitozán
permeabilitást fokozó segédanyagok: Cremophor RH 40
mukoadhezív segédanyagok: nátrium-hialuronát

IV. táblázat

Gyógyszerhordozó rendszerek nazális alkalmazás esetén

Új, modern gyógyszerhordozó rendszerek	Gyógyszerformák
mikroszférák, nanoszférák	oldatok: cseppek, oldatos spray-k
liposzómák	szuszpenziók: szuszpenziós spray-k
proliposzómák	emulziók
nioszómák	kenőcsök
nanokristályok	gélek
filmek	szilárd porok

rapiás szempontból megfelelően magas koncentrációjú egyszeri adagot állíthassunk elő, mert nazális készítmények esetén az orrüreg térfogata limitált, korlátozó tényezőt jelenthet. Oldékonyság növelésre alkalmazhatunk prodrugokat, ko-szolvenseket, ciklodextrineket, valamint a hatóanyag só formáját [2]. Farmakonok nazális abszorpciója pH-függő folyamat, például savi karakterű gyógyszereknél jobb felszívódás figyelhető meg, ha a pH alacsonyabb, mint a farmakon pK_a értéke [1].

A részecskeméret csökkentése szintén egy lehetséges technológiai eljárás, mely lehetővé teszi oldhatatlan kristályok átjutását az ornyálkahártyán. A nanomérettartományba (100-1000 nm) eső kristályok nemcsak jobb oldhatósággal, de kedvezőbb permeabilitási tulajdonságokkal is rendelkeznek. Arra mindenképpen figyelmet kell fordítani a szemcseméret kialakításánál, hogy azok a részecskék, amelyek 10 μm alatti mérettartományba esnek, bejutnak a légzőrendszerbe, a 0,5 μm -nél kisebbeket viszont ki is lélegezzük. Nazális alkalmazáshoz 5-7 μm közötti részecske- illetve cseppméret az ideális [15]. Tehát a nanorészecskéket hordozóba kell ágyazni (mukoadhezív vivőanyag), vagy mikrométeres tartományba eső ún. nanokompozitokat kell előállítani.

4.2. Segédanyagok jellemzői

Az intranazális gyógyszerbevitel segédanyagai: szolubilizáló szerek, pufferek, antioxidánsok, illat- és ízanyagok, tartósítószer, gélképző és viszkozitás-növelő anyagok, abszorpció-fokozók [16].

Rendkívül sokféle abszorpció-fokozó segédanyagot használnak a hatóanyagok felszívódásának növelése érdekében, melyek megváltoztathatják a membrán-flu-iditást, csökkenthetik a nyálkahártya viszkozitását, gátolhatják a proteolitikus enzimek aktivitását, fokozhatják a sejtek közötti zárókapcsolatok permeabilitását, serkenthetik a paracelluláris vagy transzcelluláris transzportot, fokozhatják az ornyálkahártya vérellátottságát [6]. Ezen abszorpció-fokozó segédanyagok kiválasztásánál ügyelni kell arra, hogy a lehető legkisebb, de még hatásos koncentrációban alkalmazzuk az irritáció elkerülése, mérséklése miatt [13].

Ilyen segédanyagnak tekinthető a kitozán. Pozitív

töltésű egyenes láncú poliszacharid, amely átmenetileg nyitja a sejtmembránok közötti zárókapcsolatokat és bioadhezív tulajdonsággal is rendelkezik, így lehetővé teszi poláros anyagok transzportját, amelyek nem jutnának át az ornyálkahártyán. A kitozán további előnyös tulajdonsága, hogy az ornyálkahártyára nem toxikus és nem is irritálja. Különösen biztató formulációnak bizonyult morfin kitozánnal együtt való intranazális adagolása [17].

Mukoadhezív tulajdonságokkal rendelkező rendszerek alkalmazása előnyös lehet nazális bevitel esetén, akár direkt agyszövetbe irányuló transzportra is a vér-agy gát megkerülésével. Horvát és munkatársainak eredményei az abszorpció-fokozó segédanyagok és a bioadhezív polimerek szerepére világítanak rá [18].

Egy polimer mukoadhezívitását befolyásoló tényezők a következők: megfelelő funkciós csoportok a hordozó polimeren, a polimer molekulatömege megfelelő tartományban legyen a keresztkötésekhez, a térbeli elrendeződés, az érintkezési idő a nyálkahártyával, a polimer koncentrációja, valamint a környezet kémhatása és fiziológiai változatossága (pl. mucin réteg megújulása) [10].

4.3. Gyógyszerkészítmény sajátosságai

A készítmény fizikai kémiai sajátosságai alapvetően befolyásolják a gyógyszerfelszívódást. A kémhatásnak pH 4,5-6,5 közötti tartományban kell lennie. Megfelelő kémhatás kialakítása és pufferekkel történő fenntartás esetén az ornyálkahártya irritációja elkerülhető, kedvezőbb abszorpció biztosítható, megelőzhető a bakteriális fertőzés kialakulása [16]. Az ozmolaritás és a viszkozitás szintén befolyásoló tényezők. Általánosságban izotóniás formuláció preferált, de ismert tény, hogy a tonicitás változásával módosul az ornyálkahártyán keresztüli felszívódás [16]. Nagyobb viszkozitású készítmények kellemetlen érzetet keltenek és a fiziológiai tulajdonságokat is negatívan befolyásolják [6].

Nazális alkalmazás esetén különböző gyógyszerformák jöhetnek szóba. Folyékony készítményeket tekintve lehetnek oldatok, szuszpenziók, különféle típusú emulziók. Alkalmazhatunk azonban szilárd halmazállapotú porokat is, ezek a készítmények DPI-szerű rendszerek (*Dry Powder Inhalation*) és modern technológi-

ai eljárások útján lehet őket előállítani. Félszilárd készítmények közül a kenőcsök és a gélek jöhetnek számításba.

Új, modern gyógyszerhordozó rendszerek a nazális bevitel jövőjét jelentik. Egyes mikroszférás rendszerek gélesedő tulajdonságokkal rendelkező segédanyagokat is tartalmaznak, melyek hatására jobb abszorpciós profillal jellemezhetőek. A zárókapcsolatok átmeneti kiszélesedése figyelhető meg mikroszférák jelenlétében [16], mert ezek a rendszerek vizet vonnak el a nyálkahártyarétegből, ezáltal duzzadnak. Az epitel sejtek dehidratálódnak és ez okozza a zárókapcsolatok megnyílását. A készítmény orrüregben való tartózkodási idejét növelni lehet bioadhezív mikroszférák alkalmazásával. A leggyakrabban használt mikroszférás rendszerek a lebomló keményítő mikroszférák, melyekkel növelni lehet a nazális abszorpciót számos hatóanyag esetén (pl. inzulin, gentamicin, humán növekedési hormon, metoklopramid és dezmozpresszin) [19]. A nanotechnológiával előállított termékek szintén ígéretesek lehetnek, mert ezeknek a nano mérettartományban (10^{-9} m) lévő részecskéknél kedvező felszívódási profilja van. A liposzómák, illetve a kevésbé ismert nioszómák beépülnek a biológiai membránokba, így az ilyen rendszerekben lévő hatóanyagok átjutása nem ütközik nehézségekbe, valamint ezek növelik a retenciós időt is az orrüregben. Bioadhezív polimerekből (poliakrilsav) álló gélek szintén a jövőt jelentik [19].

5. Jövőkép

A jövőt az új technológiákkal előállított készítmények jelentik szisztémás keringésbe irányuló nazális gyógyszerbevitellel, melyekkel célzott terápia érhető el. A nazális alkalmazási utat fogjuk vizsgálni az SZTE Gyógyszertechnológiai Intézetében együttműködve az MTA Szegedi Biológiai Központ Biofizikai Intézetének Molekuláris Neurobiológiai Csoportjával különféle *in vitro*, *in vitro* sejtvonalas, *ex vivo* és *in vivo* módszerekkel.

IRODALOM

1. Chien, Y. W. *et al.*: Nasal systemic drug delivery. Informa Healthcare Inc. New York (1989) – 2. Costantino, H. R. *et al.*: Intranasal delivery: Physicochemical and therapeutic aspects, *Intern. J. Pharm.* 337, 1–24. (2007) – 3. Illum, L. *et al.*: Chitosan as a novel nasal system for vaccines, *Adv. Drug. Deliv. Rev.* 51,

81–96. (2001) – 4. Illum, L. *et al.*: Transport of drugs from the nasal cavity to the central nervous system, *Eur. J. Pharm. Sci.* 11, 1–18. (2000) – 5. Chow, H. *et al.*: Direct transport of cocaine from the nasal cavity to the brain following intranasal cocaine administration in rats, *J. Pharm. Sci.* 88, 754–758. (1999) – 6. Arora, P. *et al.*: Permeability issues in nasal drug delivery, *Drug Discovery Today Vol. 7* (2002) – 7. Illum, L. *et al.*: Nasal drug delivery – possibilities, problems and solutions, *J. Contr. Release* 87, 187–198 (2003) – 8. Striebel, H. W. *et al.*: Pharmakokinetische Studie zur intranasalen Gabe von Fentanyl, *Der Schmerz* 7, 122–125 (1993) – 9. Inagaki, M. *et al.*: Macromolecular permeability of the tight junction of the human nasal mucosa, *Rhinology* 23, 213–221 (1985) – 10. Ugwoke, M. *et al.*: Nasal mucoadhesive drug delivery: Background, applications, trends and future perspectives, *Adv. Drug Deliver. Rev.* 57, 1640–1665. (2005) – 11. Hussain, A. *et al.*: Intranasal drug delivery, *Adv. Drug Deliver. Rev.* 29, 39–49 (1998) – 12. Illum, L. *et al.*: Nasal drug delivery: new developments and strategies; *DDT Vol. 7, No. 23* (2002) – 13. Behl, C.R. *et al.*: Optimization of systemic nasal drug delivery with pharmaceutical excipients, *Adv. Drug Deliver. Rev.* 29, 117–133 (1998) – 14. Merkus, P. *et al.*: Classification of cilio-inhibiting effects of nasal drugs, *Laryngoscope* 111, 595–602 (2001) – 15. Szente, V., Zelkó, R.: Helyspecifikus hatóanyagleadást biztosító rendszerek III., Nazális gyógyszerformák, *Acta Pharm. Hung.* 78, 87–90 (2008) – 16. Behl, C.R. *et al.*: Effects of physicochemical properties and other factors on systemic nasal drug delivery, *Adv. Drug Deliver. Rev.* 29, 89–116 (1998) – 17. Illum L. *et al.*: Bioadhesive formulations for nasal peptide delivery, *Drug Delivery-issues in Fundamentals*, pp. 507–539. (1998) – 18. Horvát, S. *et al.*: Sodium hyaluronate as a mucoadhesive component in nasal formulation enhances delivery of molecules to brain tissue, *Eur. J. Pharm. Biopharm.* in press (2009) – 19. Türker, S. *et al.*: Nasal route and drug delivery systems, *Pharm World Sci* 26, 137–142 (2004).

Kürti, L., Deli, M. and Szabó-Révész, P.: *Novel opportunities for nasal systemic drug delivery*

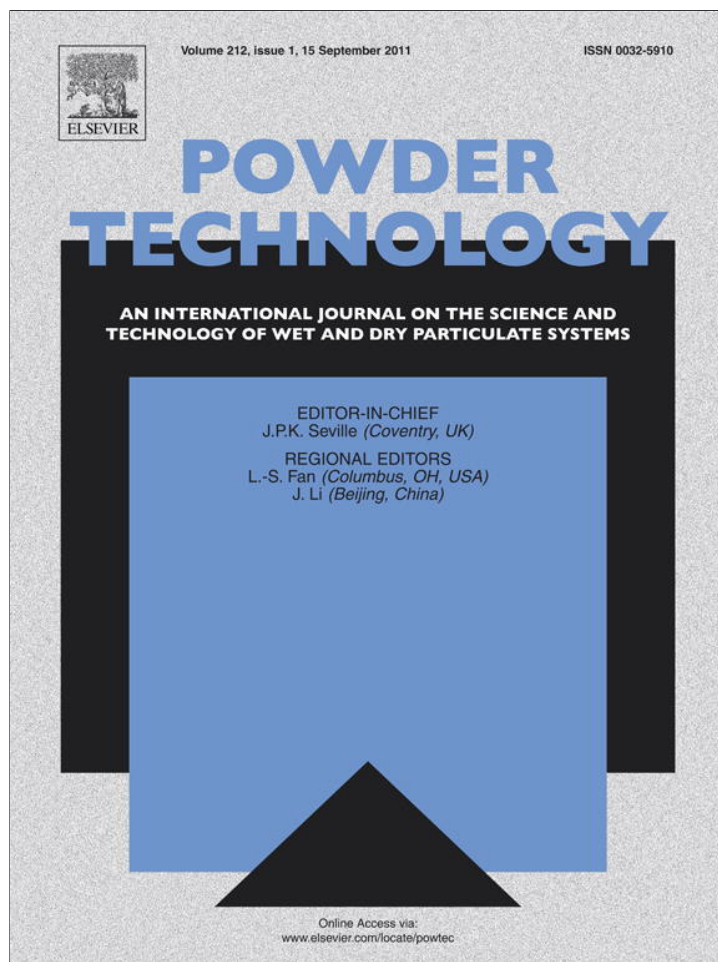
Recently, focus has been on the nasal mucosa as an alternate route to achieve faster and higher drug absorption. Knowledge of the nasal mucosa's high permeability and use of the nasal route for drug administration can be traced to ancient times. Realization of the nasal mucosa as a therapeutically viable alternate route came in the last three decades. Nasal drug administration has been used as an alternative route for the systemic availability of drugs restricted to intravenous administration. This is due to the large surface area, porous endothelial membrane, high total blood flow, the avoidance of first-pass metabolism, and ready accessibility. The nasal administration of drugs, including numerous compound, peptide and protein drugs, for systemic medication has been widely investigated in recent years. Further research with novel nasal therapeutic systems is needed to increase the absorption of drugs through the nasal mucosa without compromising normal function.

¹Szegedi Tudományegyetem Gyógyszertechnológiai Intézet, 6720 Szeged, Eötvös u. 6.

²MTA Szegedi Biológiai Központ Biofizikai Intézet Molekuláris Neurobiológiai Csoport, Szeged, Temesvári krt. 62. – 6726



PUBLICATION II.



This article appeared in a journal published by Elsevier. The attached copy is furnished to the author for internal non-commercial research and education use, including for instruction at the authors institution and sharing with colleagues.

Other uses, including reproduction and distribution, or selling or licensing copies, or posting to personal, institutional or third party websites are prohibited.

In most cases authors are permitted to post their version of the article (e.g. in Word or Tex form) to their personal website or institutional repository. Authors requiring further information regarding Elsevier's archiving and manuscript policies are encouraged to visit:

<http://www.elsevier.com/copyright>



Contents lists available at ScienceDirect

Powder Technology

journal homepage: www.elsevier.com/locate/powtec

Study of the parameters influencing the co-grinding process for the production of meloxicam nanoparticles

Levente Kürti ^{a,c}, Ákos Kukovecz ^b, Gábor Kozma ^b, Rita Ambrus ^a, Mária A. Deli ^c, Piroska Szabó-Révész ^{a,*}

^a Department of Pharmaceutical Technology, University of Szeged, Szeged, Hungary

^b Department of Applied & Environmental Chemistry, University of Szeged, Szeged, Hungary

^c Laboratory of Molecular Neurobiology, Institute of Biophysics, Biological Research Centre, Hungarian Academy of Sciences, Szeged, Hungary

ARTICLE INFO

Article history:

Received 9 July 2010

Received in revised form 31 March 2011

Accepted 21 May 2011

Available online 1 June 2011

Keywords:

Nanoparticle

Meloxicam

Co-grinding

Scanning electron microscopy

Factorial experimental design

Nasal powder system

ABSTRACT

Co-grinding is a procedure for the preparation of nanoparticles in which the drug is ground together with one or more excipients. The grinding of meloxicam, a crystalline solid, together with amorphous polyvinylpyrrolidone (PVP) or semi-crystalline polyethylene glycol (PEG) as excipients, is expected to lead to a drastic reduction in particle size. We optimized meloxicam grinding using a three level full factorial response surface design. In the case of PVP the optimum co-grinding parameter set in our study proved to be a meloxicam to PVP-C30 ratio of 1:1, and a rotation frequency of 400 rpm. The best size reduction was achieved at a meloxicam to PEG 6000 ratio=1:2 at a rotation frequency of 400 rpm: nanoparticles averaging $d_{SEM} = 174$ nm in diameter and with a very narrow size distribution (standard deviation 35% of mean) were obtained. X-ray powder diffraction analysis indicated that the optimized products contained amorphous meloxicam nanoparticles in the PVP-C30 composition, although meloxicam nanocrystals could also be detected in the samples which contained PEG 6000. The dissolution properties were significantly increased under nasal conditions (pH 5.1, temperature 30 °C), especially in the case of the amorphous product. Such dry powder systems can offer novel opportunities in systemic nasal drug delivery.

© 2011 Elsevier B.V. All rights reserved.

1. Introduction

Nanonization offers an excellent possibility to overcome mucosal barriers [1,2] and has several advantages in drug delivery [3,4]. It is believed that nanoparticles can be transported across barriers into the bloodstream without prior dissolution [5]. Nano-sized drugs with carriers can overcome the resistance offered by the physiological barriers in the body because the efficient delivery of drugs to various parts of the body is directly affected by the particle size [6].

Several techniques are available for the production of drug nanoparticles [7]. Basically, bottom-up and top-down technologies can be differentiated. The bottom-up technologies start from the molecules, which are precipitated (crystallized) in a controlled fashion to yield the desired particle size. Nowadays, bottom-up techniques are not the main choice for drug nanoparticle production due to the use of organic solvents. The top-down technologies are disintegration methods e.g. various types of milling (high-intensity ultrasonication, high-pressure homogenization, grinding or co-grinding) are more frequently used [8].

The size reduction of pharmaceutical materials is often performed by means of dry milling [9,10], but the size reduction possible by dry

milling is known to be limited to around 3 μ m due to aggregation of the particles. Experiments focusing on a particle size reduction to the submicron region by co-grinding with additives have recently been attempted [11–14].

Nanonization has become a popular approach to produce particles in the size range of 200–400 nm, to improve both the dissolution rate and the solubility of the compound [15]. The latter phenomenon is due to the well-known dependency of solubility on particle size as described by the Ostwald–Freundlich equation. Breakage of micron-sized drug crystals into nanoparticles creates an increased particle surface area, which is thermodynamically unfavorable. Thus, nano-sized particles tend to agglomerate to reduce their surface area. Particle agglomeration can be prevented by steric stabilization using polymeric excipients [16].

Co-grinding is a top-down disintegration procedure for the preparation of nanoparticles by grinding of the drug together with one or more excipients [17,18]. A main advantage of co-grinding as compared to other methods is that it is a simple procedure and organic solvents are not needed for the preparation of nanoparticles; it is therefore an economically and environmentally desirable technology [19]. It is important to control the parameters (e.g. duration of grinding, the grinding rate, the material and the volume of the grinding pot, the material and the number of the grinding balls, the grinding excipients and the drug/excipient ratio) by means of a factorial experimental design [20,21].

* Corresponding author at: H-6720 Eötvös utca 6., Szeged, Hungary. Tel.: +36 62 545572; fax: +36 62 545571.

E-mail address: revesz@pharm.u-szeged.hu (P. Szabó-Révész).

Meloxicam, a non-steroidal anti-inflammatory and analgesic water-insoluble drug (NSAID), is an enolic acid oxamic derivative [22,23]. The single oral dose of meloxicam is 7.5–15 mg. The favorable side-effect profile and the low quantity of a single dose make this NSAID suitable for administration via alternative pathways, e.g. intranasally. This may result in novel opportunities for the easing of pain, which affects the region of the head.

A reduction of the particle size of meloxicam into the nano-size range (100–1000 nm) is possible by crystallization methods through formulation of the drug in a nanosuspension [24]. However, co-grinding offers a simpler and environmentally friendly way of preparing meloxicam nanoparticles. Nanoparticles are a formulation principle for all poorly soluble drugs for which the dissolution velocity is the rate limiting step for absorption and thus the reason for a too low bioavailability. The increase in surface area leads to an increase in the dissolution velocity.

Water-soluble polymers have typically been used as co-grinding excipients [13,25,26]. An example is polyvinylpyrrolidone (PVP), an amorphous excipient which does not melt during the grinding process therefore it could also help particle size reduction and to prevent the agglomeration, as stabilizer agent [27–29]. On the contrary, polyethylene glycol (PEG) is a semicrystalline grinding excipient with low melting point which could melt due to friction work and as a consequence it cannot help as efficiently as PVP the size reduction.

The grinding of meloxicam, a crystalline solid, together with amorphous PVP or semicrystalline PEG as excipients is expected to lead to a drastic reduction in particle size and to possible changes in the crystallinity of meloxicam without any harmful alterations in its pharmaceutical effect. The crystalline and the amorphous form of an active agent have no difference in their effect, although the onset of action can be improved with faster dissolution rate.

Multivariate problems similar to meloxicam grinding are often optimized by using the COST (Change One Separate factor at a Time) approach: all parameters but one are fixed, and the response of the system is studied as a function of the changing variable. Each variable is scanned in this way, and the combination of their optimum values is accepted as the overall optimum. Unfortunately, this method is slow, since the number of necessary experiments increases considerably with the number of variables. Moreover, the COST approach can seldom find the true overall optimum of a system since it assumes that the effects of all variables are completely independent, whereas the response of a real system to change in any single parameter often appears as the overall effect of several parameter alterations (i.e. real-life multidimensional parameter spaces are seldom orthogonal). A good strategy for finding the overall optimum of a multivariate problem is to fit the response surface on the basis of the responses obtained from well-chosen parameter sets. Since the effect of any single variable can usually be accounted for by a second-order polynomial, it is customary to test parameters at three different levels: a high, a medium and a low setting. Such designs, called three-level full factorial designs, have been applied successfully in the past to optimize the synthesis of carbon nanotubes [20,30], the deposition of titanate nanowires on glass [31] and the wet peroxidation of aqueous phenol solution [32]. The simplest three-level full factorial design is to pick three values for one independent variable (x_1 : rotation speed), chart the three corresponding response (d : particle diameter) values in a standard two dimensional Cartesian coordinate system and fit the $d = f(x_1)$ function by a parabola. In case of two independent variables (x_1 : rotation speed and x_2 : meloxicam to excipient ratio) we need to sample $3 \times 3 = 9$ points in the x_1x_2 plane and chart the corresponding d values as elevation above the x_1x_2 plane in a three dimensional coordinate system.

The aim of our present research work was to produce meloxicam nanoparticles by co-grinding process with PVP and PEG, investigating the influence of different parameters on particle size and optimizing them by using a three-level full factorial design so that nano-sized

meloxicam particles of uniform size distribution are obtained. The optimized products were investigated from the aspects of crystallinity and extent of dissolution under *in vitro* nasal circumstances.

2. Materials and methods

2.1. Materials

Meloxicam (4-hydroxy-2-methyl-N-(5-methyl-2-thiazolyl)-2H-benzothiazine-3-carboxamide-1,1-dioxide) was obtained from EGIS Ltd. (Budapest, Hungary). The grinding additives, polyvinylpyrrolidone (PVP) K25 and C30 were purchased from BASF (Ludwigshafen, Germany). Types of PVP (K25 and C30) differ in molecular weight, viscosity and field of application. Molecular weight of PVP-K25 is about 34,000 and PVP-C30 has a higher molecular weight (about 58,000). Because their viscosity relating to molecular weight so the viscosity of PVP-C30 is higher, than for K25. In the case of PVP the letter "C" indicates applicability also for preparation of aseptic dosage forms. Polyethylene glycol (PEG) 6000 and 20,000 were from Sigma-Aldrich Chemie GmbH, Germany. The numbers of PEG (6000 and 20,000) refer to the molecular weight of the polymer.

2.2. Methods

2.2.1. Preliminary experiments

Several pharmaceutical excipients were tested, and the results of the co-grinding of meloxicam with PVP and PEG were the most promising in the aspect of particle size reduction. In these preliminary experiments some optimum parameters of the grinding (the duration of grinding, the material and the volume of the grinding pot and the material and the number of grinding balls) were also set.

2.2.2. Preparation of co-ground formulations and their physical mixtures

Binary mixtures of as-received meloxicam powder and the carriers PVP-C30, PVP-K25, PEG 6000 and PEG 20,000 were mixed and charged into the chamber of the planetary monomill (Fritsch Pulverisette 6, Fritsch GmbH, Idar-Oberstein, Germany) in various drug-carrier ratios (1:0.5, 1:1 and 1:2). The grinding was performed in an 80 cm³ silicon nitride (Si₃N₄) milling drum containing 25 silicon nitride balls 10 mm in diameter. In each experiment, 1.0 g of meloxicam was ground together with the calculated amount of polymer additive.

The milling parameters are given in Table 1 and the investigated parameters are listed in Table 2. After grinding, the samples were stored in plastic vials until use.

The physical mixtures of drug-carrier were prepared by accurately weighing the calculated amounts of meloxicam and carrier, mixing them well in a porcelain mortar and storing in plastic vials until use.

2.2.3. Determination of particle size by scanning electron microscopic image analysis

2.2.3.1. Scanning electron microscopy (SEM). Co-ground products were washed and centrifuged three times in distilled water to separate the water-soluble excipient from the water-insoluble meloxicam (the solubility of meloxicam is 4.4 ± 0.7 µg/mL [24]), so that individual meloxicam particles could be studied. The particle size and the surface

Table 1
General parameters of co-grinding, independent variables.

Material of the grinding pot	Si ₃ N ₄
Material of the grinding balls	Si ₃ N ₄
Number of the grinding balls	25
V _{grinding pot}	80 mL
D _{grinding ball}	10 mm
t _{milling}	2 h

Table 2
Compositions of different samples, parameters of optimization.

Meloxicam/excipient ratio	1:0.5, 1:1, 1:2
Excipients	PVP-C30, PVP-K25, PEG 6000, PEG 20,000
Revolutions per minute (rpm)	200, 300, 400

morphology of the meloxicam particles were visualized by SEM. Samples were fixed onto a metallic stub with double-sided conductive tape (diameter 12 mm, Oxon, Oxford Instruments, UK). Images were taken in secondary electron image mode on a Hitachi S-4700 Type II instrument at an acceleration voltage of 10 kV.

2.2.3.2. Image analysis. Meloxicam particle diameter distributions were obtained by analyzing several SEM images with the ImageJ software environment [33]. Over 150 individual particle measurements were made in at least five different images in order to determine the particle size accurately. Although less frequently used than TEM or dynamic light scattering, SEM image analysis is an established method for nanoparticle size analysis: for instance, it was applied successfully for the characterization of carbon nanotube networks [30], Zn-glycerolate microstacks [34] and co-grinding products of PVP and CaCO_3 [35].

2.2.3.3. Design of experiments. In a series of pre-screening experiments the following parameters were fixed (see Table 1): (i) the milling drum size and material, (ii) the ball size and number, and (iii) the milling duration. The remaining variables, i.e. the excipient type, the excipient-to-meloxicam ratio and the milling rate were the parameters featuring in the optimization. A full factorial design plan was created and carried out with the meloxicam particle size distribution defined as response factor. All calculations were performed by using Minitab 14 (Minitab Statistical Software).

2.2.4. Further investigations of the optimized products

2.2.4.1. X-ray powder diffraction analysis (XRPD). The physical state of meloxicam in the different samples was evaluated by XRPD. Diffraction patterns were analyzed with a Miniflex II X-ray Diffractometer (Rigaku Co. Tokyo, Japan), where the tube anode was Cu with $\lambda = 1.5405 \text{ \AA}$. The pattern was collected with a tube voltage of 30 kV and a tube current of 15 mA in in-step scan mode ($4^\circ/\text{min}$). The instrument was calibrated by using Si.

2.2.4.2. Studies of the extent of dissolution under in vitro nasal conditions. The dissolution of different powder samples containing the same amount of drug (10 mg) was determined according to the European Pharmacopoeia (6th Edition) paddle method (Pharma test, Heinburg, Germany), which means a rotating paddle in the dissolution vessel. 50.0 mL of phosphate buffer solution ($\text{pH } 5.6 \pm 0.1$) at $30 \pm 0.5^\circ \text{C}$ was used as a dissolution medium and the rotation speed of the paddles was 100 rpm. At predetermined times, 1 mL samples were withdrawn and immediately filtered (cut-off $0.2 \mu\text{m}$, Minisart SRP 25, Sartorius, Germany) and the amount of dissolved drug was determined spectrophotometrically ($\lambda = 364 \text{ nm}$). Withdrawn samples were replaced with 1 mL of fresh medium.

3. Results and discussion

Fig. 1 presents typical SEM images of meloxicam particles before grinding (A) and after grinding in the presence of the various excipients (B–D). The particle size was reduced by roughly one order of magnitude, regardless of the additive used. This primary effect originated from the high-energy collisions taking place in the planetary ball mill [36]. Ball milling is a process with complex mechanics, analyzed in detail by Chattopadhyay et al. [37]. On the basis of their model, it was possible to calculate the energetics of the co-grinding experiments performed. The results in Table 3 indicate

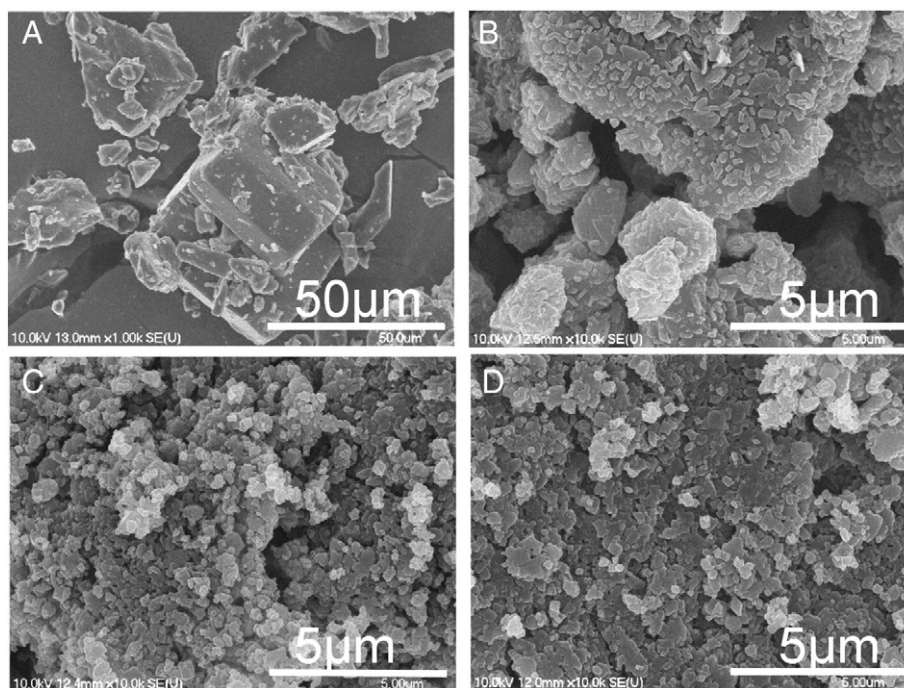


Fig. 1. Scanning electron microscopic images from meloxicam before grinding (A), after co-grinding with PVP-K25 in a ratio of 1:0.5 at 300 rpm (B), with PEG 20,000 in a ratio of 1:0.5 at 400 rpm (C), with PEG 6000 in a ratio of 1:0.5 at 400 rpm (D)/from all of the products PVP and PEG were dissolved by distilled water due to the visualization of meloxicam particles/.

Table 3
Milling energetics map of the experiments performed.

Rotation speed (rpm)	Collision frequency (s ⁻¹)	Cumulative collision energy transferred (kJ·g ⁻¹)			
		Meloxicam to additive weight ratio			
		No additive	1:0.5	1:1	1:2
200	240	8.56	5.71	4.28	2.85
300	360	28.89	19.27	14.45	9.63
400	480	68.50	45.67	34.25	22.83

that the total energy transferred to the meloxicam–excipient mixture via collisions in our system lies in the range of 2.80–68.50 kJg⁻¹.

A closer analysis of the SEM micrographs revealed that there were considerable differences in nanoparticle size distribution as a function of the excipient type used. The size distribution function is characterized by the mean particle diameter and the standard deviation of the diameter (given as a percentage of the mean and denoted as SD%). These values are reported in Table 4, and their relationship with the grinding variables is analyzed quantitatively in the main effects plots (Figs. 2 and 3) and interaction plots (Figs. 4 and 5). The main effects plot shows the average response for each value of each variable, combining the effects of the other variables as if all variables were independent. The main effects plots for the meloxicam particle diameter indicate that the tested excipients can all promote size reduction (Fig. 2). Increasing the relative amount of meloxicam in the system resulted in larger product particles, whereas increasing the milling energy (grinding rate) reduced the particle size. Since our goal was to grind meloxicam into uniformly small particles so that its administration can be controlled, it was important to study the main effects plots characterizing the broadness of the particle size distribution curve (SD%) (Fig. 3). It is evident from Fig. 3 that the excipients PVP-K25 and PEG 6000 provide significantly broader and narrower diameter distributions, respectively, than the other two tested additives. Increase of the meloxicam to additive ratio resulted in a less uniform product. On the other hand, the distribution uniformity as a function of the milling energy exhibited a minimum at 300 rpm.

Interaction plots illustrate the effects between variables, which are not independent by showing the means of the responses for each level of a factor for each level of a second factor pairwise for all factors involved in the study. Therefore, the interaction plots presented in Figs. 4 and 5 for the mean diameter and the SD%, respectively, can be used to gain insight into the complex interactions between the grinding parameters. For example: (i) all additives but PVP-C30 result in a particle diameter increase at higher milling rates, (ii) increasing the milling frequency can compensate the diameter differences introduced by changing the meloxicam to additive ratio, (iii) the use of PEG 6000 as additive results in particularly narrow size distributions, regardless of the choice of the other two parameters, etc.

We are now in a position to summarize the grinding behavior of the novel NSAID meloxicam in a high-energy ball mill with Si₃N₄ as grinding material. In the absence of any grinding additives, the final product particles are too large at low milling energy ($d_{SEM} = 364$ nm at 200 rpm) and aggregate rapidly at high energy ($d_{SEM} = 343$ nm at 400 rpm). There is an optimum at 300 rpm. However, even at this setting, the average product particle size is above $d_{SEM} = 270$ nm. It is interesting to note that, without additives, the relative broadness of the particle size distribution function was independent of the milling energy (SD~61%).

With PVP-C30, it was possible to push the average meloxicam particle size below 250 nm and the average SD below 50%. This was a significant improvement relative to the additive-free grinding result. The optimum co-grinding parameter set for PVP-C30 was a meloxicam to excipient ratio = 1:1, and a rotation frequency of 400 rpm.

Table 4
Particle diameter (d_{SEM}) of meloxicam particles in different compositions.

Excipient	Meloxicam/excipient ratio	Rotation speed (rpm)	$d_{SEM} \pm SD$ (nm)
–	1:0	–	2643.6 ± 2629.1
–	1:0	200	364.5 ± 228.1
–	1:0	300	275.0 ± 170.6
–	1:0	400	343.5 ± 205.9
PVP-C30	1:0.5	200	511 ± 333
PVP-C30	1:1	200	267 ± 158
PVP-C30	1:2	200	221.7 ± 105.4
PVP-C30	1:0.5	300	243 ± 115
PVP-C30	1:1	300	242 ± 141
PVP-C30	1:2	300	302.3 ± 115.7
PVP-C30	1:0.5	400	209.9 ± 85.3
PVP-C30	1:1	400	140.4 ± 69.2
PVP-C30	1:2	400	238.6 ± 147.9
PVP-K25	1:0.5	200	203.6 ± 190.0
PVP-K25	1:1	200	192.7 ± 74.4
PVP-K25	1:2	200	229.1 ± 203.2
PVP-K25	1:0.5	300	266.3 ± 117.0
PVP-K25	1:1	300	351.7 ± 227.7
PVP-K25	1:2	300	277.6 ± 139.9
PVP-K25	1:0.5	400	251.5 ± 362.6
PVP-K25	1:1	400	246.4 ± 108.5
PVP-K25	1:2	400	262.8 ± 124.7
PEG 6000	1:0.5	200	175.2 ± 57.4
PEG 6000	1:1	200	212.3 ± 92.0
PEG 6000	1:2	200	–
PEG 6000	1:0.5	300	165.0 ± 59.6
PEG 6000	1:1	300	204.4 ± 88.9
PEG 6000	1:2	300	358.1 ± 145.3
PEG 6000	1:0.5	400	197.3 ± 84.8
PEG 6000	1:1	400	229.5 ± 92.3
PEG 6000	1:2	400	173.8 ± 60.3
PEG 20,000	1:0.5	200	368.7 ± 238.0
PEG 20,000	1:1	200	318.8 ± 136.2
PEG 20,000	1:2	200	200.0 ± 134.6
PEG 20,000	1:0.5	300	235.5 ± 117.7
PEG 20,000	1:1	300	217.6 ± 103.7
PEG 20,000	1:2	300	–
PEG 20,000	1:0.5	400	185.1 ± 73.7
PEG 20,000	1:1	400	234.5 ± 122.9
PEG 20,000	1:2	400	333.8 ± 151.0

If the target drug administration task allows the application of PEG 6000 as additive, then it is possible to improve the co-grinding process further. The parameter setting meloxicam to PEG 6000 = 1:2 at a rotation frequency of 400 rpm yields nanoparticles averaging $d_{SEM} = 174$ nm in diameter and a very narrow size distribution, characterized by SD = 35%. This set is the overall optimum result in our study.

The most promising products of the co-grinding process were further investigated by XRPD analysis. The optimized products (Table 5, Fig. 6) differ in their crystallinity, which can be observed in the diffraction spectra (Fig. 7). The XRPD patterns of meloxicam, physical mixtures and products containing meloxicam and excipients in the optimized ratio are presented. The presence of numerous distinct peaks in the XRPD spectrum indicates that meloxicam is a crystalline material; its characteristic peaks appear at diffraction angles 2θ of 13.22, 15.06, 26.46 and 26.67°. The crystallinity of meloxicam was decreased in the co-grinding process with PVP-C30; in the other optimized product, which contains PEG 6000 the crystallinity of meloxicam did not change significantly comparing to the physical mixture. The crystalline meloxicam was altered in the co-grinding process with the amorphous excipient, PVP-C30, leading to amorphous nanoparticles. With PEG 6000 as excipient, the crystallinity of meloxicam was proved (Fig. 7), i.e. meloxicam nanocrystals were prepared.

The extent of dissolution was determined under conditions of nasal drug delivery (Fig. 8). Under *in vitro* circumstances, we attempted to mimic the physiological conditions of the human nose; the temperature of the dissolution medium was 30 °C and the

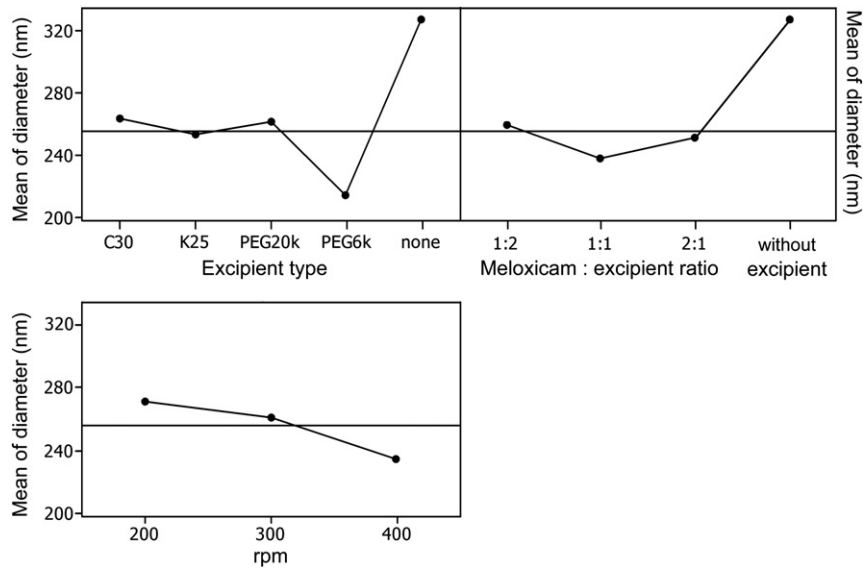


Fig. 2. Influence of different parameters (main effects plot, data means) on meloxicam crystal diameter (C30 = PVP-C30, K25 = PVP-K25, PEG20k = PEG 20,000, PEG6k = PEG 6000).

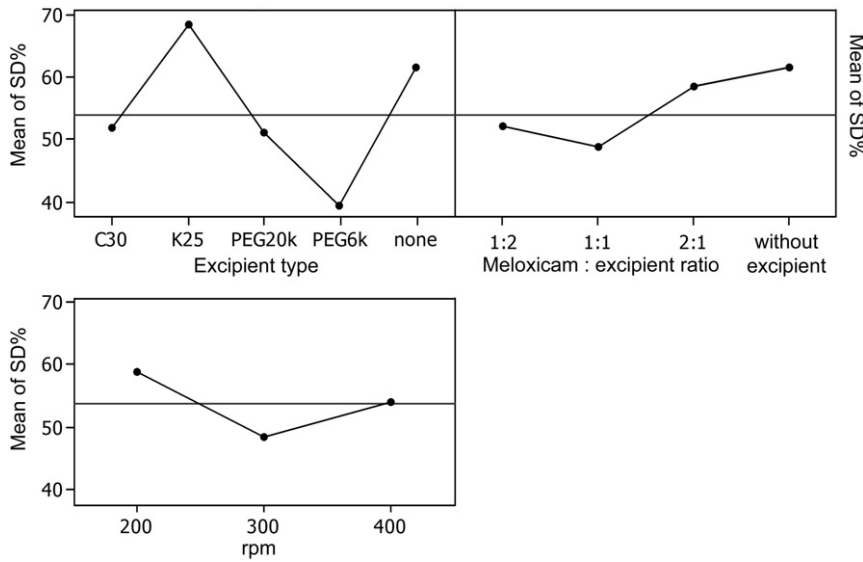


Fig. 3. Main effects plot (data means) for SD% (C30 = PVP-C30, K25 = PVP-K25, PEG20k = PEG 20,000, PEG6k = PEG 6000).

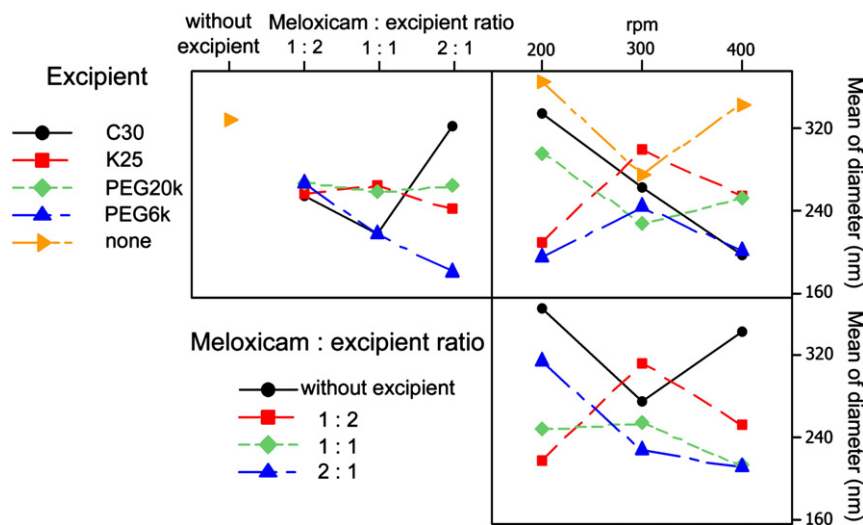


Fig. 4. Interaction plot (data means) for diameter (C30 = PVP-C30, K25 = PVP-K25, PEG20k = PEG 20,000, PEG6k = PEG 6000).

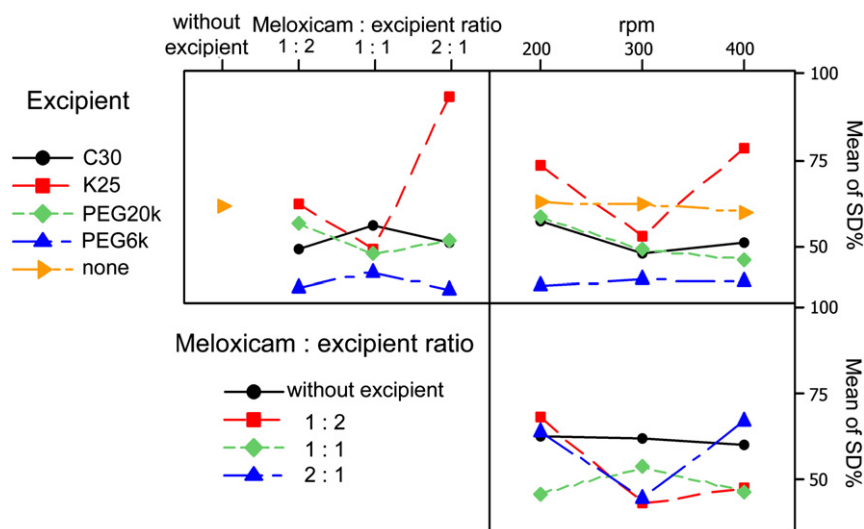


Fig. 5. Interaction plot (data means) for SD% (C30 = PVP-C30, K25 = PVP-K25, PEG20k = PEG 20,000, PEG6k = PEG 6000).

Table 5

Optimized products.

Grinding excipient of meloxicam	Drug to excipient ratio	Rotation speed (rpm)
PVP-C30	1:1	400
PEG 6000	1:2	400

pH was 5.6. These conditions alter the dissolution properties of the effective agent: lower temperature and pH decreases the extent of meloxicam dissolution, although the particle size reduction enhances the extent of dissolution. In the meloxicam PVP-C30 composition, the extent of dissolution after 60 min increased in case of the co-ground product from $4.1 \pm 0.21\%$ to $66.2 \pm 4.73\%$ relative to the physical mixture of the effective agent and the excipient. In the background of this phenomenon stands in one hand the reduction of the particle size (nanonization) and on the other hand the decrease in crystallinity of the effective agent (amorphization). Nanoparticles improve dissolution rate and bioavailability of poorly water-soluble drugs [38–41] owing to increased surface area available for dissolution as described by the Noyes–Whitney equation [42]. The co-grinding technique has already been employed for amorphization of drugs [43,44].

A two-fold enhancement of the extent of meloxicam dissolution was observed in the case of the meloxicam PEG 6000 co-ground product, in which meloxicam is in nanocrystal form. By now, main attention was focussed on size and related surface area. It was recently reported that the interfacial reaction resistance is getting the velocity determining parameter for crystals below $1 \mu\text{m}$. Design of nanocrystals

with faster interfacial reaction can further enhance the dissolution velocity [45]. In addition, nanomaterials possess improved adhesiveness to biological membranes [7]. The extent of meloxicam dissolution after 60 min in the physical mixture was $4.1 \pm 0.21\%$, while that for the optimized product was $8.3 \pm 0.08\%$. In the physical mixtures the excipient had no influence on the extent of meloxicam dissolution, contrary products, which were undergone nanonization with co-grinding process, showed significantly higher extent of dissolution.

Nanonization and amorphization of meloxicam resulted in significantly better dissolution properties in the *in vitro* dissolution studies under conditions, which mimic the physiological pH and temperature of the human nose.

Insoluble powders are likely to be effective for nasal systemic drug delivery [46]. The nasal powder formulations enhance systemic bioavailability, and are superior to liquid formulations [47,48] from the aspects of increased chemical stability of the drug, no requirement for preservatives in the formulations, and the feasibility of administering relatively large amounts of drug [49–51].

4. Conclusions

This study explored the effects of additives on the co-grinding behavior of the frequently applied NSAID meloxicam in a high-energy planetary ball mill. It was shown that both PVP and PEG as additives can act as efficient excipients in the mechanical size reduction of meloxicam particles. The influence of the grinding parameters: additive type, meloxicam to additive ratio and milling frequency on the product particle size distribution function was studied via a full

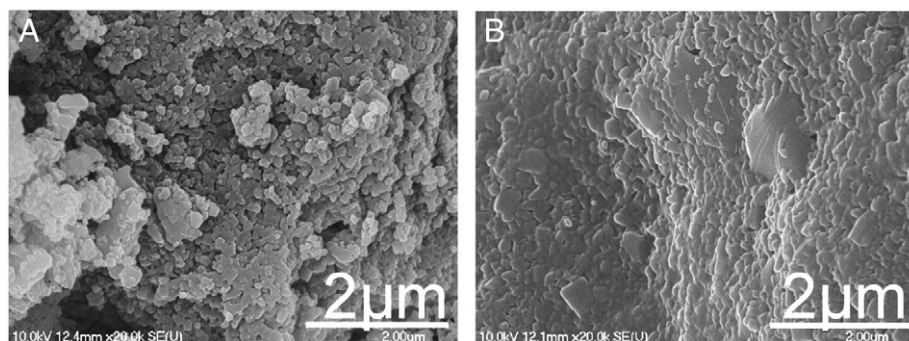


Fig. 6. Scanning electron microscopic images from the optimized products: meloxicam after co-grinding with PVP-C30 in a ratio of 1:1 at 400 rpm (A), meloxicam after co-grinding with PEG 6000 in a ratio of 1:2 at 400 rpm (B)/from all of the products PVP and PEG were dissolved with distilled water due to the visualization of meloxicam particles/.

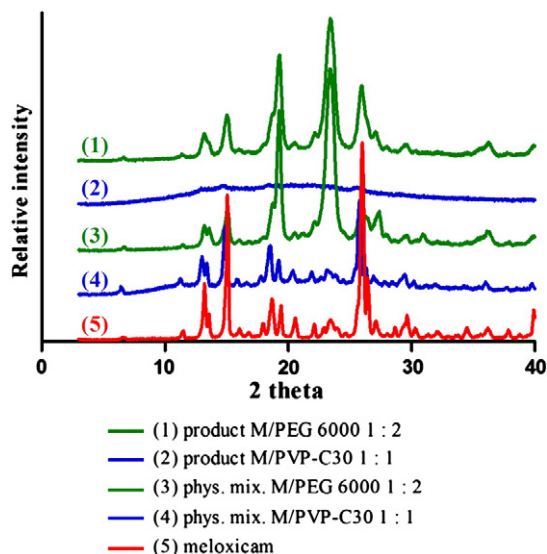


Fig. 7. X-ray powder diffraction spectra of meloxicam (5), physical mixtures (4, 3) and products of meloxicam co-grinded with PVP-C30 (2), meloxicam with PEG 6000 (1).

factorial design. Optimum grinding parameter sets for the nitrogen-containing additive PVP (meloxicam to PVP-C30 ratio = 1:1, rotation frequency 400 rpm) and for nitrogen-free PEG 6000 (meloxicam to PEG 6000 = 1:2, rotation frequency 400 rpm) were identified.

XRPD analysis indicated that the optimized products contained amorphous meloxicam nanoparticles in the PVP-C30 composition, although meloxicam nanocrystals could be detected in the samples which contained PEG 6000. The dissolution properties are also significantly increased under nasal conditions (pH 5.1, temperature 30 °C), especially in the case of the amorphous product. These dry powder systems can offer novel opportunities in systemic nasal drug delivery.

These products are suitable for further investigations in *in vitro* cell culture models, in *ex vivo* tissue models and in *in vivo* animal experiments with the aim of intranasal systemic drug delivery.

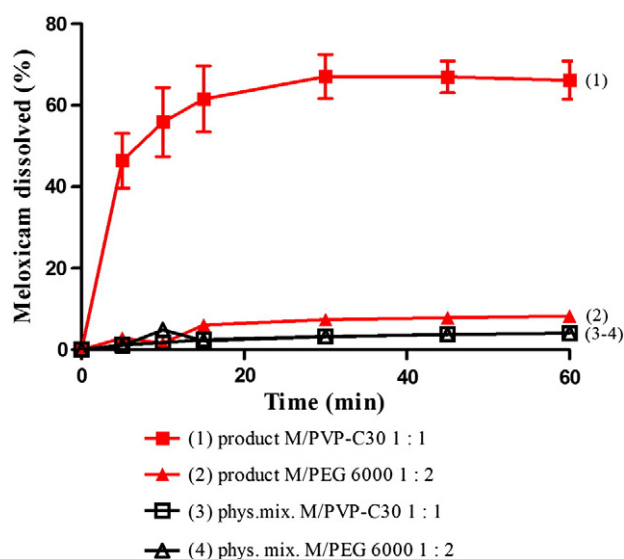


Fig. 8. The extent of meloxicam dissolution in the optimized products and in the physical mixtures, dissolution circumstances: pH 5.6 ± 0.1 , 30 ± 0.5 °C.

Acknowledgement

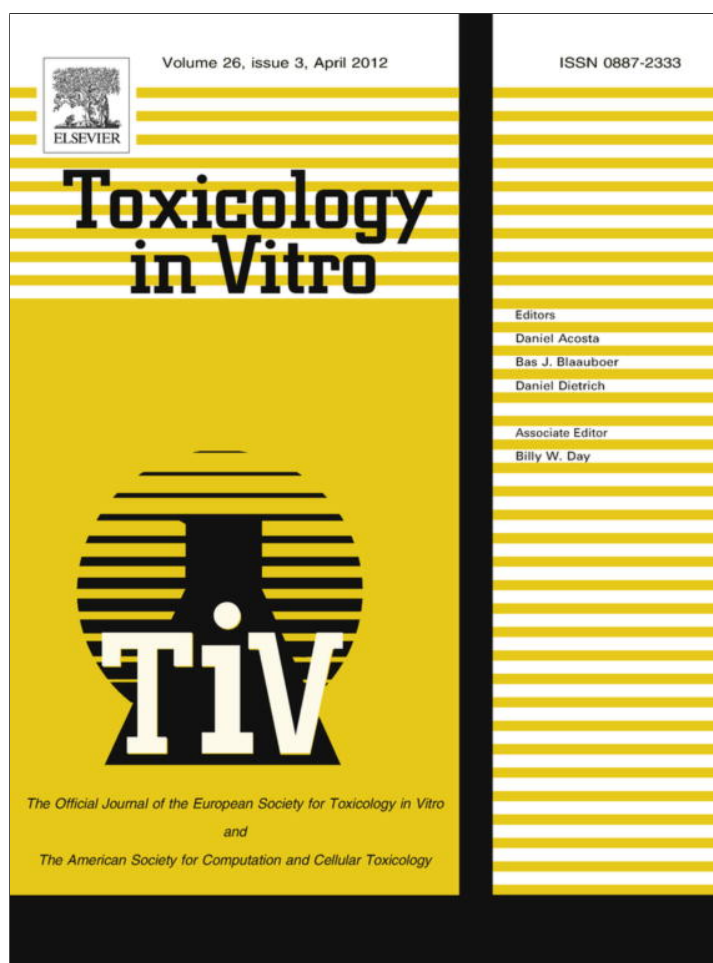
This work was supported by the TÁMOP research project TÁMOP-4.2.1/B-09/1/KONV-2010-0005 and the OTKA-NNF 78920 project.

References

- [1] M.J. Alonso, Nanomedicines for overcoming biological barriers, *Biomed. Pharmacother.* 58 (2004) 168–172.
- [2] A. Graf, E. Ablinger, S. Peters, A. Zimmer, S. Hook, T. Rades, Microemulsions containing lecithin and sugar-based surfactants: nanoparticle templates for delivery of proteins and peptides, *Int. J. Pharm.* 350 (2008) 351–360.
- [3] W.H. De Jong, P.J.A. Borm, Drug delivery and nanoparticles: applications and hazards, *Int. J. Nanomed.* 3/2 (2008) 133–149.
- [4] H. Chen, C. Khemtong, X. Yang, X. Chang, J. Gao, Nanonization strategies for poorly water-soluble drugs, *Drug Discov. Today* (2010), doi:10.1016/j.drudis.2010.02.009.
- [5] J. Brookings, S.S. Davis, L. Illum, Transport of nanoparticles across the rat nasal mucosa, *J. Drug Target* 9 (2001) 267–279.
- [6] M. Rawat, D. Singh, S. Saraf, Nanocarriers: promising vehicle for bioactive drugs, *Biol. Pharm. Bull.* 29/9 (2006) 1790–1798.
- [7] R. Shegokar, R.H. Müller, Nanocrystals: industrially feasible multifunctional formulation technology for poorly soluble actives, *Int. J. Pharm.* 399 (2010) 129–139.
- [8] C.M. Keck, R.H. Müller, Drug nanoparticles of poorly soluble drugs produced by high pressure homogenisation, *Eur. J. Pharm. Biopharm.* 62 (2006) 3–16.
- [9] O.d. Veigt, H. Vromans, J.d. Toonder, K.v.d.V. Maarschalk, Influence of flaws and crystal properties on particle fracture in a jet mill, *Powder Technol.* 191 (2009) 72–77.
- [10] G. Delagrammatikas, M. Delagrammatikas, S. Tsimas, Particle size distributions a new approach, *Powder Technol.* 176 (2007) 57–65.
- [11] H. Kubo, T. Osawa, K. Takashima, M. Mizobe, Enhancement of oral bioavailability and pharmacological effect of by micronization in co-ground mixture with d-mannitol, *Biol. Pharm. Bull.* 19 (1997) 741–747.
- [12] G.G. Liversidge, K.C. Cundy, Particle size reduction for improvement of oral bioavailability of hydrophobic drugs: absolute oral bioavailability of nanocrystalline danazol in beagle dogs, *Int. J. Pharm.* 125 (1995) 91–97.
- [13] M. Sugimoto, T.S. Okagaki, S. Narisawa, Y. Koida, K. Nakajima, Improvement of dissolution characteristics and bioavailability of poorly water-soluble drugs by novel cogrinding method using water-soluble polymer, *Int. J. Pharm.* 160 (1998) 11–19.
- [14] T. Yamada, N. Saito, T. Imai, M. Otagiri, Effect of grinding with hydroxypropyl cellulose on the dissolution and particle size of a poorly water-soluble drug, *Chem. Pharm. Bull.* 47 (1999) 1311–1313.
- [15] G.G. Liversidge, K.C. Cundy, J. Bishop, D. Czekai, Surface modified drug nanoparticles, *US Patent* (1992) 5,145,684.
- [16] B.E. Rabinow, Nanosuspensions in drug delivery, *Nat. Rev. Drug Discov.* 3 (2004) 785–796.
- [17] K. Moribe, A. Pongpeerapat, Y. Tozuka, K. Yamamoto, Drug nanoparticle formation from drug/HPMC/SDS ternary ground mixtures, *Pharmazie* 61 (2006) 97–101.
- [18] C. Zapata, C. Frances, N. Le Bolay, S. Molina-Boisseau, Production of small composite particles by co-grinding in a media mill. Characterization of the granulometric and the mechanical properties, *Trans. IChemE, Part A, Ch. E. R. D.* 82 (A5) (2004) 631–636.
- [19] M. Barzegar-Jalali, H. Valizadeh, M.-R. Siahi Shadbad, K. Adibkia, G. Mohammadi, A. Farahani, Z. Arash, A. Nokhodchi, Cogrounding as an approach to enhance dissolution rate of a poorly water-soluble drug (gliclazide), *Powder Technol.* 197 (2010) 150–158.
- [20] Á. Kukovecz, D. Méhn, E. Nemes-Nagy, R. Szabó, I. Kiricsi, Optimization of CCVD synthesis conditions for single-wall carbon nanotubes by statistical design of experiments (DoE), *Carbon* 43 (2005) 2842–2849.
- [21] S.L.A. Hennart, M.C. Domingues, W.J. Wildeboer, P. van Hee, G.M.H. Meesters, Study of the process of stirred ball milling of poorly water soluble organic products using factorial design, *Powder Technol.* 198 (2010) 56–60.
- [22] M. Fahmy, Ca-alginate beads loaded with meloxicam: effect of alginate chemical composition on the properties of the beads and ulcerogenicity of the drug, *J. Drug Del. Sci. Technol.* 16 (2006) 183–189.
- [23] G. Hanft, D. Turck, S. Scheuerer, R. Sigmund, Meloxicam oral suspension: a treatment alternative to solid meloxicam formulations, *Inflamm. Res.* 50 (2001) 35–37.
- [24] R. Ambrus, P. Kocbek, J. Kristl, R. Sibanc, R. Rajkó, P. Szabó-Révész, Investigation of preparation parameters to improve the dissolution of poorly water-soluble meloxicam, *Int. J. Pharm.* 381 (2009) 153–159.
- [25] M. Jafar, M.H.G. Dehghan, A. Shareef, Enhancement of dissolution and antiinflammatory effect of meloxicam using solid dispersions, *Int. J. App. Pharm.* 2/1 (2010) 22–27.
- [26] T.P. Shakhshneider, M.A. Vasilchenko, A.A. Politov, V.V. Boldyrev, The mechanochemical preparation of solid disperse systems of ibuprofen–polyethylene glycol, *Int. J. Pharm.* 130 (1996) 25–32.
- [27] K. Ioth, A. Pongpeerapat, Y. Tozuka, T. Oguchi, K. Yamamoto, Nanoparticle formation of poorly water-soluble drugs from ternary ground mixtures with PVP and SDS, *Chem. Pharm. Bull.* 51 (2) (2003) 171–174.
- [28] L.S. Taylor, G. Zografi, Spectroscopic characterization of interactions between PVP and indomethacin in amorphous molecular dispersion, *Pharm. Res.* 14 (1997) 1691–1698.

- [29] T. Watanabe, S. Hasegawa, N. Wakiyama, A. Kusai, M. Senna, Comparison between polyvinylpyrrolidone and silica nanoparticles as carriers for indomethacin in a solid state dispersion, *Int. J. Pharm.* 250 (2003) 283–286.
- [30] R. Smajda, Á. Kukovecz, Z. Kónya, I. Kiricsi, Structure and gas permeability of multi-wall carbon nanotube buckypapers, *Carbon* 45/6 (2007) 1176–1184.
- [31] M. Daranyi, Á. Kukovecz, E. Horváth, Z. Kónya, I. Kiricsi, Fine tuning the coverage of a titanate nanowire layer on a glass substrate, *Chem. Phys. Lett.* 460 (1–3) (2008) 191–195.
- [32] J.A. Melero, G. Calleja, F. Martinez, R. Molina, M.I. Pariente, Nanocomposite Fe₂O₃/SBA-15: an efficient and stable catalyst for the catalytic wet peroxidation of phenolic aqueous solutions, *Chem. Eng. J.* 131 (1–3) (2007) 245–256.
- [33] M.D. Abramoff, P.J. Magelhaes, S.J. Ram, Image processing with image, *J. Biophotonics Int.* 11/7 (2004) 36–42.
- [34] R. Remias, Á. Kukovecz, M. Daranyi, G. Kozma, S. Varga, Z. Kónya, I. Kiricsi, Zn-glycerolate microstacks, *Eur. J. Inorg. Chem.* 24 (2009) 3622–3627.
- [35] C. Zapata-Massot, C. Frances, N. Le Bolay, On the use of scanning electron microscopy for the modelling of co-grinding kinetics in a tumbling ball mill, *Powder Technol.* 143–144 (2004) 215–229.
- [36] J. Alkebro, S. BeHgin-Colin, A. Mocellin, R. Warren, Modeling high-energy ball milling in the alumina–yttria system, *J. Solid State Chem.* 164 (2002) 88–97.
- [37] P.P. Chattopadhyay, I. Manna, S. Talapatra, S.K. Pabi, A mathematical analysis of milling mechanics in a planetary ball mill, *Mater. Chem. Phys.* 68 (2001) 85–94.
- [38] R.H. Muller, A. Akkar, Drug nanocrystals of poorly soluble drugs, in: J.A. Schwarz, C. Contescu, K. Putyera (Eds.), *Encyclopedia of Nanoscience and Nanotechnology*, Marcel Dekker, New York, 2004, pp. 627–638.
- [39] V.B. Patravale, A.A. Date, R.M. Kulkarni, Nanosuspensions: a promising drug delivery strategy, *J. Pharm. Pharmacol.* 56 (2004) 827–840.
- [40] M. Mosharraf, C. Nystrom, The effect of particle size and shape on the surface specific dissolution rate of micronized practically insoluble drugs, *Int. J. Pharm.* 122 (1995) 35–47.
- [41] F. Kesiosoglou, S. Panmai, Y. Wu, Nanosizing — oral formulation development and biopharmaceutical evaluation, *Adv. Drug Deliv. Rev.* 5916 (2007) 31–44.
- [42] A.A. Noyes, W.R. Whitney, The rate of solution of solid substances in their own solutions, *J. Am. Chem. Soc.* 19 (1897) 930–934.
- [43] M. Senna, S. Nakayama, Preparation and properties of nano-amorphous organic and inorganic particles via chemical and mechanochemical routes, *J. Alloys Compd.* 483 (2009) 265–270.
- [44] R.S. Dhumal, S.V. Biradar, S. Yamamura, A.R. Paradkar, P. York, Preparation of amorphous cefuroxime axetil nanoparticles by sonoprecipitation for enhancement of bioavailability, *Eur. J. Pharm. Biopharm.* 70 (2008) 109–115.
- [45] M.T. Crisp, C.J. Tucker, T.L. Rogers, R.O. Williams III, K.P. Johnston, Turbidimetric measurement and prediction of dissolution rates of poorly soluble drug nanocrystals, *J. Control. Release* 117 (2007) 351–359.
- [46] F. Ishikawa, M. Murano, M. Hiraishi, T. Yamaguchi, I. Tamai, A. Tsuji, Insoluble powder formulation as an effective nasal drug delivery system, *Pharm. Res.* 19 (2002) No. 8.
- [47] N. Fransén, S. Bredenberg, E. Björk, Clinical study shows improved absorption of desmopressin with novel formulation, *Pharm. Res.* 26 (2009) 1618–1625.
- [48] N. Fransén, E. Björk, C. Nyström, Development and characterisation of interactive mixtures with a fine-particulate mucoadhesive carrier for nasal drug delivery, *Eur. J. Pharm. Biopharm.* 67 (2007) 370–376.
- [49] F. Ishikawa, M. Katsura, I. Tamai, A. Tsuji, Improved nasal bioavailability of elcatonin by insoluble powder formulation, *Int. J. Pharm.* 224 (2001) 105–114.
- [50] W.A. Lee, B.A. Narog, T.W. Patapoff, Y.J. Wang, Intranasal bioavailability of insulin powder formulations: effect of enhancer-to-protein ratio, *J. Pharm. Sci.* 80 (1991) 72–729.
- [51] N.G.M. Schipper, S.G. Romejin, J.C. Verhoef, F.W.H.M. Merkus, Nasal insulin delivery with dimethyl-β-cyclodextrin as an absorption enhancer in rabbits: powder more effective than liquid formulations, *Pharm. Res.* 10 (1993) 682–686.

PUBLICATION III.



This article appeared in a journal published by Elsevier. The attached copy is furnished to the author for internal non-commercial research and education use, including for instruction at the authors institution and sharing with colleagues.

Other uses, including reproduction and distribution, or selling or licensing copies, or posting to personal, institutional or third party websites are prohibited.

In most cases authors are permitted to post their version of the article (e.g. in Word or Tex form) to their personal website or institutional repository. Authors requiring further information regarding Elsevier's archiving and manuscript policies are encouraged to visit:

<http://www.elsevier.com/copyright>



Contents lists available at [SciVerse ScienceDirect](http://www.sciencedirect.com)

Toxicology in Vitro

journal homepage: www.elsevier.com/locate/toxinvit



The effect of sucrose esters on a culture model of the nasal barrier

Levente Kürti^{a,b}, Szilvia Veszelka^a, Alexandra Bocsik^a, Ngo Thi Khue Dung^a, Béla Ózsvári^c,
László G. Puskás^c, Ágnes Kittel^d, Piroska Szabó-Révész^b, Mária A. Deli^{a,*}

^a Laboratory of Molecular Neurobiology, Institute of Biophysics, Biological Research Centre of the Hungarian Academy of Sciences, Temesvári Krt. 62, H-6726 Szeged, Hungary

^b Department of Pharmaceutical Technology, University of Szeged, Eötvös u. 6, H-6720 Szeged, Hungary

^c Avidin Ltd., Közép fasor 52, H-6726 Szeged, Hungary

^d Institute of Experimental Medicine, Hungarian Academy of Sciences, Szigony u. 43, H-1083 Budapest, Hungary

ARTICLE INFO

Article history:

Received 12 July 2011

Accepted 10 January 2012

Available online 17 January 2012

Keywords:

Cytotoxicity

Sucrose ester

Human nasal epithelial cell

RPMI 2650 cell line

Cell electronic sensing

Epithelial permeability

ABSTRACT

Sucrose esters are effective solubilizers and there is an interest to use them as pharmaceutical excipients for nasal drug delivery. We have determined for the first time the non-toxic doses of laurate and myristate sucrose esters by four independent methods, and their effects on epithelial permeability using RPMI 2650 human nasal epithelial cell line. Based on real-time cell electronic sensing, MTT dye conversion and lactate dehydrogenase release methods reference surfactant Cremophor RH40 proved to be the least toxic excipient, and could be used at 5 mg/mL concentration for 1 h in epithelial cells without cellular damage. The non-toxic dose of Tween 80 was 1 mg/mL, while the dose of laurate and myristate sucrose esters that could be safely used on cells for 1 h was 0.1 mg/mL. Both the reference surfactants and the sucrose esters significantly enhanced the permeability of epithelial cell layers for the paracellular marker FITC-labelled 4.4 kDa dextran at 0.1 mg/mL concentration. The effects of sucrose esters on epithelial permeability were dose-dependent. These data indicate that laurate and myristate sucrose esters can be potentially used as permeability enhancers in nasal formulations to augment drug delivery to the systemic circulation.

© 2012 Elsevier Ltd. All rights reserved.

1. Introduction

Intranasal administration is an effective way to deliver drugs into the systemic circulation as an alternative to the oral and parenteral routes for some therapeutic agents (Chien et al., 2008). Undoubtedly, the nasal administration of medicines has been widely used for the treatment of topical nasal conditions such as nasopharyngitis or allergic rhinitis for many years. The nasal pathway may circumvent the blood–brain barrier and allow centrally acting pharmacos a direct transport route to the central nervous system (Illum, 2000; Horvát et al., 2009). Concerning systemic delivery, drugs can be rapidly absorbed through the nasal mucosa, resulting in a quick onset of action, and avoiding degradation in the gastrointestinal tract and first-pass metabolism in the liver (Ugwoke et al., 2001; Arora et al., 2002).

Nasal absorption is affected by physicochemical, anatomical and physiological, as well as formulation factors. The bioavailability of different active agents varies between 1% and 90%. Many drugs display high bioavailability by the nasal route, particularly if they have lipophilic characteristics (Davis and Illum, 2003). The number of nasal formulations which are available on the market is rapidly growing. The use of nasal administration of drugs is

especially important in the treatment of migraine, severe pain and hormone replacement (Illum, 2003).

Lipophilic drugs can be expected to demonstrate rapid and efficient absorption when given nasally, but more polar compounds are poorly absorbed. Bioavailabilities of about 1% are to be expected for biopharmaceuticals such as insulin, calcitonin or leuproline, and even less for higher molecular weight peptides and proteins such as growth hormone, interferons and growth factors (Kissel and Werner, 1998). The poor uptake of drugs from the nasal cavity can be associated with three major factors, (i) poor transport across the nasal epithelium; (ii) possible enzymatic degradation in the nasal cavity; (iii) rapid mucociliary clearance from the absorption site (Schmidt et al., 1998).

The critical factor for nasal absorption is the penetration across the nasal epithelial cell layers. The pathways for absorption across the nasal respiratory epithelium are similar to those across other epithelia in the body. Lipophilic drugs are transported transcellularly by passive lipid-mediated free diffusion, whereas hydrophilic compounds cross the barrier passively via the paracellular pathway, or use active carrier- or receptor-mediated processes (Deli, 2009).

Since the junctions between epithelial cells constitute the strongest barrier in the nasal system (Wolburg et al., 2008), considerable effort has been directed towards the development of technologies that can improve the permeation across these cells (Illum, 2003). Methods to enhance or promote absorption by using

* Corresponding author. Tel.: +36 62 599602; fax: +36 62 433133.

E-mail address: deli@brc.hu (M.A. Deli).

Table 1
Structure and properties of reference surfactants.

	Polyoxylated 40 hydrogenated castor oil Cremophor RH40	Macrogol-glycerolhydroxystearate 40 (Ph. Eur.)
Chemical structure		
Chemical name	Polyethoxylated sorbitan and oleic acid	Polyethoxylated 40 hydrogenated castor oil
Trade name	Tween 80	Cremophor RH40
Composition	70%: oleic acid (C ₁₈ H ₃₄ O ₂) 30%: linoleic, palmitic and stearic acid	90%: ricinoleic acid (C ₁₈ H ₃₄ O ₃) 10%: linoleic, oleic, palmitic and stearic acid
Physical properties	Viscous water-soluble yellow liquid	White to yellowish thin paste at 20 °C
HLB	15	15
Applications	Non-ionic surfactant and emulsifier	

HLB, hydrophile-lipophile balance; Ph. Eur., European Pharmacopoeia.

formulation additives have therefore been extensively studied. Absorption enhancers can increase permeation of drug molecules through the barriers of the body, including the nasal epithelium (Deli, 2009). Surfactants, cationic polymers, cyclodextrins and many other types of compounds have been applied so far (Alpar et al., 2005).

Surfactants are solubilising excipients widely used in oral, injectable and nasal formulations (Davis and Illum, 2003). Non-ionic surfactants have been shown to be less toxic than ionic surfactants to biological membranes (Arechabala et al., 1999). Macrogol-glycerolhydroxystearate 40 (Cremophor RH40) and polysorbate 80 (Tween 80) are non-ionic solubilising and emulsifying agents (Table 1). These surfactants can be used to increase bio-availability of drugs by solubilising of poorly soluble compounds, increasing cell membrane fluidity, or augmenting paracellular absorption (MacDonald et al., 2010).

Sucrose fatty acid esters are non-ionic surface-active agents consisting of sucrose as hydrophilic group and fatty acids as lipophilic groups (Table 2). Sucrose contains 8 hydroxyl groups, and it is therefore possible to produce sucrose esters containing from 1 to 8 fatty acid moieties. In sucrose esters, the fatty acids are attached to sucrose, a disaccharide consisting of two monosaccharides, glucose and fructose. The commercial sucrose esters are mixtures of sucrose esters with various esterification degrees. Due to their complexity, they exhibit very diverse behaviour, like the glycerides. Sucrose esters are commonly used in food and cosmetic industries as emulsifiers, antibacterial agents or crystallization inhibitors (Mutoh et al., 2007; Garti et al., 2000). Recently there has been great interest to use them also in the field of pharmacy. There are data about the applicability of sucrose esters as permeation enhancers through the skin (Csóka et al., 2007), and our group demonstrated that sucrose esters can be successfully used in hot melt technology (Szűts et al., 2007, 2008). We have recently described an improved dissolution of gemfibrozil from a ternary solid dispersion system containing laurate sucrose ester (Szűts et al., 2011). Due to their good solubilising properties there is an interest to use sucrose esters as pharmaceutical excipients for nasal drug delivery. However there are no data on their toxicity and effect on human nasal epithelial cells.

The use of cell-based assays is crucial for understanding the toxicity and efficacy of excipients (Fernández Freire et al., 2009). For the development of relevant strategies to overcome biological barriers and in order to screen the feasibility of the nasal route for systemic delivery, a number of nasal *in vitro* models have been developed. Cell culture systems and excised nasal mucosae provide meaningful *in vitro* models to study the permeation and metabolic barrier of the nasal epithelium (Schmidt et al., 1998; Dimova et al., 2005). The RPMI 2650 cell line originates from an anaplastic nasal septum tumour and is closely related to normal human nasal epithelium (Moore and Sandberg, 1964). This immortalised human cell line has a potential as an *in vitro* model of the nasal barrier for testing various drug candidates (Bai et al., 2008).

Our aim was to study the effects of potential innovative pharmaceutical excipients, laurate and myristate sucrose esters and reference non-ionic surfactants, Tween 80 and Cremophor RH40 on cell viability and paracellular permeability of human nasal epithelial cells.

2. Materials and methods

All reagents were purchased from Sigma–Aldrich, Hungary, unless otherwise indicated. Laurate sucrose ester was of pharmaceutical grade, and myristate sucrose ester of analytical grade (Mitsubishi Kagaku Foods Co., Japan). Tween 80 and Cremophor RH40 (BASF, Germany) were of pharmaceutical grade.

Table 2
Structure and properties of sucrose esters.

Sucrose fatty acid esters	
Chemical structure	
Chemical name	Laurate sucrose ester
Trade name	Surfhope SE Pharma D-1216 (US DMF)
Fatty acid	Lauric acid (C ₁₂ H ₂₄ O ₂)
R-	
Solubility	Soluble in water
HLB	16
Applications	Non-ionic surface-active agents, emulsifiers, antibacterial agents, crystallization inhibitors, permeation enhancers
	Myristate sucrose ester Ryoto sugar ester M-1695 Myristic acid (C ₁₄ H ₂₈ O ₂) Soluble in water 16

HLB, hydrophile-lipophile balance; US DMF, US drug master file.

2.1. Cell culture

RPMI 2650 (ATCC cat. no. CCL 30) cells were grown in Eagle's minimal essential medium (MEM) supplemented with 10% foetal bovine serum (FBS) and 50 µg/mL gentamicin in a humidified 37 °C incubator with 5% CO₂. The cells were seeded in rat tail collagen (0.05%) coated culture dishes at a density of 5×10^5 cells per cm² and the medium was changed every 2 days. When RPMI 2650 cells reached approximately 80–90% confluence in the dish they were trypsinized with 0.05% trypsin–EDTA solution. For the cytotoxicity assays cells were passaged to 96-well plate, for immunohistochemistry and fluorescent staining cells were cultured on glass coverslips. For permeability studies cells were cultured in Transwell filter inserts (polycarbonate membrane, 0.4 µm pore size, 1.12 cm² surface area, Corning Costar Co., USA). All surfaces were coated with 0.05% rat tail collagen before cell seeding. For all types of experiments, including toxicity assays, independent cell cultures were used for each parameter.

2.2. Electron microscopy

RPMI 2650 cells grown on Transwell filter membrane were fixed with 3% paraformaldehyde in 0.05 M cacodylate buffer (pH 7.5) for 30 min at 4 °C. After washing with cacodylate buffer several times, the membranes of the culture inserts with the cells were removed from their support and placed into 24-well chamber slide and were postfixed in 1% OsO₄ for 30 min. Following washing with distilled water, the cells on the membrane were dehydrated in graded ethanol, block-stained with 1% uranyl acetate in 50% ethanol for 30 min and embedded in Taab 812 (Taab; Aldermaston, Berks, UK). Following polymerisation at 60 °C for 12 h, ultrathin sections were cut perpendicularly for the membrane using a Leica UCT ultramicrotome (Leica Microsystems, Milton Keynes, UK) and examined using a Hitachi 7100 transmission electron microscope (Hitachi Ltd., Japan). Electron micrographs were made by Megaview II (lower resolution, Soft Imaging System, Germany). Brightness and contrast were adjusted if necessary using Adobe Photoshop CS3 (USA).

2.3. Immunohistochemistry

RPMI 2650 cells cultured on rat tail collagen coated glass coverslips and were stained for junctional protein β-catenin. The cultures were washed in phosphate buffered saline (PBS) and fixed with 4% paraformaldehyde – PBS for 30 min. After washing with PBS cells were blocked with 3% bovine serum albumin

(BSA) – PBS and incubated with primary antibody anti-β-catenin (Invitrogen, USA) for 1 h and 30 min. Incubation with secondary antibody Cy3-labelled anti-rabbit IgG and Hoechst dye 33342 to stain cell nuclei lasted for 1 h. Between and after incubations cells were washed three times with PBS. Coverslips were mounted in Gel Mount (Biomedica, USA) and staining was examined by a Nikon Eclipse TE2000 fluorescent microscope (Nikon, Japan) and photographed by a Spot RT digital camera (Diagnostic Instruments, USA).

2.4. Treatments

The doses of laurate and myristate sucrose esters varied between 0.01 and 3 mg/mL. The reference surfactants Tween 80 and Cremophor RH40 were tested at 1–100 mg/mL concentrations in culture medium. The stock solutions were made from various excipients by dissolving them in distilled water.

2.5. Cell cytotoxicity assays

Real-time cell electronic sensing (RT-CES) is a label-free technique for dynamic monitoring of living cells (Xing et al., 2005; Xia et al., 2008). This system utilises an electronic readout called impedance to non-invasively quantify adherens cell proliferation and viability in real-time. A special 96-well E-plate (Roche, Hungary) contains microelectronic sensor arrays. The interaction between cells and electrode generates impedance response that correlates linearly with cell index reflecting cell number, adherence and cell growth (Ózsvári et al., 2010). The E-plate was coated with 0.2% gelatine – PBS solution for 20 min at 37 °C. Culture media (80 µL) was added to each well for background readings, than 80 µL cell suspension was dispensed at the density of 6×10^3 cells/well. The cells were kept in incubator at 37 °C for 24 h and monitored every 5 min. The cell index at each time point was defined as $(R_n - R_b)/15$, where R_n is the cell-electrode impedance of the well when it contains cells and R_b is the background impedance of the well with the media alone.

Lactate dehydrogenase (LDH) release, the indicator of cell membrane damage, was determined from culture supernatants by a commercially available kit (Cytotoxicity detection kit LDH, Roche). For LDH release assay RPMI 2650 cells were cultured in 96-well plates. After treatments with absorption enhancers 50 µL samples from culture supernatants were incubated with equal amounts of reaction mixture for 15 min. The enzyme reaction was stopped by 0.1 M HCl. Absorbance was measured at a wavelength of 450 nm with a microplate reader (Fluostar Optima, BMG Labtechnologies,

Germany). Cytotoxicity is calculated as percentage of the total LDH release from cells treated by 10 mg/mL Triton X-100 detergent.

Living cells convert the yellow dye 3-(4,5-dimethylthiazol-2-yl)-2,5-diphenyltetrazolium bromide (MTT) to purple, insoluble formazan crystals. RPMI 2650 cells were cultured in 96-well plates. After treatments the cells were incubated with 0.5 mg/mL MTT solution for 3 h in CO₂ incubator. The amount of formazan crystals was dissolved in dimethyl-sulfoxide and determined by measuring absorbance at 570 nm with a microplate reader (Fluostar Optima, BMG Labtechnologies, Germany).

Viability and nuclear morphology of RPMI 2650 cells were confirmed by fluorescent staining. Bis-benzimide (Hoechst dye 33342; Sigma) labels the nuclei of both viable and dead cells. Ethidium-homodimer-1 (Molecular Probes, USA) cannot pass through the plasma membrane of viable cells, therefore only stains dead cells. Cell layers grown on collagen-coated coverslips were treated with surfactants for 30 min, then 10 μ M bis-benzimide and ethidium-homodimer-1 was added for another 30 min. At the end of incubation cells were fixed in 4% paraformaldehyde in PBS for 30 min, washed three times in PBS, mounted, and analysed using a fluorescent microscope (Nikon Eclipse TE2000, Japan) and photographed by a Spot RT digital camera (Diagnostic Instruments, USA).

2.6. Measurement of transepithelial electrical resistance (TEER)

Transepithelial electrical resistance (TEER), representing the permeability of tight junctions for sodium ions in culture conditions, was measured by an EVOM resistance metre (World Precision Instruments Inc., USA) using STX-2 electrodes, and it was expressed relative to the surface area of epithelial layers ($\Omega \times \text{cm}^2$). The TEER of nasal epithelial cell layers varied between 110 and 140 $\Omega \times \text{cm}^2$. RT-CES made it also possible to monitor the TEER changes after treatments with pharmaceutical excipients. Before treatment the cell layers had reached an equilibrium phase and their TEER values were around 150 Ω measured by the xCelligence system. TEER values (R_n) were calculated from cell index and background impedance by the following equation:

$$R_n(\Omega) = (\text{cell index} \times 15) + R_b$$

2.7. Paracellular permeability experiments

The flux of fluorescein isothiocyanate labelled dextran (FITC-dextran, mw: 4.4 kDa) across epithelial cell layers was determined in permeability studies. RPMI 2650 cells were seeded onto Transwell filter inserts and grown for 2 days. The inserts were transferred to 12-well plates containing 1.5 mL Ringer–Hepes solution (118 mM NaCl, 4.8 mM KCl, 2.5 mM CaCl₂, 1.2 mM MgSO₄, 5.5 mM D-glucose, 20 mM Hepes, pH 7.4) in the basolateral compartments. In apical chambers culture medium was replaced by 500 μ L Ringer–Hepes containing 100 μ g/mL FITC-dextran and selected concentrations of surfactants. The plates were kept in a 37 °C incubator with 5% CO₂ for 1 h on a rocking platform. After incubation the concentrations of the marker molecule in samples from the apical and basolateral compartments were determined by a fluorescent microplate reader (Fluostar Optima, BMG Labtechnologies, Germany; emission: 485 nm, excitation: 520 nm). Flux across cell-free inserts was also measured. The apparent permeability coefficient (P_{app}) was calculated. Cleared volume was calculated from the concentration difference of the tracer in the abluminal compartment ($\Delta[C]_A$) after 1 h and luminal compartments at 0 h ($[C]_L$), the volume of the abluminal compartment (V_A ; 1.5 mL) and the surface area available for permeability (A ; 1.12 cm²) by the following equation:

$$P_{\text{app}}(\text{cm/s}) = \frac{\Delta[C]_A \times V_A}{A \times [C]_L \times \Delta t}$$

2.8. Statistical analysis

All data presented are means \pm S.D. The values were compared using the analysis of variance followed by Dunnett tests using GraphPad Prism 5.0 software (GraphPad Software Inc., USA). Changes were considered statistically significant at $P < 0.05$. All independent experiments were repeated at least three times, the number of parallel samples within assays varied between 4 and 12. Inter-assay precision was calculated for all types of assays, and the coefficients of variation (CV%) were below 15%.

3. Results

3.1. Characteristics of the RPMI 2650 cell culture model

Confluent layers of RPMI 2650 human nasal epithelial cells were obtained on collagen-coated surfaces. According to phase contrast microscopy and electron microscopy RPMI 2650 cells grew in mono- or multilayers (Fig. 1). A cubic and polarised cell morphology, microvilli on the apical surface, could be observed. Healthy, intact cell constituents, like mitochondria, endoplasmic reticulum and large cell nuclei with few cytoplasm were visualised by electron microscopy. These characteristics are typical for epithelial cells *in vivo* as well. Intercellular junctions play an important role in barrier function of the cell layers. Tight intercellular junctions were visualised by electron microscopy (Fig. 1C). By immunofluorescent microscopy adherens junction protein β -catenin was detected on the border of cells (Fig. 1B). Faint cytoplasmic staining was also visible in agreement with the known signalling mechanism of this protein. Besides morphological investigations the presence of nasal barrier was confirmed by functional measurements as well. The transepithelial electric resistance values of the confluent cell layers were around 150–200 Ω . The apparent permeability coefficient of RPMI 2650 cell layers for paracellular marker 4.4 kDa FITC-dextran was $9.68 \pm 0.49 \times 10^{-6}$ cm/s.

3.2. Effects of sucrose esters and reference surfactants on RPMI 2650 cell viability

The toxicity of surfactants on RPMI 2650 cells was tested by RT-CES method. Laurate and myristate sucrose esters at 0.1 mg/mL concentrations did not reduce cell index reflecting cell viability significantly, but had a profound effect in concentrations higher than 0.1 mg/mL after 1-h treatment (Fig. 2A). Tween 80 had no influence on the cell index after 1-h treatment at 1 mg/mL, but decreased the cell index below 50% at 10 mg/mL concentration (Fig. 2B). After 1-h treatment none of the studied concentrations of Cremophor RH40 (1, 10, 50 mg/mL) caused alteration in cell index, indicating no cell damage. Our toxicity control, TritonX-100 caused 90% reduction in cell index values. This drastic reduction indicates cellular death (Fig. 2), in agreement with MTT and LDH release data.

The effect of surfactants on the plasma membrane integrity of RPMI 2650 cells were determined by LDH release and on epithelial cell viability by MTT dye conversion assay (Fig. 3). The release of LDH from RPMI 2650 cells into the extracellular space increased significantly in a dose-dependent way in cultures treated with 0.3 mg/mL and higher concentrations of laurate and 0.1 mg/mL and higher concentrations of myristate sucrose esters (Fig. 3A and B). A maximal LDH release indicating 100% toxicity was observed for both sucrose esters at 1 mg/mL dose comparable to the effect of 10 mg/mL Triton X-100. The reference surfactants Tween 80, Cremophor RH40 were non-toxic for RPMI 2650 cells under 10 mg/mL concentration for 1 h treatment period (Table 3). The 4-h MTT dye conversion cell viability test, reflecting intracellular enzyme activities, and endo- and exocytosis, proved to be more

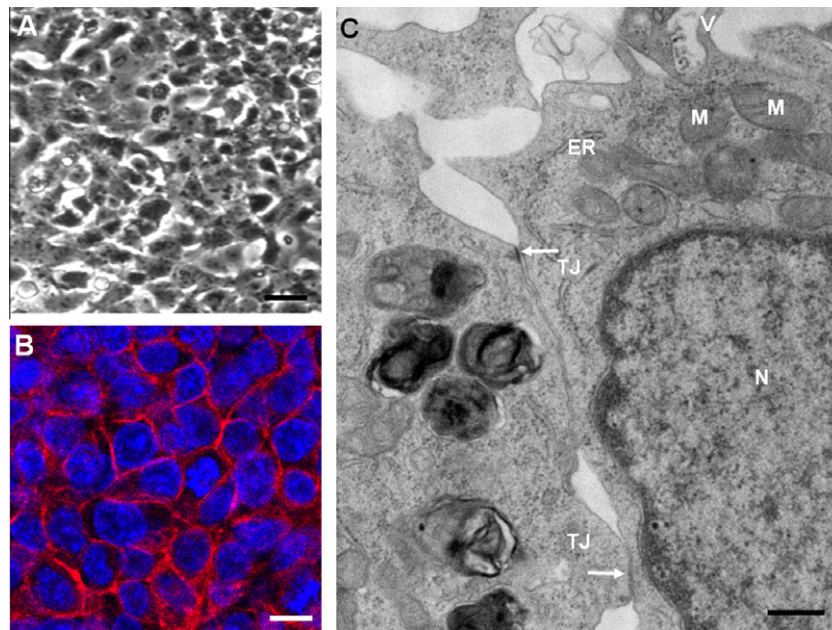


Fig. 1. Morphological characterisation of RPMI 2650 human nasal epithelial cell line. Phase contrast microscopic image of the cells (A; bar: 25 μ m) and confocal microscopic image of β -catenin immunostaining (B; bar: 10 μ m) show cobble-stone, epithelial morphology. Electron microscopic image of RPMI 2650 cells where arrows indicate tight intercellular junctions (C) (N, nucleus; M, mitochondrion; ER, endoplasmic reticulum; TJ, tight junction; V, microvilli; bar: 250 nm).

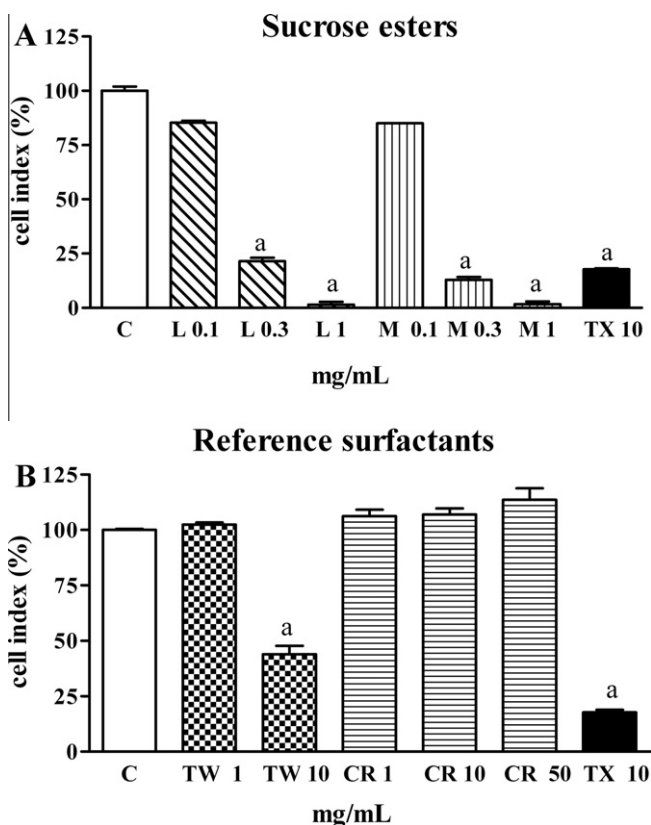


Fig. 2. Changes in cell index indicating viability of RPMI 2650 cells after 1-h treatment with sucrose esters (A) and with reference surfactants (B). a: significantly different as compared to control group, $p < 0.05$. Data are presented as mean \pm S.D., $n = 4$ parallel samples. C, control; CR, Cremophor RH40; TW, Tween 80; L, laurate sucrose ester; M, myristate sucrose ester; TX, TritonX-100.

sensitive than the LDH release assay. Sucrose esters over 0.1 mg/mL concentration significantly reduced the viability of RPMI 2650 cells in a dose-dependent way (Fig. 3C and D). In agreement with

the findings measured by LDH release, a complete loss of cell viability could be detected at sucrose ester doses higher than 0.3 mg/mL, comparable to the effect of the toxicity control. In these experiments reference surfactants were toxic over 3 mg/mL concentration (Table 3).

Besides functional tests the toxicity of excipients was proved by morphological methods as well. The double fluorescent staining of nasal epithelial cell nuclei was performed after 1-h treatment of the cells with surfactants (Fig. 4). In agreement with the results of other viability assays, the toxicity of 1 mg/mL sucrose esters and 5 mg/mL Tween 80 was confirmed, while at lower concentrations no sign of cytotoxicity was detected on RPMI 2650 cells (Fig. 4). Cremophor RH40 at both 1 and 5 mg/mL concentrations had negligible effect on cell viability.

Results from the toxicity assays on RPMI 2650 cells for all four excipients are summarised in Table 3. The non-toxic concentrations of sucrose esters as compared to Tween 80 and Cremophor RH40 were at least one order of magnitude higher. We could confirm with the cell electric sensing method, that the non-toxic dose of laurate sucrose ester was still safe after 24-h treatment period, while the non-toxic dose of Cremophor RH40 has drastically dropped to 1 mg/mL at 24 h as compared to previous time-points.

3.3. Effects of sucrose esters and reference surfactants on epithelial barrier integrity

Sucrose esters elicited dose-dependent TEER changes (Fig. 5A and B). At 0.1 mg/mL concentrations both laurate and myristate sucrose esters led to a significant and transient TEER decrease, while 0.3 mg/mL and higher concentrations caused an irreversible drop of TEER. Tween 80 at 10 mg/mL dose also resulted in a significant TEER decrease, while the smaller concentration, similarly to 1 and 10 mg/mL concentration of Cremophor RH40 did not cause changes as compared to control group.

By treating the confluent layers of RPMI 2650 epithelial cells with previously determined safe, non-toxic concentrations of various surfactants, permeability experiments with FITC-dextran, a hydrophilic paracellular marker with an average molecular weight

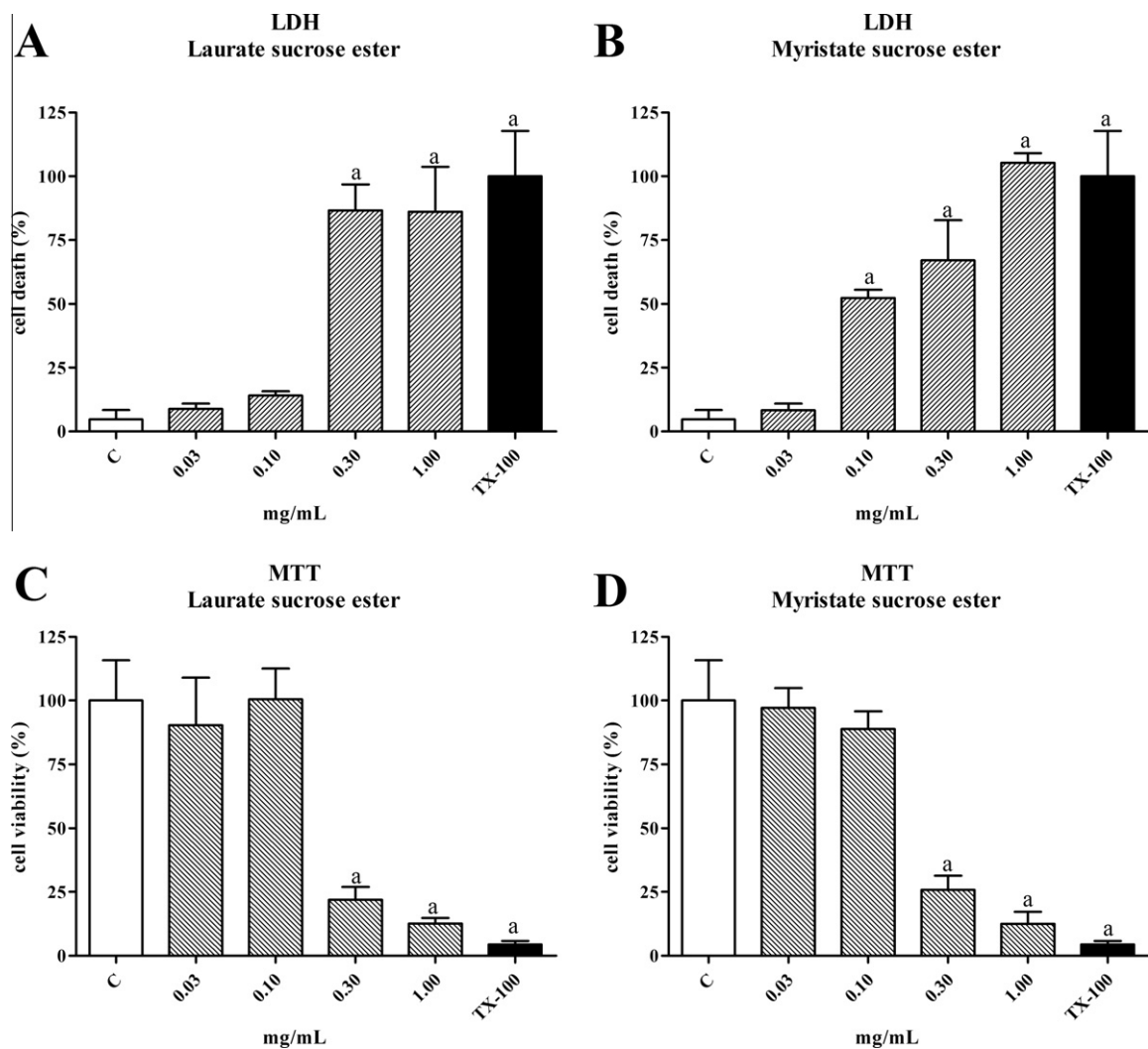


Fig. 3. Toxicity of sucrose esters on RPMI 2650 cells after 1-h treatment measured by LDH release assay (A and B) and after 4-h treatment measured by MTT reduction assay (C and D). a: significantly different as compared to control group. All values presented are means \pm S.D., three independent experiments with at least eight parallel samples, $p < 0.05$. LDH, lactate dehydrogenase; MTT, 3-(4,5-dimethylthiazol-2-yl)-2,5-diphenyltetrazolium bromide; TX, TritonX-100. Inter-assay coefficients of variation between the independent experiments: <10%.

of 4.4 kDa, the size of a peptide were performed. Laurate sucrose ester increased significantly the permeability of RPMI 2650 cell layers in a concentration-dependent manner (Fig. 6A). After 1-h treatment with 0.1 mg/mL laurate sucrose ester the apparent

permeability coefficient of FITC-dextran was increased by 50% in agreement with TEER results.

Comparing the effects of sucrose esters and the reference surfactants on the permeability for the marker molecule across

Table 3
Comparison of cellular toxicity of surfactants measured by different methods (concentrations in mg/mL).

Surfactant	RT-CES			LDH release assay 1 h			MTT reduction assay 4 h			Nucleus staining ^a 1 h
	1 h TD 0 mg/mL	4 h TD 0 mg/mL	24 h TD 0 mg/mL	TD 0 mg/mL	TD 50 mg/mL	TD 100 mg/mL	TD 0 mg/mL	TD 50 mg/mL	TD 100 mg/mL	
Laurate SE	0.10	0.10	0.10	0.10	0.20	0.30	0.10	0.20	1.00	<1.00
Myristate SE	0.10	0.10	<0.10	0.03	0.10	1.00	0.10	0.20	1.00	<1.00
TW	1.00	1.00	<1.00	10.00	>100.0	>100.00	3.00	>100.0	>100.00	<5.00
CR	>50.00	>50.00	1.00	10.00	>100.0	>100.00	3.00	60.00	>100.00	>5.00

For all types of toxicity assays independent cell cultures were used for each parameter. All independent experiments were repeated at least three times, the number of parallel samples within assays varied between 4 and 12. Inter-assay precision was calculated for all types of assays, and the coefficients of variation (CV%) were below 15%. CR, Cremophor RH40; LDH, lactate dehydrogenase; MTT, 3-[4,5-dimethylthiazol-2-yl]-2,5-diphenyl tetrazolium bromide; RT-CES, real-time cell electric sensing; SE, sucrose ester; TD 0, non-toxic dose; TD 50, dose causing 50% cellular toxicity; TD 100, dose causing 100% cellular toxicity; TW, Tween 80.

^a Nucleus staining was done by fluorescent dyes bis-benzimide and ethidium-homodimer-1 (see Fig. 4).

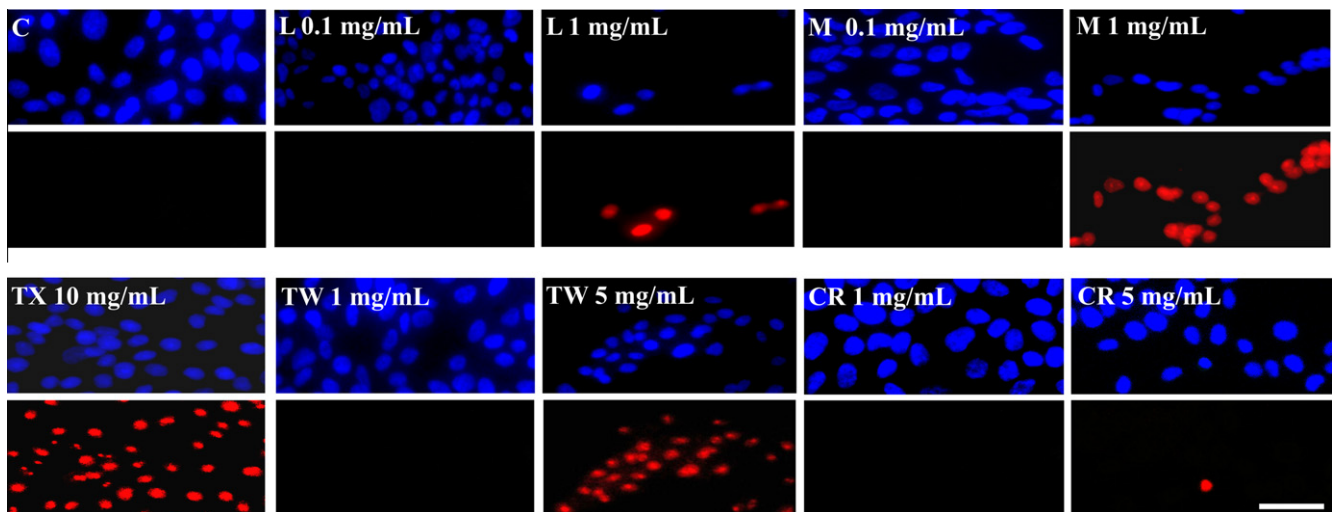


Fig. 4. Double fluorescent staining of nuclei of RPMI 2650 cells shows the cytotoxicity of excipients after 1-h treatment. Blue colour indicates cell nuclei of living and dead cells, red colour indicates cell nuclei of dead cells. C, control; CR, Cremophor RH40; L, laurate sucrose ester; M, myristate sucrose ester; TW, Tween 80; TX, TritonX-100. Bar: 30 μ m.

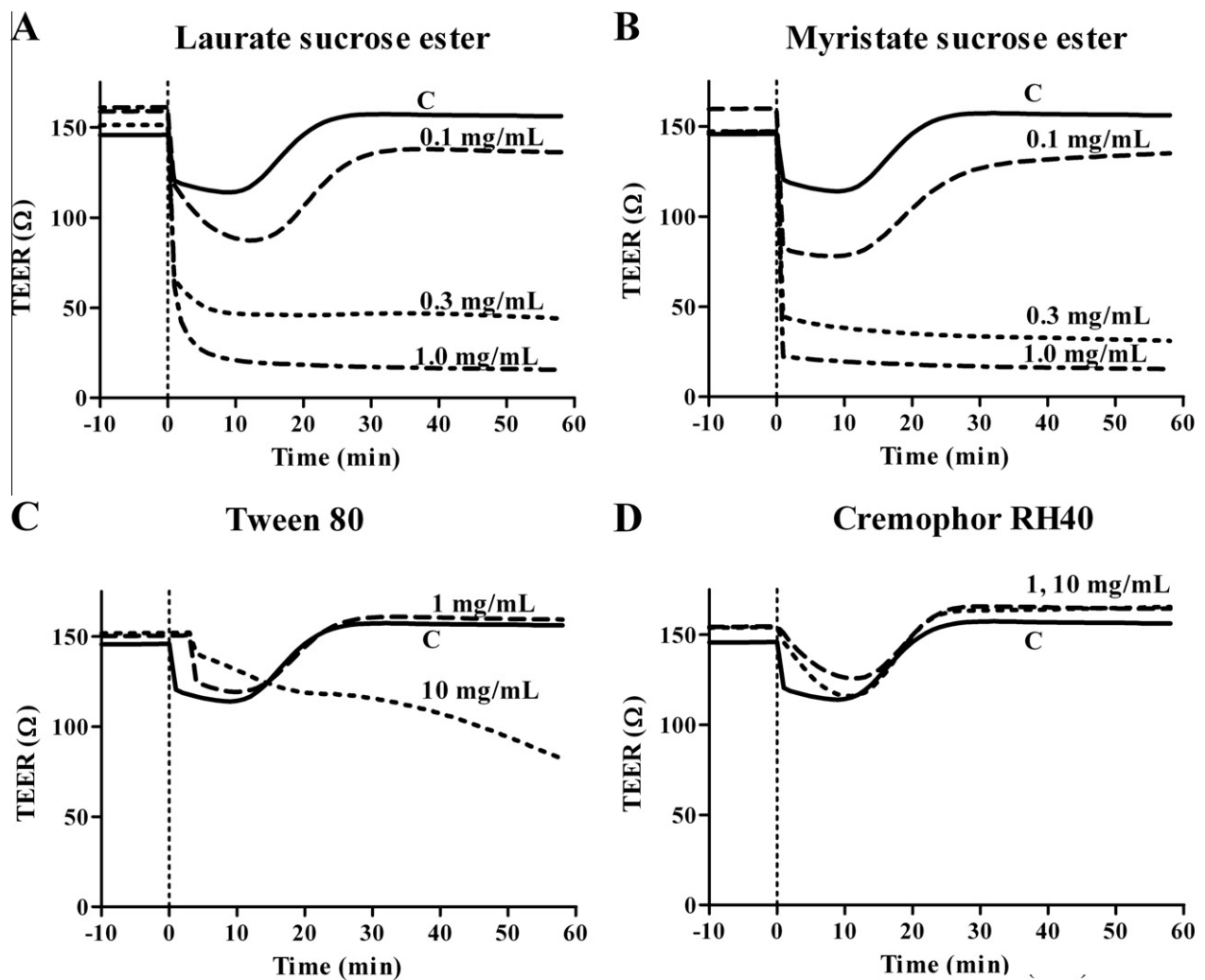


Fig. 5. Kinetics of the changes in transepithelial resistance of RPMI 2650 cells after treatment with surfactants. Broken line at 0 min indicates the onset of treatment. Data are presented as mean, $n = 4$. C, control; TEER, transepithelial electric resistance.

epithelial cell layers, the same, non-toxic concentration of 0.1 mg/mL was chosen for all compounds. All excipients increased signif-

icantly the epithelial paracellular permeability; the largest increase was seen in case of laurate sucrose ester, the P_{app} values were

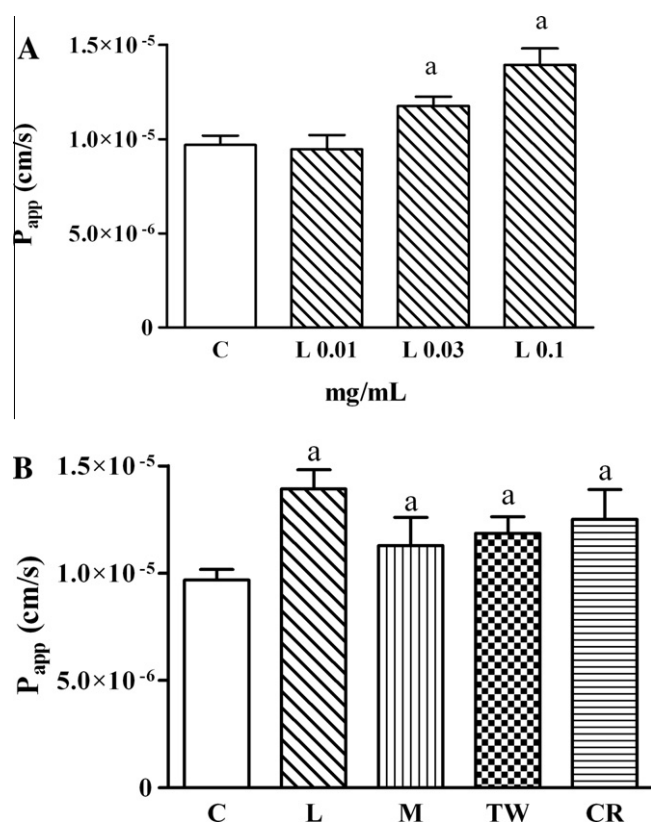


Fig. 6. The effect of non-toxic doses (0.01, 0.03, 0.1 mg/mL) of laurate sucrose ester (A) and of excipients applied in the same concentration of 0.1 mg/mL (B) on the apparent permeability coefficients of FITC-dextran on confluent RPMI 2650 cell layers. a: significantly different as compared to control group, $p < 0.05$. Data are presented as mean \pm S.D., $n = 3$. C, control; CR, Cremophor RH40; L, laurate sucrose ester; M, myristate sucrose ester; TW, Tween 80; P_{app} , apparent permeability coefficient.

elevated from $9.68 \pm 0.49 \times 10^{-6}$ cm/s to $1.39 \pm 0.09 \times 10^{-5}$ cm/s after 1-h treatment (Fig. 6B).

4. Discussion

4.1. In vitro cell culture model of the nasal barrier

Due to the importance of systemic nasal drug delivery there is a need for cell culture models of the human nasal barrier for testing various compounds for toxicity and permeability. The properties of such *in vitro* systems need to be compared with *in vivo* circumstances. Primary nasal cell cultures show several *in vivo* epithelial characteristics including proper cell differentiation, presence of apical cilia, confluent mono- or multilayer formation, production of mucoid materials and presence of intercellular junctions (Werner and Kissel, 1996). However, primary cell cultures used for transport studies have considerable limitations such as sterility, the short lifetime of cells, the low reproducibility and high cost (Kissel and Werner, 1998; Werner and Kissel, 1996; Lin et al., 2005). One of the possible solutions for these problems could be the use of *in vitro* immortalised cell lines.

The culture conditions and applicability of RPMI 2650 cells as an epithelial model are contradictory in the literature. De Fraissinette et al. (1995) discussed the limits of the use of this cell line as an *in vitro* nasal model for drug absorption. In their experiments RPMI 2650 cells formed cell clusters on filters, although they also had tendency to spread in a cell layer. The cells never showed cell polarisation, nor microvilli or tight junctions, and were not able to form tight cell layers. In another study RPMI 2650 cells grew in

multilayers, typical for the nasal epithelium, but cell polarisation and differentiation could not be detected (Schmidt et al., 1998). In contrast to the above mentioned studies, using different culture conditions including air-liquid interface RPMI 2650 cells formed layers suitable for permeability assays (Bai et al., 2008; Wengst and Reichl, 2010).

In our experiments RPMI 2650 cells grew as mono- or multilayers and reached confluence in liquid-liquid interface culture condition. The presence of intercellular junctions was confirmed by electron and immunofluorescent microscopy. Besides morphological investigations the functional properties of the nasal epithelial barrier such as resistance and paracellular permeability were also proved. Our data are in agreement with results from *in vivo* and other *in vitro* models (Schmidt et al., 1998). Advantages of the presented *in vitro* nasal system includes simplicity of culture, reproducibility, suitability for permeability studies and RT-CES. RPMI 2650 cells model the respiratory zone of the human nasal epithelium which is the most important absorption surface for nasally administered drugs to the systemic circulation. The absence of cilia and air-liquid interface can be considered as limitations of this nasal model. The presented data support that RPMI 2650 cells can be successfully used to establish an *in vitro* model of the nasal barrier and to test toxicity and epithelial permeability.

4.2. Cytotoxicity of sucrose esters and reference surfactants

Sucrose esters are widely used in cosmetic and food industry. Due to their advantageous properties as emulsifiers, solubilizers and permeation enhancers, the potential of sucrose esters to be used as pharmaceutical excipients has been investigated recently (Csóka et al., 2007; Szűts et al., 2007, 2008, 2011). The applicability of surface active agents as permeability enhancers is limited by their toxicity (Deli, 2009), therefore it is essential to determine their safe, non-toxic concentrations.

The toxicity of sucrose esters was tested for the first time in an *in vitro* model of the nasal barrier. Four different independent methods were used to measure cell viability, a label-free, real-time cell electric sensing technique, two colorimetric methods, LDH release and MTT conversion tests, and finally a morphological method, cell nucleus staining. Colorimetric methods are advisable only for the preliminary phase of a cell death study (Weyermann et al., 2005; Galluzzi et al., 2009; Fernández Freire et al., 2009). These assays suffer from several drawbacks, first, they are endpoint determinations, second, higher concentrations of excipients may interfere with the detection method (Weyermann et al., 2005). In our experiments the highest non-toxic concentrations of reference surfactants were determined by the 1-h LDH assay. This result might be due either to the interference of these excipients with the enzyme reaction or to their inability to affect cellular plasma membrane. The 4-h MTT test was more sensitive, and lower concentrations of excipients were found non-toxic. The increased sensitivity might be related not only to the longer assay time but also to the higher complexity of the MTT reduction where several cellular processes, mitochondrial and cytoplasmic enzyme activity, endo- and exocytosis are involved (Liu et al., 1997). The nucleus staining method was suitable for the morphological confirmation of the toxic concentrations of the excipients, but could not provide kinetic data and exact determination of the non-toxic, 50% or 100% toxic doses.

Due to the limitations mentioned above we have used a technological approach that provides kinetic measurement in cell-based assays (Ózsvári et al., 2010). The real-time cell electric sensing technology monitors cell viability status in a simple homogeneous assay format over a broad time frame, from minutes to several days. It is a non-invasive, highly sensitive measurement and has a reduced interference with normal cell function (Solly et al.,

2004; Boyd et al., 2008). This method was the most sensitive to determine the safe concentrations of the excipients at different incubation times. It is noteworthy that the difference between the non-toxic concentrations of sucrose esters and reference molecules dropped drastically after 24-h treatment. The epithelial cell viability at non-toxic sucrose esters doses remained constant. In contrast the toxicity of Cremophor RH40 and Tween 80 increased over time, which might indicate *in vivo* toxicity after longer treatment.

By applying various toxicity assays our results indicate that sucrose esters were more toxic than reference surfactants, especially for shorter incubation times. However, this difference significantly decreased when cells were examined with real-time monitoring for 24 h. In oral preparations the cellular toxicity of excipients can be diminished by dilution in the gastrointestinal fluids, but in the nasal mucous membrane, considerable dilution cannot be expected and the mucosa is more sensitive. Therefore, the safe concentrations of excipients determined by cellular assays need to be taken into consideration at the formulation process of nasal vehicles.

4.3. Sucrose esters as potential permeability enhancers

Real-time electric sensing provided quantitative information about the biological status of RPMI 2650 human nasal epithelial cells, including cell number, viability, and adherence indicating paracellular permeability. Sucrose esters had a dose-dependent effect on epithelial permeability in non-toxic concentration range. A transient effect on the resistance of RPMI 2650 cell layers has been observed, which was unique for sucrose esters. Although these novel excipients were not found to be more effective permeability enhancers than the reference compounds, their effect on paracellular permeability of cultured human epithelial cells have been demonstrated for the first time. The increase in paracellular permeability elicited by the non-toxic concentrations of sucrose esters might be related to their effect on intercellular junctions. No LDH release was detected at these concentrations indicating an intact plasma membrane integrity. While *in vitro* cytotoxicity correlated with the paracellular permeability on Caco-2 cells (Konsoula and Barile, 2005), in case of the tested excipients effects on paracellular permeability were seen at non-toxic concentrations. To reveal the mechanism of action of sucrose esters further experiments are necessary.

5. Conclusions

As a summary of our work, we can conclude that (i) several methods are needed to determine the cytotoxicity and the safe dose of surface active pharmaceutical excipients including real-time cell analysis; (ii) although the safe, non-toxic doses of sucrose esters that can be applied to cultured cells are lower than those of Tween 80 and Cremophor RH40, they remain constant with longer incubation time; (iii) due to their effect on epithelial resistance and permeability, sucrose esters have a potential to be applied as excipients in nasal formulations.

Conflict of Interest

No conflict of interest.

Acknowledgements

The Project named “TÁMOP-4.2.1/B-09/1/KONV-2010-0005 – Creating the Centre of Excellence at the University of Szeged” is

supported by the European Union and co-financed by the European Regional Development Fund.

References

- Alpar, H.O., Somavarapu, S., Atuah, K.N., Bramwell, V.W., 2005. Biodegradable mucoadhesive particulates for nasal and pulmonary antigen and DNA delivery. *Adv. Drug Deliv. Rev.* 57, 411–430.
- Arechabala, B., Coiffard, C., Rivalland, P., Coiffard, L.J., de Roeck-Holtzhauer, Y., 1999. Comparison of cytotoxicity of various surfactants tested on normal human fibroblast cultures using the neutral red test, MTT assay and LDH release. *J. Appl. Toxicol.* 19, 163–165.
- Arora, P., Sharma, S., Garg, S., 2002. Permeability issues in nasal drug delivery. *Drug Discovery Today* 7, 967–975.
- Bai, S., Yang, T., Abbruscato, T.J., Ahsan, F., 2008. Evaluation of human nasal RPMI 2650 cells grown at an air–liquid interface as a model for nasal drug transport studies. *J. Pharm. Sci.* 97, 1165–1178.
- Boyd, J.M., Huang, L., Xie, L., Moe, B., Gabos, S., Li, X.F., 2008. A cell–microelectronic sensing technique for profiling cytotoxicity of chemicals. *Anal. Chim. Acta* 615, 80–87.
- Chien, Y.W., Su, K.S.E., Chang, S., 2008. Nasal Systemic Drug Delivery. Informa Healthcare Inc., New York.
- Csóka, G., Marton, S., Zelkó, R., Otomo, N., Antal, I., 2007. Application of sucrose fatty acid esters in transdermal therapeutic systems. *Eur. J. Pharm. Biopharm.* 65, 233–237.
- Davis, S.S., Illum, L., 2003. Absorption enhancers for nasal drug delivery. *Clin. Pharmacokinet.* 42, 1107–1128.
- De Fraissinette, A., Brun, R., Felix, H., Vonderscher, J., Rummelt, A., 1995. Evaluation of the human cell line RPMI 2650 as an *in vitro* nasal model. *Rhinology* 33, 194–198.
- Deli, M.A., 2009. Potential use of tight junction modulators to reversibly open membranous barriers and improve drug delivery. *Biochim. Biophys. Acta* 1788, 892–910.
- Dimova, S., Brewster, M.E., Noppe, M., Jorissen, M., Augustijns, P., 2005. The use of human nasal *in vitro* cell systems during drug discovery and development. *Toxicol. In Vitro* 19, 107–122.
- Fernández Freire, P., Peropadre, A., Pérez Martín, J.M., Herrero, O., Hazen, M.J., 2009. An integrated cellular model to evaluate cytotoxic effects in mammalian cell lines. *Toxicol. In Vitro* 23, 1553–1558.
- Galluzzi, L. et al., 2009. Guidelines for the use and interpretation of assays for monitoring cell death in higher eukaryotes. *Cell Death Differ.* 16, 1093–1107.
- Garti, N., Aserin, A., Fanun, M., 2000. Non-ionic sucrose esters microemulsions for food applications. Part 1. Water solubilization. *Colloids Surf. A* 164, 27–38.
- Horvát, S., Fehér, A., Wolburg, H., Sipos, P., Veszelka, S., Tóth, A., Kis, L., Kurunczi, A., Balogh, G., Kürti, L., Erős, I., Szabó-Révész, P., Deli, M.A., 2009. Sodium hyaluronate as a mucoadhesive component in nasal formulation enhances delivery of molecules to brain tissue. *Eur. J. Pharm. Biopharm.* 72, 252–259.
- Illum, L., 2000. Transport of drugs from the nasal cavity to the central nervous system. *Eur. J. Pharm. Sci.* 11, 1–18.
- Illum, L., 2003. Nasal drug delivery: possibilities, problems and solutions. *J. Controlled Release* 87, 187–198.
- Kissel, T., Werner, U., 1998. Nasal delivery of peptides: an *in vitro* cell culture model for the investigation of transport and metabolism in human nasal epithelium. *J. Controlled Release* 53, 195–203.
- Konsoula, R., Barile, F.A., 2005. Correlation of *in vitro* cytotoxicity with paracellular permeability in Caco-2 cells. *Toxicol. In Vitro* 19, 675–684.
- Lin, H., Yoo, J.W., Roh, H.J., Lee, M.K., Chung, S.J., Shim, C.K., Kim, D.D., 2005. Transport of anti-allergic drugs across the passage cultured human nasal epithelial cell monolayer. *Eur. J. Pharm. Sci.* 26, 203–210.
- Liu, Y., Peterson, D.A., Kimura, H., Schubert, D., 1997. Mechanism of cellular 3-(4,5-dimethylthiazol-2-yl)-2,5-diphenyltetrazolium bromide (MTT) reduction. *J. Neurochem.* 69, 581–593.
- MacDonald, C., Lyzenga, W., Shao, D., Agu, U.R., 2010. Water-soluble organic solubilizers for *in vitro* drug delivery studies with respiratory epithelial cells: selection based on various toxicity indicators. *Drug Delivery* 17, 434–442.
- Moore, G.E., Sandberg, A.A., 1964. Studies of a human tumor cell line with a diploid karyotype. *Cancer* 17, 170–175.
- Mutoh, T., Kubouchi, H., Noda, M., Shiinoki, Y., Matsumura, Y., 2007. Effect of oil-soluble emulsifiers on solidification of thermally treated creams. *Int. Dairy J.* 17, 24–28.
- Ózsvári, B., Puskás, G.L., Nagy, L.I., Kanizsai, I., Gyuris, M., Madács, R., Fehér, L.Z., Gerő, D., Szabó, Cs., 2010. A cell–microelectronic sensing technique for the screening of cytoprotective compounds. *Int. J. Mol. Med.* 25, 525–530.
- Schmidt, M.C., Peter, H., Lang, S.R., Ditzinger, G., Merkle, H.P., 1998. *In vitro* cell models to study nasal mucosal permeability and metabolism. *Adv. Drug Deliv. Rev.* 29, 51–79.
- Solly, K., Wang, X., Xu, X., Strulovici, B., Zheng, W., 2004. Application of real-time cell electronic sensing (RT-CES) technology to cell-based assays. *Assay Drug Dev. Techn.* 2, 363–372.
- Szűts, A., Pallagi, E., Regdon Jr., G., Aigner, Z., Szabó-Révész, P., 2007. Study of thermal behaviour of sugar esters. *Int. J. Pharm.* 336, 199–207.
- Szűts, A., Makai, Zs., Rajkó, R., Szabó-Révész, P., 2008. Study of the effects of drugs on the structures of sucrose esters, the effects of solid-state interactions on drug release. *J. Pharm. Biomed. Anal.* 48, 1136–1142.

- Szűts, A., Láng, P., Ambrus, R., Kiss, L., Deli, M.A., Szabó-Révész, P., 2011. Applicability of sucrose laurate as surfactant in solid dispersions prepared by melt technology. *Int. J. Pharm.* 410, 107–110.
- Ugwoke, M.I., Verbeke, N., Kinget, R., 2001. The biopharmaceutical aspects of nasal mucoadhesive drug delivery. *J. Pharm. Pharmacol.* 53, 3–22.
- Wolburg, H., Wolburg-Buchholz, K., Sam, K., Horvát, S., Deli, M.A., Mack, A.F., 2008. Epithelial and endothelial barriers in the olfactory region of the nasal cavity of the rat. *Histochem. Cell Biol.* 130, 127–140.
- Wengst, A., Reichl, S., 2010. RPMI 2650 epithelial model and three-dimensional reconstructed human nasal mucosa as in vitro models for nasal permeation studies. *Eur. J. Pharm. Biopharm.* 74, 290–297.
- Werner, U., Kissel, T., 1996. In vitro cell culture models of the nasal epithelium: a comparative histochemical investigation of their suitability for drug transport studies. *Pharm. Res.* 13, 978–988.
- Weyermann, J., Lochmann, D., Zimmer, A., 2005. A practical note on the use of cytotoxicity assays. *Int. J. Pharm.* 288, 369–376.
- Xia, M., Huang, R., Witt, L.K., Southall, N., Fostel, J., Cho, M.H., Jadhav, A., Smith, C.S., Inglese, J., Portier, C.J., Tice, R.R., Austin, C.P., 2008. Compound cytotoxicity profiling using quantitative high-throughput screening. *Environ. Health Perspect.* 116, 284–291.
- Xing, J.Z., Zhu, L., Gabos, S., Xie, L., 2005. Microelectronic cell sensor assay for detection of cytotoxicity and prediction of acute toxicity. *Toxicol. In Vitro* 20, 995–1004.